Applications of Matter Reference Frames in Quantum Gravity

Yili Wang

München 2023

Applications of Matter Reference Frames in Quantum Gravity

Yili Wang

Dissertation
der Fakultät für Physik
der Ludwig-Maximilians-Universität
München

vorgelegt von
Yili Wang
aus Zhejiang, P.R.China

München, den 24.04.2023

Erstgutachter: Dr. Daniele Oriti
Zweitgutachter: PD Dr. Michael Haack
Tag der mündlichen Prüfung: 05.06.2023

Contents

List of Figures

List of Tables

Zusammenfassung

Diese Dissertation untersucht Anwendungen von materiebasierten Referenzsystemen im Gruppenfeldtheorie (GFT) Ansatz für Quantengravitation. In nichtperturbativer Quantengravitation ohne Hintergrundraumzeit werden üblicherweise Materiefelder verwendet, um relationale Beschreibungen aufzustellen. In dieser Dissertation bestehen Referenzsysteme aus Skalarfeldern und es werden drei Beispiele aufgezeigt, in denen siein GFT angewendet werden.

Im ersten Beispiel wird ein homogenes, anisotropes GFT Kondensat erstellt, welches an ein Skalarfeld gekoppelt ist. Basierend auf verschiedenen Begriffen von Anisotropie in GFT werden zwei unterschiedliche GFT Zustände konstruiert. Das Skalarfeld, wirkend als physikalische Uhr, extrahiert effektive Observablen und Dynamik jener Zustände und demonstiert hierdurch den Prozess der Isotropisierung eines frühen anisotropen Universums.

Der zweite Fall errichtet einen schwarzenQuantenloch-Zustand in einem relationen materiebasierten Referenzsystem. Es wird analysiert, wie die expliziten Skalarfelder ohne jegliche Information über ihre Dynamik rekonstruiert werden können. Aus den resultierenden Feldern, als Referenzsystem an GFT gekoppelt, wird ein GFT-Zustand entnommen, welcher eine klassische Schwarzschild-Raumzeit im Grenzwert eines Kontinuums reproduziert.

Das Abschlussprojekt zeigt die Emergenz eines Amit-Roginsky-artigen Modells als Störungen eines $3D$ Boulatov GFT-Modells auf, welches an ein Skalarfeld gekoppelt ist. Die Kopplung an das Skalarfeld führt translationsinvariante kinetische Terme in die Boulatovwirkung ein. Störungen dieser neuen Wirkung ergeben eine effektive Theorie, die durch Amit-Roginsky-Theorie beschrieben wird, falls Bedingungen gelten, aus welchen Dominanz melonischer Diagramme hergeleitet werden kann.

Summary

This dissertation studies the applications of matter reference frames in the Group Field Theory (GFT) approach to quantum gravity. In non-perturbative quantum gravity without a background space-time, matter fields are usually used to give relational descriptions. In this dissertation, the matter reference frame consists of scalar fields, and three examples of applying this reference system in GFT will be shown.

In the first example, homogeneous anisotropic GFT condensate states coupled with a scalar field are built. Based on different definitions of 'anisotropy' in GFT, two distinct GFT states are constructed parallelly. As a physical clock, the scalar field extracts effective observables and dynamics of these GFT states, demonstrating the isotropisation of an anisotropic early universe.

The second case constructs a quantum black hole state in a relational matter reference frame. We will analyse how to find the explicit scalar fields without any information about their dynamics. With the resulting scalar fields coupled to GFT states as a reference system, we obtain a GFT state that reproduces classical Schwarzschild geometry in a continuum limit.

The final project shows the emergence of an Amit-Roginsky-like model as perturbations over a $3D$ Boulatov GFT model coupled with a scalar field. The coupling of scalar fields brings translationally invariant kinetic terms to the Boulatov action. The perturbations over this new action yields an effective theory governed by Amit-Roginsky theory, and the conditions are found to recover the melonic dominance.

Chapter 1

Introduction

1.1 Approaches to Quantum Gravity

Quantum gravity, as its name indicates, is the quantum theory of gravity. General Relativity (GR), Quantum Physics, and Statistical Mechanics consist the basis of modern physics. According to quantum physics, everything is fundamentally quantum, so GR, as a classical theory, should also have a quantum description. However, GR and quantum physics are not compatible with each other. For instance, Quantum Field Theory (QFT) is a theory on a fixed background space-time, but in GR, space-time should also be involved in dynamics. Moreover, no observation has been made where both gravity and quantum effects are important. Without any experimental guidance, the task is more challenging.

Despite the difficulties, scientists spare no effort to pursue the unification of quantum physics and GR for a long time, and the preliminary scheme for the quantisation of GR was formed during 1930 to 1960 [1]. It has been more than one hundred years since Einstein proposed a quantum modification on gravitational theories in 1916 [2]:

> *Da dies in Wahrheit in der Natur nicht zutreffen dürfte, so scheint es, daß die Quantentheorie nicht nur die Maxwellsche Elektrodynamik, sondern auch die neue Gravitationstheorie wird modifizieren müssen.*
>
> [Since in nature, this should not be true, it seems that the quantum theory should not only modify Maxwell's electrodynamics, but also the gravitational theory.]

Around ten years later, Oskar Klein suggested that the concept of space-time should be changed due to the quantum effect on gravity [3–5]. The first technical work attacking the problem of quantum gravity was done by Rosenfeld in early 1930s [6, 7]. In the following two decades, much effort was made in this field [8–19]. For example, the word 'graviton', which is widely used today, was named by Blokhintsev and Gal'perin [8], denoting the quanta of a gravitational field. In late sixties, Charles W. Misner discussed four possible directions to

quantum gravity [20], covariant quantisation, canonical quantisation, Schwinger's method considering infinitesimal variations in propagator, and Feynman's sum-over-histories approach, which are very close to the classifications nowadays. Quantum gravity today can be roughly divided into two main streams: perturbative formalism and non-perturbative formalism.

The perturbative approaches corresponds to the covariant quantisation in Misner's classification, and nowadays are usually represented by the string theory [21–23]. The birth of perturbative quantum gravity traces back to 1952, when the 'flat space quantisation' of gravity was developed in Suraj N. Gupta's papers [17–19]. In perturbative quantum gravity, a space-time with metric $g_{\mu\nu}$ can be separated into a free Minkowski background $\eta_{\mu\nu}$ and a small non-linear perturbations $h_{\mu\nu}$ as interactions between gravitons,

$$g_{\mu\nu} = \eta_{\mu\nu} + h_{\mu\nu}, \tag{1.1}$$

and this is why it is named 'perturbative'. The perturbative programme thrived and its basic framework was formed with the Feynman rules for GR completed in late 1960s [24–29]. Though Gerard 't Hooft and Martinus J. G. Veltman proved that Yang-Mills theory can be renormalised [30, 31], evidence showing the non-renormalisability of GR was soon found [32–35]. To solve this problem, various attempts were made such as the idea of asymptotic safety [36], supergravity [37, 38], and higher derivative gravity [39]. However, none of them broke the bottleneck.

The perturbative approach enjoyed a rebirth thanks to the string theory. String theory, born in 1968, was initially developed as a realisation of S-matrix programme for hadronic particle physics [40]. In early 1970s, the possibility of string theory to be a quantum gravity candidate was considered [41–43], but string theory was not seriously considered until in 1984, when Michael B. Green and John H. Schwarz showed the anomaly cancellation [44], which is known as the starting point of 'the first superstring revolution' [23]. Then in the same year, the construction of heterotic string [45] and the Calabi-Yau compactification [46] built a bridge from the high-energy string theory to our low-energy real world. The superstring theory was well-established in 1987 [47, 48], combining ideas from other perturbative models such as supergravity. The string theory aims at not only quantising GR, but also constructing 'a theory of everything' [39].

On the other hand, non-perturbative approaches to quantum gravity develops parallelly, including canonical method, Feynman's sum-over-histories method, and all other relevant models. Being 'non-perturbative', these theories do not have a background space-time, strictly obeying the diffeomorphism invariance required by GR. Another difference between perturbative and non-perturbative approaches is that the only goal of non-perturbative models is to construct a consistent theory quantising gravity, instead of 'the final theory'.

The canonical programme began with the Peter G. Bergmann's work on non-linear fields [12, 13], which is the first work considering a phase quantisation with general co-

variance. Based on these papers, Bergmann defines 'true observables' in quantum theories as those whose 'values (at a given time) are independent of the choice of the frame of reference (including the gauge frame)' [14]. Meanwhile, the Hamiltonian form of GR was investigated by Dirac to explore the quantum nature of gravity [15, 16, 49]. Around ten years later, Richard Arnowit, Stanley Deser, and Misner constructed the famous ADM formulation [50], significantly simplifying the Hamiltonian formalism of GR. Bryce S. DeWitt then derived the Wheeler-DeWitt equation in 1976 and proposed a concept of 'wave function of the universe' [51]. The development of canonical quantisation then encountered a stumbling block like the covariant programme did, until the birth of loop quantum gravity after almost twenty years.

Loop Quantum Gravity (LQG) [1], a canonical quantisation of GR [52, 53], is a typical non-perturbative formalism and is a strong rival to the string theory. In 1986, Abhay Ashtekar defined new phase space variables, known as 'Ashtekar variables' [54, 55], and constructed a new Hamiltonian GR in terms of the spinorial connections, completing the project of Amitaba Sen [56]. Soon it was found that the Wilson loops for Ashtekar variables are solutions to the Wheeler-DeWitt equation [57], with the 'Loop Space Representation of Quantum General Relativity' introduced by Carlo Rovelli and Lee Smolin[58, 59] in the same year. The states of discrete space in LQG are labeled by Spin Networks (SNWs), whose concept was first brought by Penrose in 1971 [60–62]. At this moment, LQG established itself as a quantum gravity candidate, which is almost at the same time of the superstring revolution, bringing the renaissance of canonical programme.

Another major member from non-perturbative family is the Spin Foam (SF) model [53, 63–66], which approximately belongs to the sum-over-histories approach in Misner's classification. The sum-over-histories project of quantum gravity was first introduced in 1957, in 'Feynman quantization of general relativity' [20], the paper where Misner discusses four possible approaches to quantum gravity. Then from 1978, motivated by the path-integral method on deriving a black-hole radiance [67], Hawking developed the quantum gravity in Euclidean metrics [68–70]. Unlike string theory or LQG, SF is a younger candidate. A spinfoam can be thought of as the history of a SNW, which gives the building block of discretised space-time. Born in 1996 and combining techniques from topological quantum field theory [71] as well as LQG, SF revived the sum-over-histories programme [72–75].

One century has past, people have never stopped chasing a quantum gravity despite all the difficulties [76]. Though string theory belongs to the 'covariant' programme in Misner's categorisation, today a 'covariant' formalism usually refers to the SF model. The precise relation between LQG and SF still needs to be explored, and a theory of 'covariant LQG' is suggested to be the one merging LQG and SF and revealing the profound insights of quantum gravity [53, 77–79].

[1] In this dissertation, LQG always refers to the 'canonical LQG'.

Nowadays, the quantum gravity community contains a wider range of models alongside the three approaches mentioned above, such as the causal set theory [80, 81], the $2D$ matrix model [82, 83], and the twistor programme [84, 85]. Not only between LQG and SF, convergences also occur among many other quantum gravity models. This dissertation will focus on the Group Field Theory (GFT) formalism for quantum gravity [86–89], which captures some of these convergences. GFT is a non-perturbative theory, and it is a generalisation of the matrix model, adopting and adapting techniques from LQG, SF, tensor models [90–92], Regge calculus [93], and causal dynamical triangulation [94].

1.2 Group Field Theory Formalism

GFT has a very special way to define the quantum gravity, which is already summarised by its name 'group field theory'. To be precise, GFT aims to describe quantum gravity as a 'combinatorially non-local quantum field theories on group manifolds' (or on the corresponding Lie algebra) [88]. Let us explain the definition term by term.

combinatorially non-local GFT is characterised by its combinatorially non-local interactions. As illustrated later in detail, GFT is not only a generalisation of matrix model, but also an enrichment of tensor model. The field is characterised by its tensorial nature.

quantum field theories GFT uses techniques from QFT. QFT is no doubt currently the best physical theory at quantum level. Like QFT, GFT lives on a smooth domain manifold. The utilisation of QFT enables us to use concepts or techniques from it. For instance, GFT can put differential operators in its kinetic terms, and GFT can also use the standard definition of path integral. It should be mentioned that GFT is not a theory of 'graviton', since there is no background space-time in GFT. As a result, GFT has no canonical formulation or any space-time based notion.

on group manifolds Instead of a background space-time, GFT lives on a group manifold, which is an significant difference with an usual QFT on space-time. The background structure of GFT is provided by a local symmetry (Lie) group of the theory. Restricted by the group domain, the field possesses special group-theoretic symmetries. For example, the GR is invariant under Lorentz transformations, then it is natural to consider the Lorentz group in GFT. One can also consider the subgroup of Lorentz group such as $SU(2)$ rotation group.

1.2.1 Matrix Model

To begin with, let us introduce first the Hermitian matrix model. The matrix model originates in 1961, when Regge described a Riemannian manifold without using coordinates [93]. From 1982, much work was done to develop the idea of a $2D$ gravitational theory [95–99]. In a matrix model, 2-simplices, together with their sub-simplices, form a *simplicial complex* that gives a triangulation [100] of a $2D$ surface. Though it describes Euclidean gravity, a basic assumption of the matrix model is that the Lorentzian gravity can be recovered by a rotation of the Euclidean time [82, 101].

Trivially, the dynamics of a point particle $\mathcal{X}$ can be described by an action

$$S = \frac{1}{2}\mathcal{X}^2 + \frac{\lambda}{3}\mathcal{X}^3, \tag{1.2}$$

where λ is a coupling constant. The point-like nature of the particles and the locality of the interactions ensures that its Feynman diagrams are simple tri-valent diagrams with $(0+1)$-dimensional combinatorial structure [88].

To increase the combinatorial dimension, one need to deal with a 1-dimensional object, so here comes the matrix model. The dynamical objects of matrix model are rank-2 matrices M_{ij}. Generalising the action of a point particle (1.2), for example, a simple action of $N \times N$ matrices M_{ij} reads [88]

$$S = \frac{1}{2}M^i_j \mathfrak{K}^{jl}_{ki} M^k_l - \frac{\lambda}{\sqrt{N}} M^i_j M^m_n M^k_l \mathfrak{V}^{jnl}_{mki}, \tag{1.3}$$

where the kinetic kernel is

$$\mathfrak{K}^{jl}_{ki} = \delta^j_k \delta^l_i, \tag{1.4}$$

and the vertex term is

$$\mathfrak{V}^{jnl}_{mki} = \delta^j_m \delta^n_k \delta^l_i. \tag{1.5}$$

The matrices M_{ij} can be graphically represented by ribbons [90], with side lines called strand labeled by matrix indices, forming a *dual complex*. Then a ribbon vertex corresponds to a triangle, and its ribbons are dual to the edges, which is illustrated in Figure 1.1. The vertex term in action 1.3 forms a triangle, and the kinetic term tells how to glue these triangles through the edges. The ribbon graphs are the Feynman diagrams Γ of matrix model [82, 83], and let us show how this is related with a $2D$ simplicial gravity.

Assume that Γ consists of v_Γ vertices and f_Γ faces, and its dual simplicial complex contains v vertices, e edges, and t triangles. The partition function

$$Z = \int \mathcal{D}[M_{ij}] e^{-S} = \sum_\Gamma \left(\frac{\lambda}{\sqrt{N}}\right)^{1/2} Z_\gamma = \sum_\Gamma \lambda^{v_\Gamma} N^{f_\Gamma - v_\Gamma/2} \tag{1.6}$$

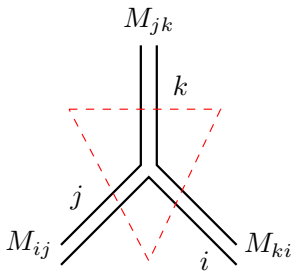

Figure 1.1: The interaction term of a matrix model (black solid lines) corresponds to a 2-simplex (red dashed line).

is obtained by summing over all possible triangulations [82, 83, 88]. Note that

$$f_\Gamma - \frac{1}{2}v_\Gamma = v - \frac{1}{2}t = v - e + t = 2 - 2h, \tag{1.7}$$

where χ is the Euler characteristic and h is the number of genus of the simplicial complex $\triangle$. Therefore,

$$Z = \sum_{\triangle} \lambda^t N^\chi. \tag{1.8}$$

Meanwhile, an Einstein action on a 2-dimensional manifold is simply

$$S_E = \int \mathrm{d}^2x\sqrt{g}(-R + \Lambda) = (-4\pi\chi + \Lambda A_M), \tag{1.9}$$

where A_M is the area of the manifold. The partition function

$$Z = \int \mathcal{D}[g]e^{-S_E} \tag{1.10}$$

is difficult to calculate, but we can first consider the discrete form of it. Suppose that we discretise the surface into equilateral triangles, and each triangle is of area a. This discretisation brings a factor of $1/G$ to the action, where G is the order of the discrete symmetry group of the triangulation. Then let $\lambda = \exp\{-\Lambda a/G\}$ and $N = \exp\{4\pi/G\}$, and one obtains

$$Z = \sum_{\triangle} \lambda^t N^\chi = \sum_{\triangle} e^{\frac{4\pi\chi}{G} - \frac{\Lambda t a}{G}}. \tag{1.11}$$

Each Feynman amplitude Z_Γ is related to simplicial path integrals of $2D$ gravity on its corresponding simplicial complex, and the total amplitude is obtained by summing over all possible geometries and all possible topologies. This reflects an idea of the *third quantisation* [102]: making topology dynamical. In this way, one considers all possible space-time geometries, rather than those limited by certain topology.

Then one may be interested in exploring the continuum limit of a matrix model. To do this, let us expands the partition function as

$$Z = N^2 Z_0(\lambda) + Z_1(\lambda) + N^{-2} Z_2(\lambda) + ... \sum_h N^{2-2h} Z_h(g), \tag{1.12}$$

so the sum of triangulations can be controlled. When $N \to \infty$, the term of Z_0 will be dominant. With $h = 0$, trivial topology will contribute most. Therefore, the large-N limit in matrix model is also named the planar limit.

In order to study the continuum limit, we first work with the triangulations with fixed topology (Z_0) to find out if a critical point can be defined. One finds that Z_0 can be written as

$$\lim_{v_\Gamma \to \infty} Z_0(\lambda) \sim \lim_{v_\Gamma \to \infty} \sum_{v_\Gamma} v_\Gamma^{\gamma-3} \left(\frac{\lambda}{\lambda_c}\right)^{v_\Gamma} \sim (\lambda - \lambda_c)^{2-\gamma}, \tag{1.13}$$

when the number of vertices are large. Note that the expectation value of area of the surface is proportional to v_Γ:

$$\langle A \rangle = a \langle v_\Gamma \rangle = a \frac{\partial}{\partial \lambda} \ln Z_0(\lambda) \sim \frac{a}{\lambda - \lambda_c}. \tag{1.14}$$

The total area diverges if $\lambda \to \lambda_c$, so we can make $a \to 0$ in order to have a finite total surface. Therefore, by sending $a \to 0$ and $v_\Gamma \to \infty$, one has a continuum limit of the matrix model, and this match the continuum path integral of $2D$ gravity through Liouville approach [82, 83, 88].

Another continuum limit is obtained by summing over all topologies alongside a summing over geometries, and this is a double-scaling limit. Considering topologies with higher genus and taking large number of vertices, the leading singular term of each partition function reads

$$Z_h(\lambda) \simeq f_h (\lambda - \lambda_c)^{\frac{(2-\beta)\chi}{2}}, \tag{1.15}$$

where β is a constant and f_h is a coefficient. Therefore, by taking $\lambda \to \lambda_c$ when $N \to \infty$, the contributions from higher-genus topologies are not necessarily compressed by Z_0. The total path integral is

$$Z \simeq \sum_h f_h \kappa^{2h-2}, \tag{1.16}$$

where $\kappa \equiv N(\lambda - \lambda_c)^{(2-\beta)/2}$. As a result, if one take $N \to \infty$ and $\lambda \to \lambda_c$ while fixing κ, which is named a double-scaled limit, all possible topologies are included. The result of this continuum limit also agrees with the $2D$ Liouville gravity [82, 83, 88].

In order to move up to higher dimensions, one may naïvely extend the matrix model to a 'tensor model', where, for instance, M_{ij} is replaced by an $N \times N \times N$ tensor T_{ijk} in $3D$ cases [103–105]. Then the action (1.3) becomes

$$S(T) = \frac{1}{2} \sum_{i,j,k} T_{ijk} T_{kji} - \lambda \sum_{ijklmn} T_{ijk} T_{klm} T_{mjn} T_{nli}, \tag{1.17}$$

and a rank-three tensor is represented by a three-strand ribbon. The path integral then reads

$$Z = \int \mathcal{D}[T_{ijk}] e^{-S(T)} = \sum_{\Gamma} \lambda^{v_\Gamma} Z_\Gamma \tag{1.18}$$

Such an extension, however, failed to describe a $3D$ quantum gravity [88]. Unlike a matrix model, this tensor model does not relate the Feynman amplitude with a $3D$ simplicial gravity. In addition, it loses the control over topologies when computing path integrals. Therefore, the $3D$ generalisation of a matrix model should be a model containing a richer structure of path integral.

1.2.2 Group Field Theory

Such a generalisation of matrix model can be achieved by GFT. The first GFT model is established by Boulatov [106], which describes a $3D$ gravity, and it was soon extended to $4D$ by Ooguri [107] in the same year. Instead of tensors with three indices, a $3D$ GFT uses fields with three variables from a Lie group or its corresponding Lie algebra, i.e. T_{ijk} is replaced by $\varphi(g_1, g_2, g_3)$, where $g_i \in G$ are group elements. Summing over indices in tensor models is replaced by an integral over the group manifold. In this way, one enriches the tensor model with more degrees of freedom (d.o.f.) while keeping the combinatorial non-local interactions. 'Determined completely by the fundamental groups of a manifold' [106], Boulatov model produces the simplicial path integral of a $SU(2)$ $3D$ BF theory [108], which is a topological theory equivalent to $3D$ GR.

Generally speaking, a d-dimensional GFT for quantum gravity is a theory of complex non-local field $\varphi(g_1, g_2, ..., g_d)$ on the d-copies of a group manifold, where

$$\varphi(g_1, g_2, ..., g_d) : G^d \to \mathbb{C}. \tag{1.19}$$

A general GFT action reads

$$\begin{aligned} S &= \int (\mathrm{d}g)^d (\mathrm{d}g')^d \bar{\varphi}(g_1, ..., g_d) \mathcal{K}(g, g') \varphi(g'_1, ..., g'_d) \\ &\quad + \sum_i \frac{\lambda_i}{n_i} \int (\mathrm{d}g_{n_1})^d ... (\mathrm{d}g_{n_i})^d \bar{\varphi}(g_{n_1}) ... \mathcal{V}_i(g_{n_1}, ..., g_{n_i}) ... \varphi(g_{n_i}), \end{aligned} \tag{1.20}$$

where $g \equiv (g_1, g_2, ..., g_d)$, and $\mathrm{d}g$ is the Haar measure on G^d. The kinetic kernel is given by $\mathcal{K}(g, g')$, and all possible interaction terms containing n_i fields are considered. The group G is a Lie group, and the choice on G depends on which local gauge symmetry that the gravity possesses. For example, $SU(2)$, $SL(2, \mathbb{R})$ are used for three dimensions, and $SL(2, \mathbb{C})$ can be chosen when studying a theory in four dimensions.

In addition to the *group representation* we used above, the Hilbert space of quantum simplices can also be written in *Lie algebra representation* [109] and spin representation. In Lie algebra representation, for instance, the field is

$$\varphi(X_1, X_2, ..., X_d) : \mathfrak{su}(2)^d \to \mathbb{C}, \tag{1.21}$$

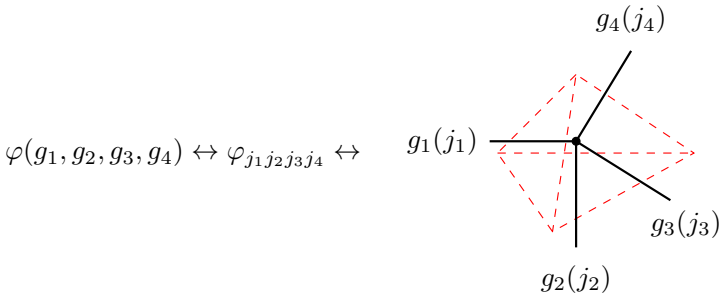

Figure 1.2: A tetrahedron (red dashed lines) corresponds to a four-valent spin network (black lines), where each link is dual to a face of tetrahedron.

when $G = SU(2)$. The group representation can be recovered through a non-commutative Fourier transform [110–113],

$$\tilde{\varphi}(X) \equiv \int_G \mathrm{d}g e_g(X)\varphi(g), \tag{1.22}$$

where e_g is the plane wave depending on the quantisation map [114]. The advantage of Lie algebra representation is that it has a clear geometric interpretation on the group element as parallel transport along the links dual to $(d-2)$-faces [88].

The *spin representation* is simpler than Lie algebra representation, and it can be translated from group representation by Peter-Weyl decomposition into irreducible representations for $G = SU(2)$ [115, 116], where the field is $\varphi_{j_1,...,j_d}$. This representation is of great importance in this dissertation, as the calculation can be significantly simplified in spin representation, and we will give a detailed introduction later.

Similar to a matrix representing an 1-simplex, $\varphi(g_1, g_2, ..., g_d)$ represents a $(d-1)$-simplex, belonging to a simplicial complex making the triangulation of a $(d-1)$-space. The dual complex is the Feynman diagram. A $(d-1)$-simplex corresponds to a vertex in dual complex, and its $(d-2)$-faces correspond to the links attached to the vertex. The group elements g_i are assigned to these links in the dual complex. Take 3-dimensional space for example, if $G = SU(2)$, then the building blocks are tetrahedra given by $\varphi(g_1, g_2, g_3, g_4)$ dual to 4-valent SNWs, as shown by Figure 1.2.

In order that these $(d-2)$-faces can form a $(d-1)$-simplex, *closure constraint* is required. In Lie algebra representation, it means $\sum_d X_d = 0$. In group representation, it is translated to right gauge invariance

$$\varphi(g_1, ..., g_d) = \varphi_(g_1 h, ..., g_d h), \quad \forall h \in G, \tag{1.23}$$

which also means a symmetry under a global parallel translation. As for spin representation, it is realised by the triangle inequality among the spins j_i.

The field φ can be promoted into creation/annihilation operators $\hat{\varphi}^\dagger/\hat{\varphi}$, creating or removing a $(d-1)$-simplex [117]:

$$\hat{\varphi}^\dagger(g) \equiv \sum_{\vec{S}} \hat{c}^\dagger_{\vec{S}} \psi_{\vec{S}}(g), \tag{1.24}$$

where $\hat{c}^\dagger_{\vec{S}}/\hat{c}_{\vec{S}}$ is the fundamental operator with *Bosonic* commutator, creating/annihilating a d-valent vertex state $\vec{S}$. The single-vertex wave-function $\psi_{\vec{S}} \equiv \left\langle g \middle| \vec{S} \right\rangle$ is normalised such that $\int \mathrm{d}g \psi_{\vec{S}}(g)\psi_{\vec{S}'}(g) = \delta_{\vec{S},\vec{S}'}$.

Correspondingly, one defines a Fock vacuum $|0\rangle$, which means 'no space'. As the building blocks should be indistinguishable, the field operators obey Bosonic statistics:

$$[\hat{\varphi}(g), \hat{\varphi}^\dagger(g')] = \Delta_R(g,g'), \quad [\hat{\varphi}(g), \hat{\varphi}(g')] = [\hat{\varphi}^\dagger(g), \hat{\varphi}^\dagger(g')] = 0, \tag{1.25}$$

where

$$\Delta_R(g,g') \equiv \int dk \prod_{i=1}^{d} \delta(g_i k (g_i')^{-1}) \tag{1.26}$$

is a Dirac delta over G.

Each building block and its dual complex created by $\hat{\varphi}^\dagger$ is interpreted as an 'atom of space', and its Hilbert space is

$$\mathcal{H} = L^2(G^d). \tag{1.27}$$

Then, the kinematical Hilbert space of GFT is a Fock space

$$\mathcal{F}(\mathcal{H}) = \bigoplus_{v=0}^{\infty} sym\left\{\mathcal{H}^{(1)} \otimes ... \otimes \mathcal{H}^{(v)}\right\}, \tag{1.28}$$

where *sym* represents the symmetry under 'particle permutations'.

Though GFT is originally constructed as a generalised matrix model, it combines various aspects from different non-perturbative approaches to quantum gravity, such as LQG, SF, and coloured tensor models.

LQG First of all, GFT is tightly connected with LQG. GFT and LQG share the same Hilbert space basis defining the quantum theory [118, 119]. In LQG, SNWs are the fundamental pre-geometric building blocks of a continuum space, and GFT can be viewed as a QFT of SNWs when $G = SU(2)$. Moreover, GFT can be thought of as a second quantised reformulation of LQG [117, 119]. In such a way, one is able to borrow techniques from LQG, such as area or volume operators, which are diagonalised in GFT spin representation.

SF Another important feature of GFT is that its Feynman diagrams can explicitly reproduce the same amplitude of SF model [120]. A SF σ describes the histories of a SNW. The world-sheet of a link from SNW is a *face*, and the world-line of a vertex is called an *edge*. The edges meet at the *vertex* of σ. Its Feynman amplitude is

$$Z = \sum_{\sigma} w(\sigma) \sum_{\rho} \prod_{f} A_f(\rho_f) \prod_{e} A_e(\rho_{f|e}) \prod_{v} A_v(\rho_{f|v}), \tag{1.29}$$

where $w(\sigma)$ is the weight and ρ are the representations labelling σ.

Consider $(2+1)$-dimensional GFT for example, where the building blocks of the space are 2-simplices (triangles) represented by $\varphi(g_1, g_2, g_3)$. The group-representation action reads

$$\begin{aligned} S(\varphi) &= \frac{1}{2} \int \mathrm{d}g^3 \varphi(g_1, g_2, g_3) \varphi(g_3, g_2, g_1) \\ &\quad - \frac{\lambda}{4!} \int \mathrm{d}g^6 \varphi(g_1, g_2, g_3) \varphi(g_3, g_4, g_5) \varphi(g_2, g_2, g_6) \varphi(g_6, g_4, g_1), \end{aligned} \tag{1.30}$$

and in spin representation it becomes

$$\begin{aligned} S(\varphi) = &\frac{1}{2} \sum_{j,m} \varphi^{j_1 j_2 j_3}_{m_1 m_2 m_3} \varphi^{j_3 j_2 j_1}_{m_3 m_2 m_1} \\ &- \frac{\lambda}{4!} \sum_{j,m} \begin{Bmatrix} j_1 & j_2 & j_3 \\ j_4 & j_5 & j_6 \end{Bmatrix} \varphi^{j_1 j_2 j_3}_{m_1 m_2 m_3} \varphi^{j_3 j_4 j_5}_{m_3 m_4 m_5} \varphi^{j_5 j_2 j_6}_{m_5 m_2 m_6} \varphi^{j_6 j_4 j_1}_{m_6 m_4 m_1}, \end{aligned} \tag{1.31}$$

where $\begin{Bmatrix} j_1 & j_2 & j_3 \\ j_4 & j_5 & j_6 \end{Bmatrix}$ is a Wigner $6j$ symbol. The interactions among four triangles φ^4 form a tetrahedron, and the kinetic term glues these tetrahedra to form a $3D$ triangulation. The Feynman amplitude of this GFT is

$$Z = \int \mathcal{D}[\varphi] e^{-S(\varphi)} = \sum_{\Gamma} \frac{\lambda^n}{sym[\Gamma]} Z(\Gamma), \tag{1.32}$$

where the Γ are Feynman diagrams (dual to $3D$ simplicial complex) with n vertices, and $sym[\Gamma]$ is the symmetry factor of a graph. By assigning each face and edge with an irreducible representation of $SU(2)$ and an intertwiner respectively, one obtains [88, 106]

$$Z(\Gamma) = \left(\prod_{f} \sum_{j_f} \right) \prod_{f} (2j_f + 1) \prod_{v} \begin{Bmatrix} j_1 & j_2 & j_3 \\ j_4 & j_5 & j_6 \end{Bmatrix}, \tag{1.33}$$

which is the Ponzano-Regge SF amplitude.

Extending to $(3+1)$ dimensions, we have a field $\varphi(g_1, g_2, g_3, g_4)$, and obtain a Feynman amplitude as the simplicial path integral of a BF theory [107]. A classical $4D$ Riemannian

GR (Palatini-Holst continuum gravity) can be expressed as a constrained BF theory via Plebanski formulation [88, 121, 122], and there are various methods to put the Plebanski constraint in order to build a GFT for $4D$ gravity (see [123] for example).

Having introduced the basics of GFT, let us continue to fulfil the expectation of emergent space-time and geometry in GFT. To this end, it is necessary to investigate the GFT condensates in a material reference system.

1.3 Quantum Gravity Condensates in Relational Reference Frame

As mentioned, the GFT building blocks, encoded with *pre-geometric* fundamental d.o.f., are the 'atoms of space'. One may wonder, if the geometry and the space-time are fundamentally discrete, then how do we build a bridge connecting GFT with a continuum world, which is closely related with our daily life?

To answer the question, it is useful to consider the concept of 'emergent space-time and geometry'. This is not a unique concept that can only be found in GFT, and in fact, it is widely used in many quantum gravity models such as LQG, SF, and causal set theory. The basic idea is rather simple: the continuum is a *collective* behaviour of pre-geometric d.o.f. in an *effective* description [124]. The space-time emerges from combinatorial structures in GFT, and the pre-geometric data is given by the group elements. We assume that exists such a phase, where only the collective behaviour of pre-geometric d.o.f. is of concern, and call it a *proto-geometric* phase [125]. The continuum geometry and space-time is therefore effectively recovered from a suitable averaging or coarse graining.

However, unlike usual QFTs, which are quantum theories *on* a space-time, GFT is a quantum theory *of* space-time. Here comes another problem, that how to effectively describe a system when we lack a notion of time or coordinates?

In non-perturbative approaches, the concept of a 'background space-time' is broken [52, 126]. In Newtonian physics and QFT, coordinates $\{x_\mu\}$ defines 'where' an event is, and the space-time is a primary notion: it is what one is left with after removing all dynamical things away. But according to GR, space-time is also a dynamical object, so nothing exists if all dynamical objects are taken away. The general covariance implies that manifold is simply a mathematical tool that facilitates the description, and coordinate systems are not physical either.

To describe a GFT system, especially its effective dynamics, it is important to localise the quanta of space (or of space-time). The question is then how to define the location without a background space-time? The strategy in this dissertation is to use a *relational*

reference frame. This issue also closely related with the problem that what can be observables in quantum gravity, without any notion of 'space-time point'? One answer to it is the Dirac observable [127], which are gauge-invariant quantities in gauge theories. A further argument was made by Rovelli [128] that we should also take the reference system as dynamical objects in order to define observables and their locations.

When describing a object, one actually tells how this object evolves with respect to the local value that the gravitational field takes. Then it is reasonable to say that this object is at some 'relational' location with 'relational' dynamics to gravity. For example, to find the evolution of a dynamical quantity A, one uses another dynamical object T as a clock. When T is at some value T_o, A takes a corresponding value $A(T_o)$. In other words, only partial observables, which are physical quantities associated with a measuring procedure are meaningful in a background-independent system [52, 129, 130]. It turns out that the matter which is dynamically coupled with the gravity can be clock and rods, localising the points in a diffeomorphism-invariant manner [128].

Choosing a clock is related with the problem of time [131]. The core of problem of time, in short, is to figure out whether time is an observable in quantum gravity. In general, there are three ways to attack the problem of time, *tempus ante quantum*, *tempus post quantum*, and *tempus nihil est*. In 'tempus ante quantum' approach, a clock is selected before quantising the system, and the 'tempus nihil est' method keeps the quantum system timeless without any specific notion of time. In GFT, we use 'tempus post quantum' method, such that the notion of time is made after the quantisation. In this way, we will have a 'clock operator' $\hat{T}$, such that its expectation value over a quantum state $|o\rangle$ corresponds to a classical clock time $T = T_o$, with very small quantum fluctuations from $\hat{T}$. For example, if

$$\langle o|\, \hat{T}\, |o\rangle \simeq T_o, \tag{1.34}$$

then

$$A(T_o) \simeq \langle o|\, \hat{A}\, |o\rangle\,. \tag{1.35}$$

The similar techniques are also applied when defining a rod. In short, in this dissertation, clock and rods will all be defined after a time-neutral quantisation.

In quantum gravity, a simple but useful matter reference is the scalar field ϕ, whose general action reads

$$S_\phi = \frac{1}{2}\int \sqrt{-g}\left[(\partial\phi)^2 + (\mathfrak{m}^2 + \tilde{\alpha}R)\phi^2\right] + \int \sqrt{-g}V(\phi) + ..., \tag{1.36}$$

with $\mathfrak{m}$ the mass, $\tilde{\alpha}$ the coupling constant, and $V(\phi)$ a potential term. As a clock or a rod, ϕ is assumed to be minimally coupled such that it will not largely affect the system to be measured, so $\tilde{\alpha} = 0$. The mass term and the potential term will be chosen depending on the situation.

There are usually two methods to discretise the scalar fields: one is to assign d.o.f. on simplicial complex, like lattice gauge theory [132, 133]; the other is to discretise the matter field on dual complex. For simplicity, we choose the second method, so the value of ϕ is associated on nodes of a SNW [52]. In this way, GFT yields the same Feynman amplitude of a gravity coupled with scalar fields [134]. To localise the GFT quanta, d scalar fields are needed at most, 1 clock and $(d-1)$ rods in usual. Then the field is generalised such that

$$\varphi(g_1, ..., g_d; \phi_1, ..., \phi_d) : G^d \times \mathbb{R}^d \to \mathbb{C}, \tag{1.37}$$

with a non-trivial commutator between field operators

$$[\hat{\varphi}(g, \phi), \hat{\varphi}^\dagger(g', \phi')] = \Delta_R(g, g')\delta^d(\phi - \phi'). \tag{1.38}$$

Having coupled GFT with a relational matter reference frame, let us now show how GFT effectively describes the emergence of continuum space-time. Interested in the collective behaviour of GFT quanta, one may finds that the situation is quite similar with condensed matter physics [135]. A simple but powerful GFT states that used to study a large number of quanta on average is the *GFT condensate state* [136–138], and this technique will also be applied in this dissertation. The simplest definition of a GFT condensate coherent state is

$$|\sigma\rangle \equiv \mathcal{N}_\sigma \exp\Big\{\int \mathrm{d}g\mathrm{d}\phi\sigma(g;\phi)\hat{\varphi}^\dagger(g;\phi)\Big\}|0\rangle\,, \tag{1.39}$$

where $\mathcal{N}_\sigma = \exp\{-\|\sigma\|^2/2\}$ with $\|\sigma\|^2 = \int dgd\phi|\sigma(g;\phi)|^2$ such that the state is normalised $\langle\sigma|\sigma\rangle = 1$. The state (1.39) has a very similar form with bosonic coherent states in condensed matter theory [135], and akin to the boson coherent state, it is an eigen-state of GFT field operators, i.e.

$$\hat{\varphi}(g;\phi)\,|\sigma\rangle = \sigma(g;\phi)\,|\sigma\rangle\,. \tag{1.40}$$

State (1.39) gives a natural mean-field approximation of GFT. Since $\langle\hat{\varphi}(g;\phi)\rangle = \sigma(g;\phi)$, $\sigma(g,\phi)$ can be thought of as an order parameter [139]. Every quanta in (1.39) is determined by the same wave-function $\sigma(g;\phi)$, which also equips homogeneity to the state. Because of all the reasons above, (1.39) is named a GFT 'condensate state'.

The next task is to localise the coherent state in a matter reference frame. Let us take homogeneous cosmological cases for example, where one only needs a clock ϕ_1 to define 'when' a GFT condensate state is. The simplest choice is to take away $\mathrm{d}\phi$ in (1.39), and claim that

$$|\sigma(\phi_o)\rangle = \mathcal{N}_\sigma \exp\Big\{\int \mathrm{d}g\sigma(g;\phi_o)\hat{\varphi}^\dagger(g;\phi_o)\Big\}|0\rangle \tag{1.41}$$

represents a condensate of tetrahedra at clock time $\phi_1 = \phi_o$ [140].

However, this definition suffers from infinitely large quantum fluctuations when calculating the momentum of the scalar field, ∂_{ϕ_1}. To control divergence, one can instead use

coherent peaking state by introducing a peaking function η_ϵ [125]. Assume that at $\phi_1 = \phi_o$, the scalar field has momentum π_o, and the condensate state is governed by a wave-function $\sigma_{\epsilon;\phi_o}(g;\phi_1)$

$$\sigma_{\epsilon;\phi_o}(g;\phi_1) = \eta_\epsilon(g;\phi_1-\phi_o,\pi_o)\varsigma(g;\phi_1), \tag{1.42}$$

with ς a 'reduced wave-function'. The peaking function η_ϵ reads

$$\eta_\epsilon(\phi_1-\phi_o,\pi_o) \equiv \mathcal{N}_\epsilon \exp\left(-\frac{(\phi_1-\phi_o)^2}{2\epsilon}\right)\exp(i\pi_o(\phi_1-\phi_o)), \tag{1.43}$$

and $\mathcal{N}_\epsilon^2 = (\pi_o\epsilon)^{-1/2}$ in order that $\int d\phi|\eta_\epsilon|^2 = 1$. To ensure the quantum fluctuations does not diverge, one requires $\epsilon \ll 1$ to be small but finite, and $\epsilon\pi_0^2 \gg 1$ [125, 141]. Then a state

$$|\sigma_\epsilon;\phi_o\rangle \equiv \mathcal{N}_\sigma \exp\left\{\int \mathrm{d}g\mathrm{d}\phi_1 \sigma_{\epsilon;\phi_o}(g;\phi_1)\hat{\varphi}^\dagger(g;\phi_1)\right\}|0\rangle \tag{1.44}$$

is called a coherent peaked state, picking a state approximately at $\phi_1 = \phi_o$ with negligible relative variance when the number of tetrahedra is large enough. With this tool, one can extract an effective description from GFT condensates and show the emergence of classical space-time, which will be illustrated in the following chapters.

1.4 Overview of Dissertation

This dissertation focuses on the applications of the matter reference frame, which consists of scalar fields, from various aspects of GFT.

Chapter 2 develops homogeneous anisotropic GFT condensate states coupled to a scalar field, which are expected to have a correspondence with classical Bianchi I universe. We will study the definitions of 'isotropy' in quantum cosmology, and build anisotropic GFT states according to different definitions. Both observables and dynamics over these states will be effectively described in terms of a matter clock.

In Chapter 3, a candidate quantum state of Schwarzschild black hole will be constructed at kinetic level. Coupled with scalar fields which form a relational reference system, this GFT state reproduces the observables sharing the same properties with those of a classical Schwarzschild space-time. We will demonstrate how to find a suitable matter fields as reference frame from a most general set-up.

Chapter 4 shows how Amit-Roginsky-like matter is reproduced effective as perturbations around a $3D$ Boulatov GFT, with the help of a matter reference frame that facilitate the computation.

Finally, a conclusion and outlooks will be presented in Chapter 5, discussing the future possible directions of research on GFT.

In addition, there will be three appendices. In order not to interrupt the smoothness of this dissertation, a brief introduction of $SU(2)$ recoupling theory will be given in Appendix A, on which the calculation in this dissertation heavily relies. Appendix B illustrates basics of edge-coloured graphs encoded with topology, which will be applied in chapter 3. Appendix C, as a complementary of Chapter 3 for interested readers, will illustrate a simple example for a GFT states that corresponds to a negative-mass black hole.

Chapter 2

Effective Bianchi I Universe

This chapter is based on a project in collaboration with Daniele Oriti.

In this chapter, we will build a GFT cosmological model to describe a homogeneous anisotropic universe. Working with an isotropic background, we introduce the anisotropy as perturbations. By studying two different definitions of 'isotropy' in GFT, we will parallelly construct two types of anisotropic GFT condensate states and study their effective dynamics, in terms of a matter clock. It will be shown that both models, being anisotropic at early stage, become isotropic as the clock time increases.

2.1 Background

A quantum gravity theory is expect to resolve the singularities in classical theories. In addition to the curvature singularities of black holes, another important singularity is the initial Big-Bang singularity in cosmology, where quantum effects should be considered. An important branch of quantum gravity is the quantum cosmology, which was started by Misner [142], applying the idea of canonical quantum gravity [51] to cosmology. This chapter constructs a quantum cosmological model in GFT corresponding to a classical Bianchi I universe, and demonstrates how to an extract effective description from it with a material clock.

The Standard Cosmological Model (SCM), also known as (inflation+)ΛCMD model, is based on two fundamental assumptions: i) GR correctly describes the gravity; ii) the universe is homogeneous and isotropic at large scales, which is the cosmological principle. SCM is strongly supported by a wide range of observational evidence such as Cosmic Microwave Background (CMB). In SCM, an initial singularity exists at the beginning of the universe, the Big-Bang singularity, and this singularity is inevitable according to GR [143–145]. The existence of space-time singularity implies a potential incompleteness of current cosmological model, where they may not be able to provide a correct paradigm for the early universe. Therefore, there is an argument that at Planck scale, one has to

consider the quantum effect on gravity in order to resolve the singularity.

In quantum cosmology, one solution to the Big Bang singularity problem is replacing the big bang with a 'Big Bounce' [146–148]. For example, bouncing solutions can be found for a flat Friedmann-Lemaître-Robertson-Walker (FLRW) brane-world from string theory [149]. Loop Quantum Cosmology (LQC) [150, 151] is a quantum cosmological theory where techniques from LQG are applied, and it also finds a big bounce at the early stage of our universe [152].

The investigation of the universe near the initial singularity can be largely simplified by Belinski-Khalatnikov-Lifshitz (BKL) conjecture [153, 154], which implies that the dynamics of early universe can be approximated by Bianchi models [155, 156], which are homogeneous and anisotropic.

Meanwhile, SCM is facing several challenges. An increasing number of high-precision observations finds anomalies that question the exact isotropy of the large-scale universe. For example, recent research in dipole anomaly [157, 158] finds dipole signals from number-count show a inconsistency from the prediction of CMB at around 5σ. There are several interpretations on these anomalies, and one candidate is a universe with non-trivial topology such as Bianchi universes, which suggests that our universe is likely to have a preferred direction [159–163].

As will be illustrated in detail later, GFT has managed to obtain Friedmann equations from quantum gravity condensates in a matter reference frame [136–138], where the states are set to be homogeneous and isotropic, obeying the cosmological principle. Considering the BKL conjecture for early universe as well as the anomalies observed today, it is our interest to extend the current GFT cosmological state to describe an anisotropic universe. The anisotropic GFT state has not been well developed for the time being. Based on the previous attempts [164, 165], we will try constructing a GFT state such that a Bianchi I universe, which is the simplest anisotropic model, can emerge from it effectively. It will be checked whether this GFT model can share some properties with the classical theory, which helps us to understand isotropisation during expansion from an anisotropic early state.

2.2 Bianchi I Model

Bianchi classification is a set of spatially homogeneous models, including nine types of structure constants featuring the Lie algebra formed by Killing vectors [155, 156]. The simplest one is the Bianchi I model, where the spatial curvature and structure constants are both zero. The diagonalised Bianchi I metric in a standard synchronous form reads

$$\mathrm{d}s^2 = -N(\tau)\mathrm{d}\tau^2 + a_1^2(\tau)\mathrm{d}x^2 + a_2^2(\tau)\mathrm{d}y^2 + a_3^2(\tau)\mathrm{d}z^2, \tag{2.1}$$

where $N(t)$ is the lapse function, and scale factors $a_i(t)/a_j(t) \neq$ *constant* to ensure anisotropy.

Alternatively, one can work with Misner's variables and rewrite the scale factors into [166]

$$a_1(\tau) = V^{1/3}(\tau)e^{\beta_+(\tau)+\sqrt{3}\beta_-(\tau)}, \tag{2.2}$$
$$a_2(\tau) = V^{1/3}(\tau)e^{\beta_+(\tau)-\sqrt{3}\beta_-(\tau)}, \tag{2.3}$$
$$a_3(\tau) = V^{1/3}(\tau)e^{-2\beta_+(\tau)}. \tag{2.4}$$

The mean Hubble parameter can be calculated by the mean scale factor $a := (a_1a_2a_3)^{1/3}$,

$$H = \frac{\dot{a}}{a} = \frac{1}{3}(H_1 + H_2 + H_3), \tag{2.5}$$

where '$\cdot$' denotes $\mathrm{d}/\mathrm{d}\tau$, and

$$H_i = \frac{\dot{a}_i}{a_i}. \tag{2.6}$$

The $\tau\tau-$component of Einstein equation is

$$H_1H_2 + H_2H_3 + H_3H_1 = 8\pi G\rho_m, \tag{2.7}$$

which can also be obtained from Hamiltonian constraint [167], where ρ_m is the energy density. This equation can be recast into a generalised Friedmann equation

$$H^2 = \frac{8\pi G}{3}\rho_m + \frac{\Sigma^2}{a^6}, \tag{2.8}$$

where

$$\Sigma^2 = \frac{a^6}{18}\left[(H_1 - H_2)^2 + (H_2 - H_3)^2 + (H_3 - H_1)^2\right] \tag{2.9}$$

is the *shear term* measuring contribution from anisotropy.

Now let us remember the argument on observables made in Chapter 1, so we should consider only relational observables in a matter reference frame instead of the coordinates $\{t, x, y, z\}$. The scalar fields will play the role of material frame, so let us continue to a Bianchi I universe coupled with scalar fields. Since Bianchi I universe is homogeneous, there is no spatial dependence and one clock is enough to describe the system. For convenience, we choose a free massless scalar field ϕ and work with Misner's variables. The parameters $\beta_\pm$ can be treated as a couple of free massless scalar fields. Then we find the equation of motion in terms of the clock time ϕ from the Hamiltonian formalism of such a Bianchi I universe [165]

$$S = \int \mathrm{d}\tau \left(p_V\dot{V} + p_+\dot{\beta}_+ + p_-\dot{\beta}_- + p_\phi\dot{\phi} - NC\right), \tag{2.10}$$

where C is the Hamiltonian constraint such that

$$NC = -6\pi GNVp_V^2 + \frac{2\pi GNp_+^2}{3V} + \frac{2\pi GNp_-^2}{3V} + \frac{Np_\phi^2}{2V}. \tag{2.11}$$

The momentum of scalar field p_ϕ is a constant of motion [165, 167], and $\{p_\phi, NC\} = 0$. The equations of motion are

$$\dot{\phi} = \{\phi, NC\} = \frac{Np_\phi}{V}, \tag{2.12}$$

$$\dot{V} = \{V, NC\} = -12\pi GNVp_V, \tag{2.13}$$

$$\dot{\beta_\pm} = \{\beta_\pm, NC\} = \frac{4\pi GNp_\pm}{3V}. \tag{2.14}$$

$$\tag{2.15}$$

Combining (2.12) and (2.14), one obtains

$$\frac{\mathrm{d}\beta_\pm}{\mathrm{d}\phi} = \frac{4\pi G}{3}\frac{p_\pm}{p_\phi}. \tag{2.16}$$

Taking $NC = 0$, one finds the generalised Friedmann equation for Bianchi I universe:

$$\left(\frac{V'(\phi)}{3V(\phi)}\right)^2 = \left(\frac{\mathrm{d}\beta_+}{\mathrm{d}\phi}\right)^2 + \left(\frac{\mathrm{d}\beta_-}{\mathrm{d}\phi}\right)^2 + \frac{4\pi G}{3}, \tag{2.17}$$

and ' means $\mathrm{d}/\mathrm{d}\phi$. A general solution for a Bianchi I universe coupled with a free massless scalar field reads [168, 169]

$$a_i(\phi) = a_{i,o}e^{\sqrt{8\pi G}\kappa_i(\phi-\phi_i)}, \tag{2.18}$$

where κ_i and ϕ_i are some constants playing no role in our case. From (2.18), one finds that the left-hand side of (2.17) is a constant, so its right-hand side should be a constant as well.

Then let us think about a question: what quantities can one use to show how anisotropic a space-time is? Two common anisotropy criteria are the shear term Σ^2 2.9 and the *mean anisotropy parameter* $\mathcal{A}$ [170–173]

$$\mathcal{A} := \sum_{i=1}^{3} \frac{H_i^2 - H^2}{H^2}. \tag{2.19}$$

At first sight, one may also use β_+ and β_- to characterise the anisotropy, since metric reduces to isotropic one when $\beta_+ = \beta_- = 0$. However, $\{\beta_+, \beta_-\}$ are not unique to determine a Bianchi I spacetime. For example, suppose one redefines the parameters such that

$$\beta_+ = -\frac{1}{2}\left(\tilde{\beta}_+ + \sqrt{3}\tilde{\beta}_-\right), \tag{2.20}$$

$$\beta_- = -\frac{1}{2}\left(\sqrt{3}\tilde{\beta}_+ - \tilde{\beta}_-\right), \tag{2.21}$$

then the scale factors can be rewritten into

$$\tilde{a}_3(\tau) \equiv a_1(\tau) = V^{\frac{1}{3}} e^{-2\tilde{\beta}_+}, \tag{2.22}$$

$$\tilde{a}_2(\tau) \equiv a_2(\tau) = V^{\frac{1}{3}} e^{\tilde{\beta}_+ - \sqrt{3}\tilde{\beta}_-}, \tag{2.23}$$

$$\tilde{a}_1(\tau) \equiv a_3(\tau) = V^{\frac{1}{3}} e^{\tilde{\beta}_+ + \sqrt{3}\tilde{\beta}_-}. \tag{2.24}$$

The spatial metric then becomes

$$\mathrm{d}q^2 = \tilde{a}_1^2(t)\mathrm{d}\tilde{x}^2 + \tilde{a}_2^2(t)\mathrm{d}\tilde{y}^2 + \tilde{a}_3^2(t)\mathrm{d}\tilde{z}^2, \tag{2.25}$$

where $\tilde{x} = z$, $\tilde{y} = y$ and $\tilde{z} = x$, which is an equivalent space-time. It can be verified that $[(\mathrm{d}\beta_+/\mathrm{d}\phi)^2 + (\mathrm{d}\beta_-/\mathrm{d}\phi)^2]$ is the quantity that invariant under redefinition of coordinates, and this is simply a shear term written in Misner's variables. Therefore, the shear term and the mean anisotropy parameter will act as 'observables' characterising the anisotropy in this chapter.

2.3 Quantum Dynamics

2.3.1 GFT Equations of Motion

To continue, let us construct a homogeneous and anisotropic quantum model in terms of the GFT condensate $|\sigma\rangle$ (1.39). Coupled with one scalar field, the basic GFT field is

$$\varphi(g_v, \phi) : SU(2)^4 \times \mathbb{R} \to \mathbb{C}. \tag{2.26}$$

This field is then promoted to operators $\hat{\varphi}$ and $\hat{\varphi}^\dagger$ to build the condensate state. A simple choice to extract the effective dynamics of GFT condensates is to compute the Schwinger-Dyson equation derived from a general GFT action (1.20) where

$$\langle\sigma| \frac{\delta S[\hat{\varphi}, \hat{\varphi}^\dagger]}{\delta\hat{\varphi}^\dagger} |\sigma\rangle = 0, \tag{2.27}$$

and it yields

$$\int \mathrm{d}g_v \mathrm{d}\phi_v \mathcal{K}(g_v, g_w; (\phi_v - \phi_w)^2)\sigma(g_v, \phi_v) + \mathcal{V}\delta\bar{\sigma}(g_w, \phi_w) = 0, \tag{2.28}$$

similar to a Gross-Pitaevskii equation in condensed matter theory [138, 139]. We use a generalised GFT model [164, 174–176] based on Engle-Pereira-Rovelli-Livine SF model [177] such that

$$\mathcal{K} = \delta(g_w g_v^{-1})\delta(\phi_v - \phi_w)\left[-\tau\partial_\phi^2 + \eta\sum_i \Delta_{g_i} + M^2\right], \tag{2.29}$$

where Δ_{g_i} is Laplace-Beltrami operator acting on the group manifold. This choice on kinetic kernel is also required due to the renormalisability of GFT [178–182].

As is shown in Figure 1.2, a tetrahedron is created by $\hat{\varphi}^\dagger(g;\phi)$, and its dual complex is a SNW. For computational simplicity, we will work in spin representation from now on. One first decompose the wave-function according to Peter-Weyl theorem,

$$\sigma(g_v,\phi_v)=\sum_{\{j\},\{m\},l_L,l_R}\iota^{j_1j_2j_3j_4l_L}_{m_1m_2m_3m_4}\iota^{j_1j_2j_3j_4l_R}_{n_1n_2n_3n_4}\sigma^{j_1j_2j_3j_4l_Ll_R}(\phi_v)\prod_{i=1}^{4}D^{j_i}_{m_in_i}(g_{v,i}), \tag{2.30}$$

where the intertwiner

$$\iota^{j_1j_2j_3j_4l}_{m_1m_2m_3m_4}=\sum_{m,m'}C^{j_1j_2l}_{m_1m_2m}C^{j_3j_4l'}_{m_3m_4m'}C^{ll'0}_{mm'0} \tag{2.31}$$

is assigned on the vertex of a SNW to combine four links together, and $C^{jj_1j_2}_{mm_1m_2}$ the Clebsch-Gordon coefficient [115, 116]. The subscript L and R of the intertwiner ι denotes invariance under local frame rotations (left invariance) and the closure condition (right gauge invariance).

First of all, we want to fix the shape of a tetrahedron with the areas of its faces and require that the the intertwiner is an eigen-vector of the LQG volume operator that yields the largest possible eigenvalue. This implies

$$\iota^{j_1j_2j_3j_4l_R}_{n_1n_2n_3n_4}=\iota^{j_1j_2j_3j_4l_\star}_{n_1n_2n_3n_4}, \tag{2.32}$$

where $\iota^{j_1j_2j_3j_4l_\star}_{n_1n_2n_3n_4}$ is the intertwiner yielding the largest volume eigen-value. Then requiring that $l_L=l_R=l_\star$ since the volume is invariant under parallel transport, the wave-function satisfies [140]

$$\sigma(g_v,\phi_v)=\sum_{j,m}\iota^{j_1j_2j_3j_4l_\star}_{m_1m_2m_3m_4}\iota^{j_1j_2j_3j_4l_\star}_{n_1n_2n_3n_4}\sigma^{j_1j_2j_3j_4}(\phi_v)\prod_{i=1}^{4}D^{j_i}_{m_in_i}(g_{v,i}). \tag{2.33}$$

Usually, the argument above is valid for 'isotropic' GFT condensates. However, as will be illustrated below, the intertwiners of anisotropic building blocks will be fixed such that they also have the largest eigen-values [164]. Then we may assume that the anisotropic perturbations over an isotropic GFT state also satisfy the dynamics of the same type [176].

With the interaction terms neglected, the equation of motion (2.28) of σ_{j_v} approximately satisfies

$$A_{j_v}\partial^2_\phi\sigma_{j_v}-B_{j_v}\sigma_{j_v}\simeq 0, \tag{2.34}$$

where $A_{j_v}=-\tau$, and $B_{j_v}=-(\eta\sum_{j_i}j_i(j_i+1)+M^2)$.

To control the momentum of the scalar field ϕ, we apply coherent peaked state to define the condensate state at clock time $\phi = \phi_o$, say $|\sigma_\epsilon; \phi_o\rangle$ (1.44), and its wave-function reads

$$\sigma_{\epsilon,\phi_o}(g,\phi) = \eta_\epsilon(g; \phi - \phi_o, \pi_o)\varsigma(g,\phi). \tag{2.35}$$

Consequently, in spin representation, the Schwinger-Dyson equation receives corrections from the peaking function such that [125]:

$$\varsigma''_{j_v}(\phi_o) - 2i\frac{\pi_o}{\epsilon\pi_o^2 - 1}\varsigma'_{j_v}(\phi_o) - \left(\epsilon^{-1}\frac{2}{\epsilon\pi_o^2 - 1} + \frac{B_{j_v}}{A_{j_v}}\right)\varsigma_{j_v}(\phi_o) \simeq 0. \tag{2.36}$$

If $\varsigma_{j_v} = \rho_{j_v}\exp(i\theta_{j_v})$ with ρ_{j_v} and θ_{j_v} real, the equation above then becomes

$$\rho''_{j_v}(\phi_o) - \frac{Q_{j_v}^2}{\rho_{j_v}^3(\phi_o)} - \Upsilon_{j_v}^2\rho_{j_v}^2(\phi_o) = 0, \tag{2.37}$$

where

$$\Upsilon_{j_v}^2 = \frac{\pi_o^2}{\epsilon\pi_0^2 - 1}\left(\frac{2}{\epsilon\pi_o^2} - \frac{1}{\epsilon\pi_0^2 - 1}\right) + \frac{B_{j_v}}{A_{j_v}}. \tag{2.38}$$

For convenience, we denote ϕ_o with ϕ, and a general solution of differential equations in form (2.37) is [183]

$$\rho_{j_v}(\phi) = \frac{e^{\sqrt{\Upsilon_{j_v}^2}(\Phi-\phi)}\sqrt{\Omega_{j_v}e^{4\sqrt{\Upsilon_{j_v}^2}(\phi-\Phi)} + \Omega_{j_v} - 2\mathfrak{E}_{j_v}\sqrt{\Omega_{j_v}}e^{2\sqrt{\Upsilon_{j_v}^2}(\phi-\Phi)}}}{2\sqrt{\Upsilon_{j_v}^2}\sqrt[4]{\Omega_{j_v}}}, \tag{2.39}$$

where Φ is the clock time of ϕ when a quantum bounce happens (usually $\Phi = 0$), and

$$\Omega_{j_v} = \mathfrak{E}_{j_v}^2 + 4Q_{j_v}^2\Upsilon_{j_v}^2. \tag{2.40}$$

There are three conserved quantities due to the introduction of coherent peaked states [125]. The first is a charge Q_j related with $U(1)$ symmetry,

$$Q_{j_v} = \rho_{j_v}^2\left(\theta'_j - \frac{\pi_0}{\epsilon\pi_0^2 - 1}\right). \tag{2.41}$$

The others are 'bulk GFT energy' $\mathfrak{E}_{j_v}$, a charge generating translations of the reduced background wave-function along the clock time direction ϕ_0, which takes the form

$$\mathfrak{E}_{j_v} = (\rho'_{j_v})^2 + \frac{Q_{j_v}^2}{\rho_j^2} - \Upsilon_{j_v}^2\rho_{j_v}^2, \tag{2.42}$$

and 'relational energy' $\tilde{\mathfrak{E}}_{j_v}$

$$\tilde{\mathfrak{E}}_{j_v} = \mathfrak{E}_{j_v} + 2Q_{j_v}\frac{\pi_0}{\epsilon\pi_0^2 - 1}, \tag{2.43}$$

where an 'energy injection' occurs due to the precise choice of the peaking function η_ϵ.

2.3.2 Generic Operators

Here we discuss operators most used in GFT. A generic GFT (1+1)-body operator acts on a vertex w and results in another vertex v, without changing the combinatorial structure of the state, which reads

$$\hat{\mathcal{O}}_t \equiv \int \mathrm{d}g_v \mathrm{d}g_w \mathrm{d}\phi_v \mathrm{d}\phi_w O(g_v, g_w; \phi_v, \phi_w) \hat{\varphi}_t^\dagger(g_v; \phi_v) \hat{\varphi}_t(g_w; \phi_w), \tag{2.44}$$

where

$$O(g_v, g_w; \phi_v, \phi_w) \equiv \langle g_v; \phi_v | \, \hat{O} \, | g_w; \phi_w \rangle \tag{2.45}$$

is the matrix element, and (2.44) is a 'second quantised' version of a 'first quantised' (1+1)-body operator $\hat{O}$, acting on states in the Fock space.

An important operator is the *number operator*:

$$\hat{N} = \int \mathrm{d}g \mathrm{d}\phi \hat{\varphi}^\dagger(g, \phi) \hat{\varphi}(g, \phi), \tag{2.46}$$

and its expectation value at ϕ_0 in spin representation reads

$$\langle \hat{N} \rangle(\phi_o) = \int \mathrm{d}g \mathrm{d}\phi |\sigma_{\epsilon, \phi_o}(g, \phi; \phi_o, \pi_o)|^2 \simeq \sum_{j_v} \rho_{j_v}^2(\phi_o). \tag{2.47}$$

The area of the i^{th} face of a tetrahedron is measured by an *area operator*

$$\hat{A}_i = \kappa \int \mathrm{d}g \mathrm{d}\phi \hat{\varphi}^\dagger(g, \phi) \sqrt{E_i^I E_i^J \delta_{IJ}} \rhd \hat{\varphi}(g, \phi), \tag{2.48}$$

where $I = \{1, 2, 3\}$. Here $\kappa = 8\pi\gamma\ell_P^2$ with γ the Barbero-Immirzi parameter, and E_I^i is the LQG flux operators proportional to Lie derivatives on $SU(2)$. The action of LQG flux operator is [184–186]

$$E_i^I \rhd f(g_j) := \lim_{\epsilon \to 0} i \frac{\mathrm{d}}{\mathrm{d}\epsilon} f(g_1, ..., e^{-i\epsilon\tau^I} g_j, ..., g_4), \tag{2.49}$$

for a function $f : SU(2)^4 \to \mathbb{C}$, where τ^I is the Pauli matrix, and $\tau^I \tau^I = j(j+1)\mathbb{1}$ is the $SU(2)$ Casimir operator. The eigen-value of an area operator over a SNW is $\ell_0^2 \sqrt{j_i(j_i+1)}$, and ℓ_0 is a fundamental length scale parameter.

The *volume (density) operator* is

$$\hat{V} = \int \mathrm{d}g \mathrm{d}\phi \hat{\varphi}^\dagger(g_v, \phi_v) V(g_v, g_w) \hat{\varphi}^\dagger(g_w, \phi_w). \tag{2.50}$$

Its expectation value over $|\sigma_\epsilon; \phi_o\rangle$ is

$$\langle \hat{V} \rangle(\phi_o) \simeq \sum_{j_v} V_{j_v} \rho_{j_v}^2(\phi_o), \tag{2.51}$$

with V_{j_v} the eigenvalue of volume operator when acting on the vertex v of a SNW. Finally is the scalar field operator, which can defined as [140]

$$\hat{\Phi} = \int \mathrm{d}g_v \mathrm{d}\phi \hat{\varphi}^\dagger(g_v, \phi)\hat{\varphi}(g_v, \phi)\phi. \tag{2.52}$$

However, $\langle\hat{\Phi}\rangle$ will show a dependence on the total number of tetrahedra, so $\langle\hat{\Phi}\rangle$ is an extensive quantity depending on the scale of a system. As a scalar field, it should be an intensive quantity independent of the scale, so we can redefine this operator as:

$$\hat{\phi} := \frac{\hat{\Phi}}{\langle\hat{N}\rangle}, \tag{2.53}$$

such that

$$\langle\hat{\phi}\rangle(\phi_o) = \frac{\langle\hat{\Phi}\rangle(\phi_o)}{\langle\hat{N}\rangle(\phi_o)} \simeq \phi_o, \tag{2.54}$$

which makes sense.

2.4 Anisotropic Quantum Gravity Condensates I

2.4.1 Measurement of Anisotropy

As mentioned, we can use the shear and the anisotropy parameter $\mathcal{A}$ to tell how 'anisotropic' a universe is. However, we do not have the corresponding quantum operators in GFT. An alternative way to calculate these quantities is to express them as functions of area or volume operators, which is well-defined already. To this end, let us first find the relations in a classical Bianchi I universe, and apply them to quantum states to obtain the expectation values approximately.

To begin with, it is necessary to define what is 'isotropy' before we study 'anisotropy'. Generally, there are two definitions of spatial 'isotropy' in GFT: i) One uses regular tetrahedra as the building blocks of an isotropic space, which is widely used in GFT quantum cosmology [140]; ii) One chooses re-rectangular tetrahedra, where three orthogonal edges of a tetrahedron meeting at one vertex are of the same length [176], which shares a similar spirit with the 'isotropy' in LQC [167, 169]. In this chapter, these definitions will be considered separately.

This section is based on the first definition of 'isotropy'. To describe the anisotropy of GFT condensates, let us first find observables in classical Bianchi I space-time. Suppose we have a regular tetrahedron, whose faces are equilateral triangles with edges of length l. Then let us embed this tetrahedron in a Bianchi I space-time, so the physical area of the triangles as well as the physical length of the edges will change accordingly. Assume that one face of this tetrahedron $\triangle ABC$ is parallel to $x-y$ plane, and the edge AC of this

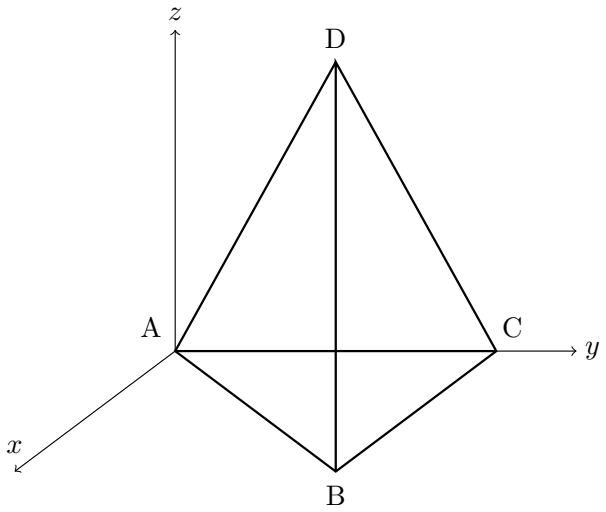

Figure 2.1: A tetrahedron in Bianchi I universe, which is regular if the space is isotropic.

triangle is parallel to $y-$axis, so $z-$axis represents the direction orthogonal to $\triangle ABC$, as illustrated by Figure 2.1. Such embedding also yields a volume closest to the eigen-value of the volume operator [165]

As a result, $\triangle ABD \cong \triangle BCD$, so faces of a tetrahedron have three different physical areas. Let the physical areas of $\triangle ABC$, $\triangle ACD$, $\triangle ABD$ (or $\triangle BCD$) to be $\mathfrak{A}$, $\mathfrak{B}$ and $\mathfrak{C}$ respectively, then one finds

$$\mathfrak{A} = \frac{\sqrt{3}}{4} e^{2\beta_+} V^{\frac{2}{3}} l^2, \tag{2.55}$$

$$\mathfrak{B} = \frac{e^{-(\beta_+ + \sqrt{3}\beta_-)}}{4\sqrt{3}} \sqrt{8 + e^{6\beta_+ + 2\sqrt{3}\beta_-}} V^{\frac{2}{3}} l^2, \tag{2.56}$$

$$\mathfrak{C} = \frac{e^{-(\beta_+ + \sqrt{3}\beta_-)}}{4\sqrt{3}} \sqrt{2 + 6e^{4\sqrt{3}\beta_-} + e^{6\beta_+ + 2\sqrt{3}\beta_-}} V^{\frac{2}{3}} l^2, \tag{2.57}$$

in terms of Misner's variables $\{\beta_+, \beta_-\}$. Because the relation between the volume V and Misner's variables $\{\beta_+, \beta_-\}$ is ill-behaved at quantum level [165], this dissertation only consider the observables as functions of areas.

By requiring that $\beta_- = 0$ if $\mathfrak{B} = \mathfrak{C}$ and $\beta_+ = \beta_- = 0$ if $\mathfrak{A} = \mathfrak{B} = \mathfrak{C}$, one finds

$$\beta_- = \frac{1}{4\sqrt{3}} \ln\left(\frac{\mathfrak{A}^2 + 3\mathfrak{B}^2 - 12\mathfrak{C}^2}{\mathfrak{A}^2 - 9\mathfrak{B}^2}\right), \tag{2.58}$$

and

$$\beta_+ = \frac{1}{6} \ln\left(\frac{8\mathfrak{A}^2 \sqrt{\frac{\mathfrak{A}^2 + 3\mathfrak{B}^2 - 12\mathfrak{C}^2}{\mathfrak{A}^2 - 9\mathfrak{B}^2}}}{12\mathfrak{C}^2 - \mathfrak{A}^2 - 3\mathfrak{B}^2}\right). \tag{2.59}$$

Additionally, we define the ratios between scale factors

$$k_1 := \frac{a_3}{a_1} = \sqrt{\frac{1}{8}\left(9\frac{\mathfrak{B}^2}{\mathfrak{A}^2} - 1\right)}, \tag{2.60}$$

$$k_2 := \frac{a_3}{a_2} = \sqrt{\frac{1}{8}\left(9\frac{4\mathfrak{C}^2 - \mathfrak{B}^2}{3\mathfrak{A}^2} - 1\right)}, \tag{2.61}$$

which are 1 in an isotropic universe. The anisotropy parameter $\mathcal{A}$ can be rewritten in two ways:

$$\mathcal{A}_1(\phi) := \frac{18V^2(\beta_+'^2 + \beta_-'^2)}{V'^2}, \tag{2.62}$$

$$\mathcal{A}_2(\phi) := \frac{2V^2(k_1^2 k_2'^2 + k_2^2 k_1'^2 - k_1 k_2 k_1' k_2')}{V'^2 k_1^2 k_2^2}, \tag{2.63}$$

and they are equivalent in classical theory. Finally one can find the physical volume of a tetrahedron as a function of the areas:

$$V^2 = \frac{\mathfrak{A}\left(-\mathfrak{A}^2 - 3\mathfrak{B}^2 + 12\mathfrak{C}^2\right)}{\left(27\sqrt{3}\right)\sqrt{\frac{\mathfrak{A}^2+3\mathfrak{B}^2-12\mathfrak{C}^2}{\mathfrak{A}^2-9\mathfrak{B}^2}}}. \tag{2.64}$$

All these relations above depend on how one embeds the tetrahedron, but they are reliable quantities to measure the anisotropy. As discussed above, $\{\beta_+, \beta_-\}$ are not unique to characterise a Bianchi I space-time, so change embedding (for example, make $\triangle ACD$ parallel to $x-z$ plane) is equivalent to change coordinates and thus get a different set of $\{\beta_+, \beta_-\}$. Similar with the Bianchi I universe in LQC [167], different embedding in GFT does not change the dynamics, and this is what really matters. Moreover, these relations have a one-to-one correspondence to embedding, so once the way to embed a tetrahedron is fixed, we are always able to describe its exact properties unambiguously. Speaking about the volume, it is possible that other embedding cannot produce a volume similar to quantum expectation values from fixed areas of the triangles. However, this issue is beyond the dissertation, and we leave this for future.

Equipped with the knowledge on classical space-time, let us now move to the quantum side. The strategy we use is to substitute the area eigenvalues into the classical expressions and assume that the results are their quantum correspondence [165]. The eigen-value of GFT (or LQG) volume operator depends on the intertwiner ι_v associated to the vertex v that connects four links together [187–191]. Simply substituting eigenvalues of area operator into equation (2.64) does not yield the explicit eigenvalue of the volume operator. However, the relative difference between (2.64) and the exact GFT volume eigenvalues are very small [165], and we only care about the ratio V'/V in (2.17), so it does not change to result qualitatively if one use (2.64) to study the properties of volume. Hence, for convenience, the following calculation involving V will be based on (2.64).

2.4.2 Anisotropic Perturbations

An interesting fact is that Bianchi IX space can be separated into a closed FLRW background and a gravitational wave with longest wavelength [192, 193]. Though this is not directly related with what we are dealing with in this chapter, it inspires an essential conjecture in our Bianchi I GFT model: the homogeneous anisotropic states are split into an isotropic 'background' and anisotropic 'perturbations'. It should be mentioned that the use of 'background' and 'perturbation' is an abuse of notation. We require that isotropy will emerge from an anisotropic state asymptotically, so the isotropic part of the GFT state will be dominant. In this regime, the contribution from the anisotropic part is so small that they can be viewed as perturbations over an isotropic background. However, this does not mean that the anisotropy is also negligible at early stage. In fact, it is expected that our GFT state is highly anisotropic at this stage. Moreover, we expect that the tetrahedron assigned with four equal smallest spins will dominate at later time [194].

The embedding in Figure 2.1 results in a tetrahedron with three different faces, and accordingly we consider SNWs assigned with spins of three different values $j_v = (j, j, j_a, j_b)$. Let the links assigned with j correspond to $\triangle ABD$ and $\triangle BCD$, and those with j_a and j_b are dual to $\triangle ABC$ and $\triangle ACD$ separately. These SNWs are quantum counterparts of the classical tetrahedra we discuss above. As mentioned above, only with areas of the triangles, one cannot specify the shape of a tetrahedron, so we further require that each quantum building blocks should take the largest possible volume eigen-value with given face areas. In this way, we obtain a regular tetrahedron when its faces are of same area.

Tetrahedra with $j = j_a = j_b$ are the building blocks of the isotropic background, and the rest modes are called 'anisotropic perturbation'. One finds that the order of spins in a SNW is important, but this should not be a defect. Anisotropy means that there is a preferred direction, and the correspondence between spin and the classical triangle contain the information of embedding, so the order of spins tells us which direction is preferred.

According to (2.47) and (2.51) for instance, GFT geometric observables usually require a sum of all SNW modes j_v, and this means that tetrahedra with all possible shapes should be included. It seems to be rather challenging, but one can simplify the situation through the following analysis.

First of all, let $\jmath \equiv (\eta \sum_{i=1}^{4} j_i(j_i+1) + M^2)/\tau$. Assume the correction from peaking function is very small, and when $\jmath < 0$, $\Upsilon^2_{j_v^s} < 0$, according to solution (2.39), $\rho_{j_v} \propto \cos\Big(\sqrt{|\jmath|}\phi\Big)$. When $\jmath > 0$, $\Upsilon^2_{j_v^s} > 0$, so $\rho_{j_v} \propto \exp\Big(\sqrt{\jmath}\phi\Big)$ at large ϕ. By convention, one usually choose $\tau < 0$, $\eta > 0$, and $M^2 < 0$. Then $\jmath$ increases as j decreases, so $|\sigma_{j_v}|$ grows fastest for $j = 0$. Because $|\sigma_{j_v}|^2 = \rho^2_{j_v}$ gives the number expectation value for the mode j_v, $j = 0$ becomes dominant for large $|\phi|$. However, there is no clear interpretation for a tetrahedron with $j = 0$, so we can ignore it and set $1/2$ be the minimum possible spin. At late time, the condensate is almost occupied by the modes whose $j = 1/2$. Consequently,

the wave-function

$$\begin{aligned}\sigma(g_v,\phi) &= \sum_{j_v} \iota^{j_1j_2j_3j_4l_L}_{m_1m_2m_3m_4}\iota^{j_1j_2j_3j_4l_R}_{n_1n_2n_3n_4}\sigma^{j_1j_2j_3j_4l_Ll_R}(\phi)\prod_{i=1}^{4}D^{j_i}_{m_in_i}(g_{v,i}) \\ &\simeq \iota^{1/2}_{m_1m_2m_3m_4}\iota^{1/2}_{n_1n_2n_3n_4}\sigma_{1/2}(\phi)\prod_{i=1}^{4}D^{1/2}_{m_in_i}(g_{v,i}) \end{aligned} \tag{2.65}$$

for large ϕ in spin representation. Then one can approximately only deal with $j = 1/2$ when work in spin representation, and the kinematic kernel reads

$$K \simeq \delta(g_w g_v^{-1})\delta(\phi_v - \phi_w)\left[-\tau\partial_\phi^2 + 4\eta\frac{1}{2}\left(\frac{1}{2}+1\right) + M^2\right], \tag{2.66}$$

which means that the dynamics are governed by $j = 1/2$ state at late time. Therefore at large ϕ, our model will become isotropic and satisfy Friedmann equation of flat space [138].

Solution (2.39) oscillates when the spins associated to a vertex takes some value j_v^s such that$\Upsilon^2_{j_v^s} < 0$. Let us take $\tau = -1$ for convenience, which loses no generality. Due to the conditions required by low-spin dominance, the parameters we choose make $\Upsilon^2_{j_v^s}$ declines when $\jmath$ increases, so only modes that $(j_a + j_b + 2j) < j_v^s$ bring non-trivial contributions which are non-oscillating [194].

Let us consider an isotropic background consisting of three modes: $j_v = \{1/2\}$, $j_v = \{1\}$, and $j_v = \{3/2\}$, which are dual to regular tetrahedra. We further assume that $j_v = \{2\}$ yields oscillating solutions. This assumption can be achieved by requiring $-24\eta < M^2 < -15\eta$. With background modes fixed, one can do perturbations on them respectively. Let $\eta = 1$ for simplicity, we choose $M^2 = -23.9$ in order to include anisotropic perturbative mode as many as possible.

Furthermore, (2.58) and (2.59) put constraints on the perturbations as well, requiring

$$\frac{\mathfrak{A}^2 + 3\mathfrak{B}^2 - 12\mathfrak{C}^2}{\mathfrak{A}^2 - 9\mathfrak{B}^2} > 0, \tag{2.67}$$

which means that its quantum counterpart should also satisfy

$$\frac{j_a(j_a+1) + 3j_b(j_b+1) - 12j(j+1)}{j_a(j_a+1) - 9j_b(j_b+1)} > 0. \tag{2.68}$$

Finally the $SU(2)$ recouping theory [115, 116] demands that the sum of spins on a spin network should be integer. With all restrictions mentioned above, only a finite number of modes are allowed in our model, as shown in table 2.1.

Therefore, GFT condensates here are composed of these 25 modes, and we assume that the wave-function of the full state is a sum over all wave-functions which are solutions to (2.36) respectively:

$$\sigma = \sigma_{1/2} + \sigma_1 + \sigma_{3/2} + \sigma_{1/2,1/2,1/2,3/2} + ... + \sigma_{3/2,3/2,1,3}. \tag{2.69}$$

background	perturbations
$(\frac{1}{2},\frac{1}{2},\frac{1}{2},\frac{1}{2})$	$(\frac{1}{2},\frac{1}{2},\frac{1}{2},\frac{3}{2})$ $(\frac{1}{2},\frac{1}{2},1,1)$
$(1,1,1,1)$	$(1,1,1,2)$ $(1,1,2,1)$ $(1,1,1,3)$ $(1,1,\frac{1}{2},\frac{1}{2})$ $(1,1,\frac{1}{2},\frac{3}{2})$ $(1,1,\frac{3}{2},\frac{1}{2})$ $(1,1,\frac{3}{2},\frac{3}{2})$ $(1,1,\frac{3}{2},\frac{5}{2})$
$(\frac{3}{2},\frac{3}{2},\frac{3}{2},\frac{3}{2})$	$(\frac{3}{2},\frac{3}{2},\frac{3}{2},\frac{1}{2})$ $(\frac{3}{2},\frac{3}{2},\frac{1}{2},\frac{1}{2})$ $(\frac{3}{2},\frac{3}{2},\frac{5}{2},\frac{1}{2})$ $(\frac{3}{2},\frac{3}{2},1,1)$ $(\frac{3}{2},\frac{3}{2},2,1)$ $(\frac{3}{2},\frac{3}{2},3,1)$ $(\frac{3}{2},\frac{3}{2},\frac{1}{2},\frac{3}{2})$ $(\frac{3}{2},\frac{3}{2},\frac{5}{2},\frac{3}{2})$ $(\frac{3}{2},\frac{3}{2},1,2)$ $(\frac{3}{2},\frac{3}{2},2,2)$ $(\frac{3}{2},\frac{3}{2},\frac{3}{2},\frac{5}{2})$ $(\frac{3}{2},\frac{3}{2},1,3)$

Table 2.1: All possible modes of tetrahedra labelled by four spins that do not oscillate.

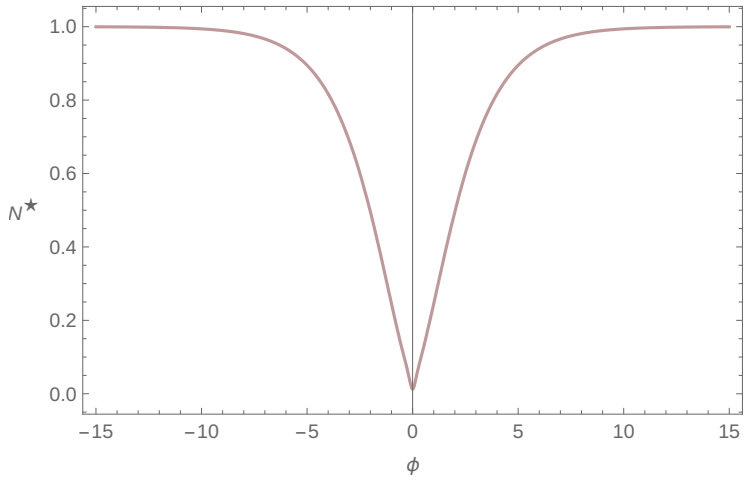

Figure 2.2: The behaviour of $N_\star$ when $\epsilon = 0.0001$ and $\pi_0 = 10000$. The value of ϵ bring slight change to the plot which is indistinguishable.

Now let us move on to extract effective description and dynamics from this model.

2.4.3 Observables

This part investigates the behaviour of the observables over perturbed GFT condensates, and we will compute the expectation value of number operator and the parameters measuring anisotropy introduced before. In the following computation, $\mathfrak{E}_{\frac{1}{2}} = \mathfrak{E}_1 = \mathfrak{E}_{\frac{3}{2}} = 10$ with all perturbations has $\mathfrak{E}_i = 1$.

Let us first study the number operator. An important quantity is the ratio between numbers of small-spin background and the total number, which is defined as

$$N_\star(\phi) \equiv \frac{N_{\frac{1}{2}}(\phi)}{\langle \hat{N}(\phi) \rangle} = \frac{\rho_{\frac{1}{2}}(\phi)^2}{\sum_{j_v} \rho_{j_v}^2(\phi)}. \tag{2.70}$$

This goes to 1, which not only shows the model becomes isotropic, but also agrees with the statement that small spin dominate later at late time, as is illustrated in Figure 2.2.

Then for a tetrahedron with spins $j_v = (j, j, j_a, j_b)$, the ratio between scale factors can be written into

$$k_1^{j_v} = \sqrt{\frac{1}{8}\left(9\frac{j_b(j_b+1)}{j_a(j_a+1)} - 1\right)}, \tag{2.71}$$

$$k_2^{j_v} = \sqrt{\frac{1}{8}\left(9\frac{4j(j+1) - j_b(j_b+1)}{3j_a(j_a+1)} - 1\right)}, \tag{2.72}$$

according to their classical expressions (2.60) and (2.61). Thus, we can compute $k_{i(\sigma)}$ to

measure the anisotropy of the whole condensate state, with definition

$$k_{i(\sigma)} = \frac{1}{\langle \hat{N} \rangle} \sum_{j_v} (\rho_{j_v}^2 k_i^{j_v}), \tag{2.73}$$

which is an intensive quantity. From Figure 2.3, one finds both $k_{1(\sigma)}$ and $k_{2(\sigma)}$ go to 1 as $|\phi|$ becomes larger, which is consistent with the fact that the universe becomes isotropic later.

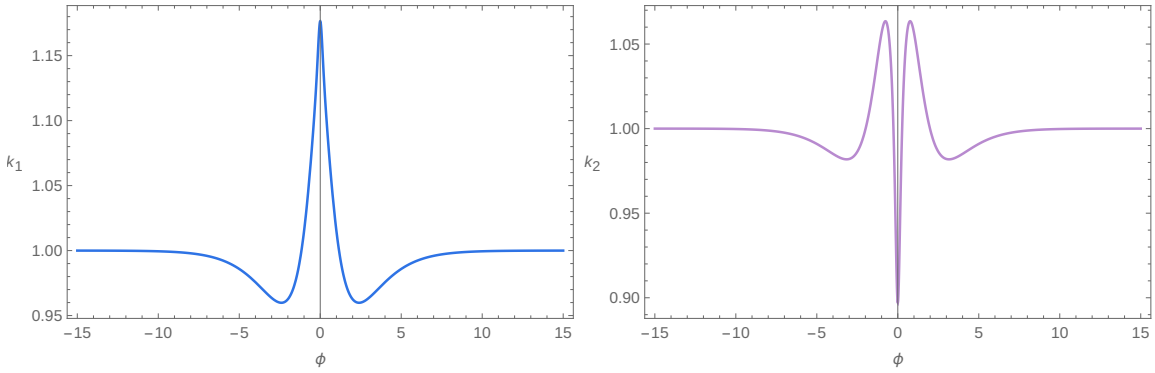

Figure 2.3: The behaviour of k_1 and k_2, where $\epsilon = 0.0001$ and $\pi_0 = 10000$.

The Misner's variables $\{\beta_+, \beta_-\}$ is calculated in a similar way, where

$$\beta_+^{j_v} = \frac{1}{6} \ln \left(\frac{8 j_a (j_a+1) \sqrt{\frac{j_a(j_a+1)+3j_b(j_b+1)-12j(j+1)}{j_a(j_a+1)-9j_b(j_b+1)}}}{12j(j+1) - j_a(j_a+1) - 3j_b(j_b+1)} \right), \tag{2.74}$$

$$\beta_-^{j_v} = \frac{1}{\sqrt{3}} \ln \left(\frac{j_a(j_a+1) + 3j_b(j_b+1) - 12j(j+1)}{j_a(j_a+1) - 9j_b(j_b+1)} \right), \tag{2.75}$$

in accordance with (2.58) and (2.59). Then let

$$\beta_\pm^J \equiv \frac{1}{\langle \hat{N} \rangle} \sum_{j_v} (\rho_{j_v}^2 \beta_\pm^{j_v}), \tag{2.76}$$

and one finds they becomes zero at late time, as is shown in Fig.2.4.

For the mean anisotropy parameter $\mathcal{A}$, one need to compute the volume as well. Here we simply substitute the area eigen-values into (2.64)

$$V_{j_v}^2 \simeq \ell_0^6 \frac{\sqrt{j_a(j_a+1)}\,(-j_a(j_a+1) - 3j_b(j_b+1) + 12j(j+1))}{\left(27\sqrt{3}\right) \sqrt{\frac{j_a(j_a+1)+3j_b(j_b+1)-12j(j+1)}{\mathfrak{A}^2-9j_b(j_b+1)}}}, \tag{2.77}$$

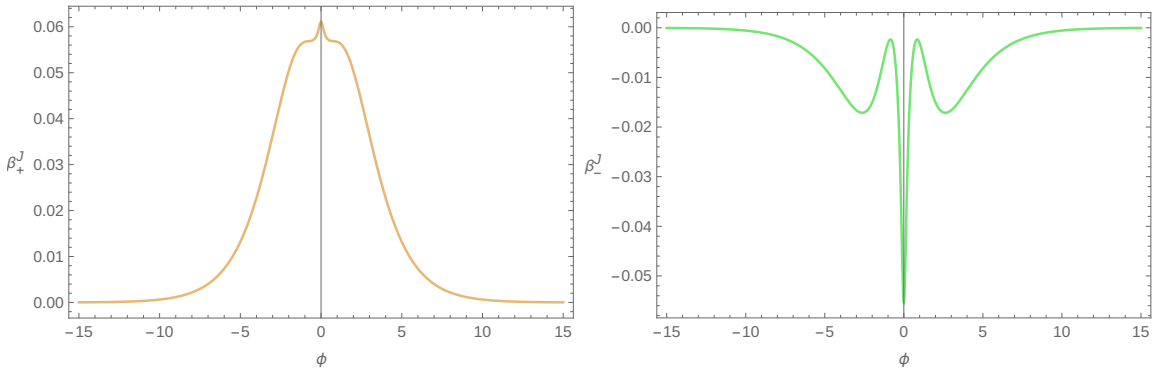

Figure 2.4: The behaviour of β_+ and β_- in accordance with the embedding in this paper, where $\epsilon = 0.0001$ and $\pi_0 = 10000$.

and use (2.51) to find the total volume. Then one can obtain $\mathcal{A}$ from volume, ratio k, and Misners's variables, substituting $k_{i(\sigma)}$ or $\beta_\pm^J$ into (2.62) or (2.63)

$$\mathcal{A}_1(\phi) \equiv \frac{18V^2\left((\beta_+^{J\prime})^2 + (\beta_-^{J\prime})^2\right)}{V'^2}, \tag{2.78}$$

$$\mathcal{A}_2(\phi) \equiv \frac{2V^2(k_{1(\sigma)}^2 k_{2(\sigma)}'^2 + k_{2(\sigma)}^2 k_{1(\sigma)}'^2 - k_{1(\sigma)}k_{2(\sigma)}k_{1(\sigma)}'k_{2(\sigma)}')}{V'^2 k_{1(\sigma)}^2 k_{2(\sigma)}^2}. \tag{2.79}$$

Both of them go to zero when $|\phi|$ increases, as is demonstrated in Figure 2.5. The calculations of these observables are consistent among each other, all showing that the anisotropy is relevant near bounce and isotropy is dominant at later time.

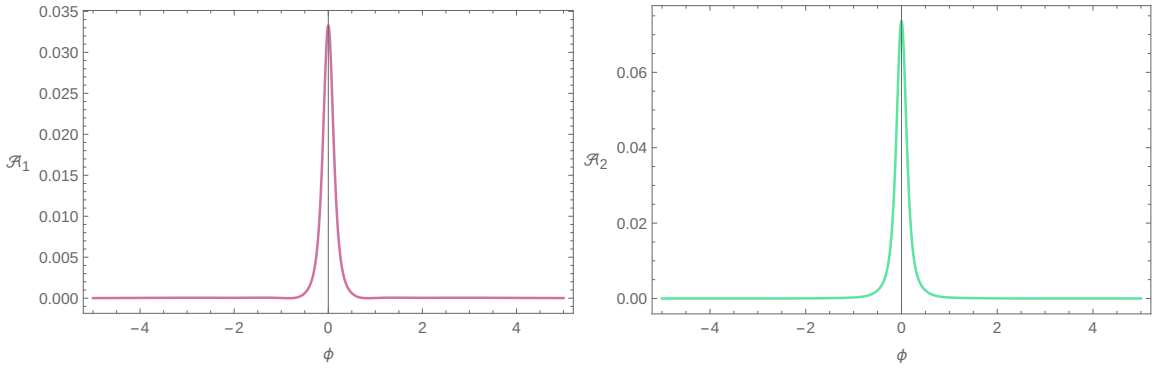

Figure 2.5: The behaviour of $\mathcal{A}_1$ and $\mathcal{A}_2$, where $\epsilon = 0.0001$ and $\pi_0 = 10000$.

2.4.4 Quantum Fluctuations

This subsection demonstrates the reliability of the computation with the application of coherent peaked states. By calculating the relative variances of the observables, the quantum

fluctuations from the clock field ϕ turns out to be very small at large number of tetrahedra.

The relative variance of an observable O is defined in a usual way:

$$\Delta_O^2 \equiv \frac{\langle \hat{O}^2 \rangle - \langle \hat{O} \rangle^2}{\langle \hat{O} \rangle^2}. \tag{2.80}$$

For number operator, one finds [141]

$$\Delta_N^2 = \frac{1}{\sum_{j_v} N_{j_v}} \simeq \frac{1}{\sum_{j_v} \rho_{j_v}^2}. \tag{2.81}$$

Since $\rho_{j_v}(\phi)$ grows exponentially for any mode j_v in the state, the relative variance of number operator definitely becomes negligible at late time, when the number of tetrahedra goes to infinity.

Similarly for volume operator, one has

$$\Delta_V^2 \simeq \frac{\sum_{j_v} V_{j_v}^2 \rho_{j_v}^2}{(\sum_{j_v} V_{j_v} \rho_{j_v}^2)^2}. \tag{2.82}$$

The relative variance of area operator takes the same form with that of the volume operator, except different eigen-values, so we do not repeat the result. No doubt, the relative variance of both volume operator and area operator goes to zero for large ϕ.

The main difficulty arises when one tries to find the relative variance of k_i, $\beta_\pm$, and $\mathcal{A}$. Unlike number operator, area operator, or volume operator, k_i, $\beta_\pm$, and $\mathcal{A}$ do not have GFT operators measuring their values straightforwardly. Instead, they are obtained as functions of area or volume expectation values. If one simply treats them as functions of areas, then the relative variance can be found through the formula of error propagation. However, this will result in a diverging number. On the other hand, suppose we have such operators who has eigenvalues k_i or $\beta_\pm$, then the fluctuations are similar with that of volume or area operator, converging as the number increases. Since we do not have exact operators, this issue is left open currently, and it is of interest that how can one construct a GFT operator measuring anisotropy.

2.5 Anisotropic Quantum Gravity Condensates II

2.5.1 Measurement of Anisotropy

Let us continue to the other definition of 'isotropy', where tri-rectangular tetrahedra are the building blocks of a three-dimensional space. Again, the embedding is performed, as illustrated in Figure 2.6. Edges AD, BD, and CD of the tetrahedron are orthogonal to each other, so it is convenient to require that they are parallel to $x-$, $y-$, and $z-$ axis

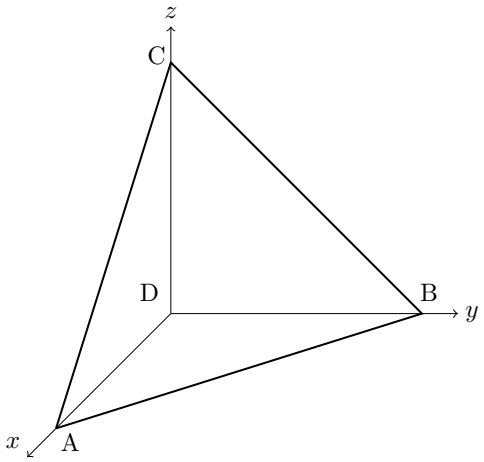

Figure 2.6: A tetrahedron in Bianchi I universe, where tri-rectangular tetrahedra are building blocks.

respectively. Assume $AD = BD = CD = l$, so they have the same physical length if the universe is isotropic. The physical areas of $\triangle ADB$ ($\mathfrak{A}$), $\triangle ACD$ ($\mathfrak{B}$), and $\triangle DCB$ ($\mathfrak{C}$) read

$$\mathfrak{A} = \frac{1}{2}a_1 a_2 l^2, \tag{2.83}$$

$$\mathfrak{B} = \frac{1}{2}a_1 a_3 l^2, \tag{2.84}$$

$$\mathfrak{C} = \frac{1}{2}a_2 a_3 l^2. \tag{2.85}$$

It is straightforward to define the ratio between scale factors

$$\mathfrak{k}_1 := \frac{a_1}{a_3} = \frac{\mathfrak{A}}{\mathfrak{C}}, \tag{2.86}$$

$$\mathfrak{k}_2 := \frac{a_1}{a_2} = \frac{\mathfrak{B}}{\mathfrak{C}}. \tag{2.87}$$

$$\tag{2.88}$$

Similarly, the Misner's variables $\beta_\pm$ can also be written in terms of the physical areas, where

$$\beta_+ = \frac{1}{6}\ln\left(\frac{\mathfrak{A}^2}{\mathfrak{B}\mathfrak{C}}\right), \tag{2.89}$$

$$\beta_- = \frac{1}{4\sqrt{3}}\ln\left(\frac{\mathfrak{B}^2}{\mathfrak{C}^2}\right). \tag{2.90}$$

In addition, the anisotropy parameter $\mathcal{A}$ is expressed in the same way as (2.62) and (2.63). Finally, the volume reads

$$V = \frac{\sqrt{2}}{3}(\mathfrak{A}\mathfrak{B}\mathfrak{C})^{\frac{1}{2}}. \tag{2.91}$$

Again, these relations only works with the embedding illustrated here, which is the simplest choice that we can make. But as argued, these quantities are not unique, and changing embedding is equivalent to changing a coordinate system, so one needs to keep the calculation consistent all the time with the embedding. In this case, only three orthogonal faces are needed to fix the shape of a tetrahedron, and we always demand that they determine the coordinates $\{x, y, z\}$ in the way explained above.

2.5.2 Anisotropic Perturbations

Let us choose $j_v = (1/2, 1/2, 1/2)$ to be the isotropic background mode. Given a SNW (j_a, j_b, j_c), we demand that j_a, j_b, and j_c dual to $\triangle ABD$, $\triangle ADC$, and $\triangle DBC$ separately.

With this definition, one has to less choice on the perturbations. For the perturbations discussed in the previous section, where one choose j to be a 'background spin' and vary j_a and j_b to get a perturbation (j, j, j_a, j_b). Here, however, one does not have such a 'background spin' which is fixed when performing perturbations, as no two triangles from the tetrahedron are necessarily congruent here. As a result, j_a, j_b, and j_c can be changed at the same time as a perturbation.

From (2.39), one knows that the order of spins does not affect the wave-function. Meanwhile, consider all possible permutations on (j_a, j_b, j_c) will result in an isotropic model, since the way we embed tetrahedra will make their contribution to anisotropy cancel each other. For instance, modes $(1/2, 1/2, 1)$ and $(1/2, 1, 1/2)$ are governed by the same wave-function, so they will have the same number of tetrahedra. One finds that $(1/2, 1/2, 1)$ contributes $\beta_- = -\log(8/3)/4\sqrt{3}$ and $(1/2, 1/2, 1)$ contributes $\beta_- = \log(8/3)/4\sqrt{3}$. As they are of the same number, the total contribution is 0, so consequently they together form a isotropic state. In order to avoid the situation where anisotropic modes yield an isotropic full state, we limit the perturbations such that $j_a \leq j_b \leq j_c$ to obtain an anisotropic model.

The condensate state is expected to be dominated by smallest-spin modes, which is the isotropic background as well. Therefore, everything remains almost the same with those the previous section, except that here we only sum over three spins [176]. Let us take $(1/2, 1/2, 1/2)$ to be the only background mode, and choose $3/2$ to be maximal possible spin, so $-M^2 - 45\eta/4 < 0$ while $-M^2 - 19\eta/2 > 0$. The oscillating solutions are ignored again. All possible modes are shown in Table 2.2, and we choose $\eta = 1$ and $M^2 = -10$.

background	perturbations
$\left(\frac{1}{2},\frac{1}{2},\frac{1}{2}\right)$	$\left(\frac{1}{2},\frac{1}{2},1\right)$
	$\left(\frac{1}{2},\frac{1}{2},\frac{3}{2}\right)$
	$\left(\frac{1}{2},1,1\right)$
	$\left(\frac{1}{2},\frac{3}{2},\frac{3}{2}\right)$
	$\left(\frac{1}{2},1,\frac{3}{2}\right)$
	$\left(1,1,\frac{3}{2}\right)$
	$\left(1,\frac{3}{2},\frac{3}{2}\right)$

Table 2.2: All possible modes of tri-rectangular tetrahedra labelled by three spins that do not oscillate.

2.5.3 Observables

All observables are defined in the same way. For a SNW (j_a, j_b, j_c), one defines

$$\beta_+^{j_v} = \frac{1}{6}\ln\left(\frac{j_a(j_a+1)}{\sqrt{j_b(j_b+1)j_c(j_c+1)}}\right), \tag{2.92}$$

$$\beta_-^{j_v} = \frac{1}{4\sqrt{3}}\ln\left(\frac{j_b(j_b+1)}{j_c(j_c+1)}\right), \tag{2.93}$$

and

$$\mathfrak{k}_1^{j_v} = \frac{\sqrt{j_a(j_a+1)}}{\sqrt{j_c(j_c+1)}}, \tag{2.94}$$

$$\mathfrak{k}_2^{j_v} = \frac{\sqrt{j_b(j_b+1)}}{\sqrt{j_c(j_c+1)}}. \tag{2.95}$$

Then one can define the observables over the condensates:

$$\mathfrak{k}_{i(\sigma)} = \frac{1}{\langle\hat{N}\rangle}\sum_{j_v}\rho_{j_v}^2\mathfrak{k}_i^{j_v}, \tag{2.96}$$

$$\beta_\pm^J = \frac{1}{\langle\hat{N}\rangle}\sum_{j_v}\rho_{j_v}^2\beta_\pm^{j_v}, \tag{2.97}$$

and $\mathcal{A}$ is defined in the same manner with (2.78) and (2.79).

Keeping all other parameters same with those in previous section, one obtains similar results with this new definition of 'isotropy'. Because SNWs with small spins are dominant at late time, the condensates become isotropic as ϕ grows, which is shown in Figures 2.7, 2.8, 2.9, and 2.10. As the quantum fluctuations have exactly the same qualitative behaviour as well, it is redundant to compute them again in and we simply skip the computation.

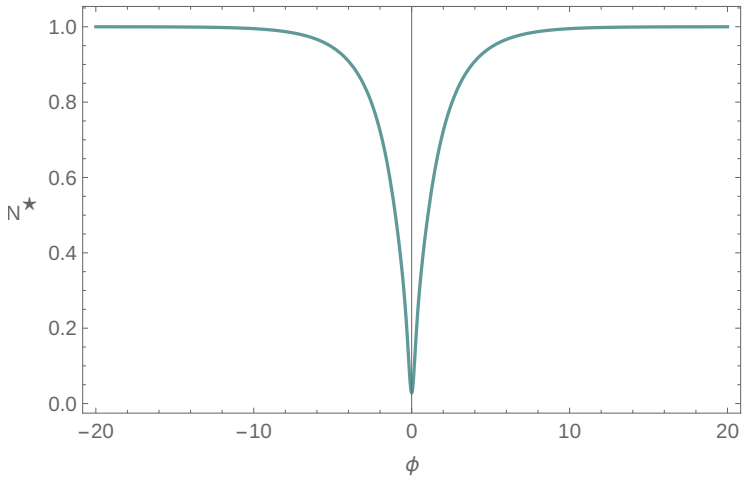

Figure 2.7: The behaviour of $N_\star$ when $\epsilon = 0.0001$ and $\pi_0 = 10000$.

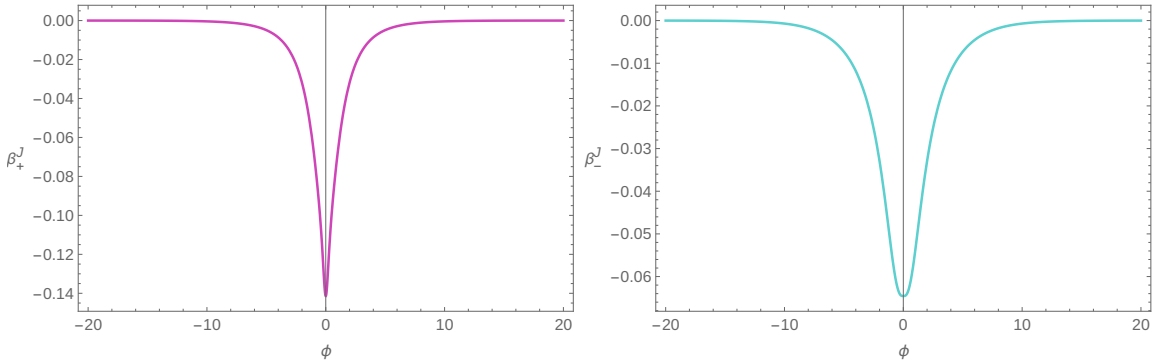

Figure 2.8: The behaviour of β_+ and β_- in accordance with the embedding in this paper, where $\epsilon = 0.0001$ and $\pi_0 = 10000$.

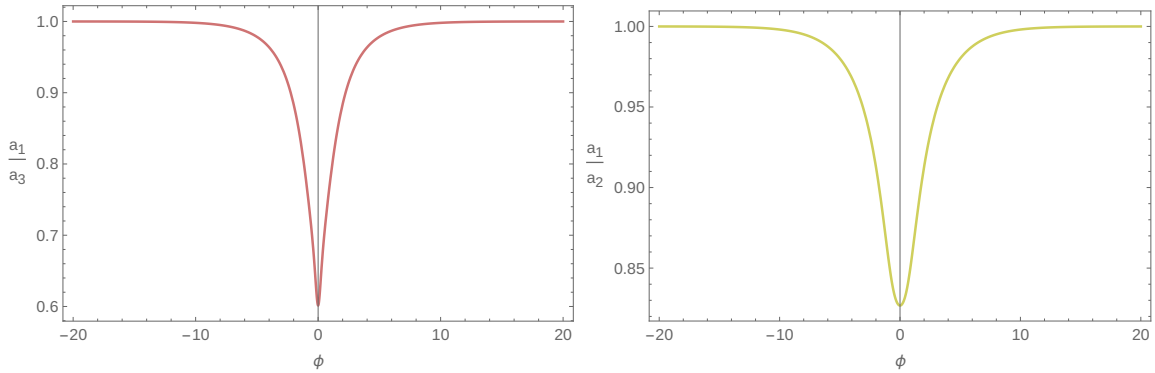

Figure 2.9: The behaviour of $\mathfrak{k}_1$ and $\mathfrak{k}_2$ in accordance with the embedding in this paper, where $\epsilon = 0.0001$ and $\pi_0 = 10000$.

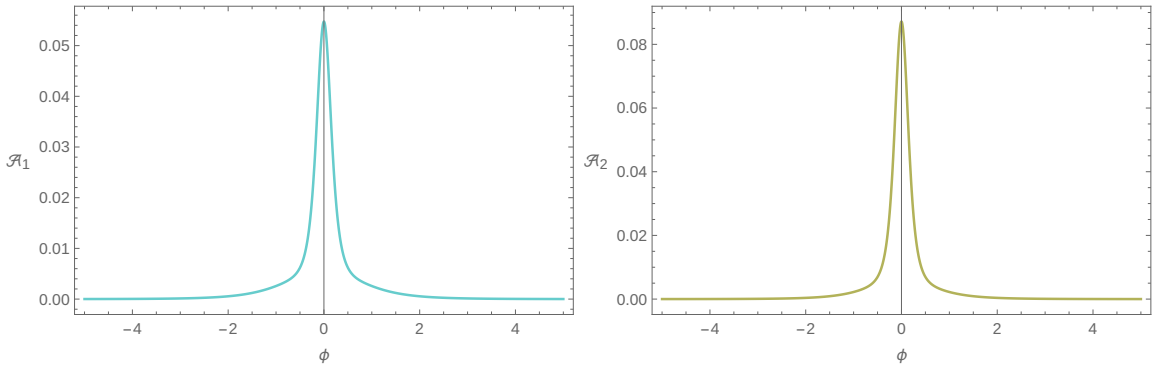

Figure 2.10: The behaviour of $\mathcal{A}_1$ and $\mathcal{A}_2$, where $\epsilon = 0.0001$ and $\pi_0 = 10000$.

2.6 Effective Dynamics

GFT condensate state has successfully extracted an effective Friedmann equation [136–138]. If one defines an isotropic GFT condensates from regular tetrahedra, and the expectation value of the volume operator at clock time ϕ over this state is $V(\phi)$, then $V(\phi)$ satisfies the equation [140, 195]:

$$\left(\frac{V'}{3V}\right)^2 = \frac{4\pi G_{eff}}{3}, \tag{2.98}$$

which is exactly the same form with an isotropic Friedmann equation where $\beta'_+ = \beta'_- = 0$ in (2.17).

The final part of the computation in this chapter is to extract the effective dynamics of GFT condensates and to compare it with that of a classical Bianchi I universe. We expect that our GFT effective equation have a similar form with (2.98) at later time since the state becomes isotropic, which has been illustrated in previous sections. At early stage, on the other hand, it is of our interest to find out if the effective equation looks similar with a classical Bianchi I equation (2.17), such that

$$\left(\frac{V'}{3V}\right)^2 = \left(\frac{\mathrm{d}\beta^J_+}{\mathrm{d}\phi}\right)^2 + \left(\frac{\mathrm{d}\beta^J_-}{\mathrm{d}\phi}\right)^2 + \frac{4\pi G_{eff}}{3}, \tag{2.99}$$

where G_{eff} is the effective GFT gravitational constant defined as

$$G_{eff} := \frac{1}{3\pi}\left(\frac{\rho'_{\frac{1}{2}}}{\rho_{\frac{1}{2}}}\right)^2. \tag{2.100}$$

As we use various quantities measuring anisotropy beside Misner's variables, we also expect the early effective dynamics of the volume satisfy

$$\left(\frac{V'}{3V}\right)^2 = \frac{\xi^2}{18} + \frac{4\pi G_{eff}}{3}, \tag{2.101}$$

where the shear

$$\xi^2 = \frac{2k'^2_{1(\sigma)}}{k^2_{1(\sigma)}} + \frac{2k'^2_{2(\sigma)}}{k^2_{2(\sigma)}} - \frac{2k'_{1(\sigma)}k'_{2(\sigma)}}{k_{1(\sigma)}k_{2(\sigma)}}, \tag{2.102}$$

and the expression of ξ^2 is the same for $\mathfrak{k}_i$ if one uses the second definition of 'isotropy'. Equation (2.99) and (2.101) are equivalent at classical level, but they are not necessarily the same for a quantum state as $\beta^J_\pm$ and $k_{i(\sigma)}$ are evaluated in different ways, so we consider two equations separately.

In both FLRW and Bianchi I space-time, V'/V is a constant. So the fact that $V'/V = const$ is not enough to figure out which kind of dynamics that a GFT state satisfy. One has to compute two terms on the right-hand side of equation (2.99) or (2.101) in order to find out how the introduction of anisotropy affects the effective GFT dynamics.

From Fig.2.11, one finds the isotropic background given by regular tetrahedra ($j_v = \{1/2\}, \{1\}, \{3/2\}$) dominates after $\phi \simeq 10$, as is shown by Figure 2.11. The situation is similar for tri-rectangular condensates according to Figure 2.7, where the universe becomes isotropic for $\phi \gtrsim 10$. In isotropic regime, the shear $(d\beta_+/d\phi)^2 + (d\beta_-/d\phi)^2$ or $\xi^2/18$ is negligible and

$$\left(\frac{V'}{3V}\right)^2 \simeq \frac{4\pi G_{eff}}{3}, \tag{2.103}$$

which means that GFT condensates reproduce FLRW dynamics effectively at late time.

It is interesting to investigate the period where anisotropy is relevant after bounce before $\phi \simeq 10$. According to Fig.2.12 and 2.13, one finds that in the regime $5 \lesssim \phi \lesssim 10$, even when anisotropy is ineligible, (2.17) is still well-satisfied, with very small contribution from anisotropic perturbations. This is result is similar with the result in a recent research on anisotropic GFT condensates [165], and it is true no matter how one defines 'isotropy' or 'anisotropy' in our case.

In a classical Bianchi space-time, when the spacial curvature is small or zero, the shear term decreases much faster than the matter term if the universe is expanding [156]. In our GFT model, we find a similar behaviour where the shear is almost negligible compared with two other terms. This may also imply that the correction from anisotropic modes is so small that one can still approximately apply isotropic homogeneous Friedmann equation in a deep Planckian regime.

In addition to the explanation above, there can be an opposite argument, that the anisotropy is not negligible, and an improvement of GFT model is needed in the future. For far, there are three main possible reasons why the GFT condensates in this chapter does not satisfy the classical anisotropic dynamics. One possibility is that the number of building blocks of GFT condensate state is too small to reproduce a continuum behaviour. As mentioned in Chapter 1, the emergence of continuum geometry and space-time requires

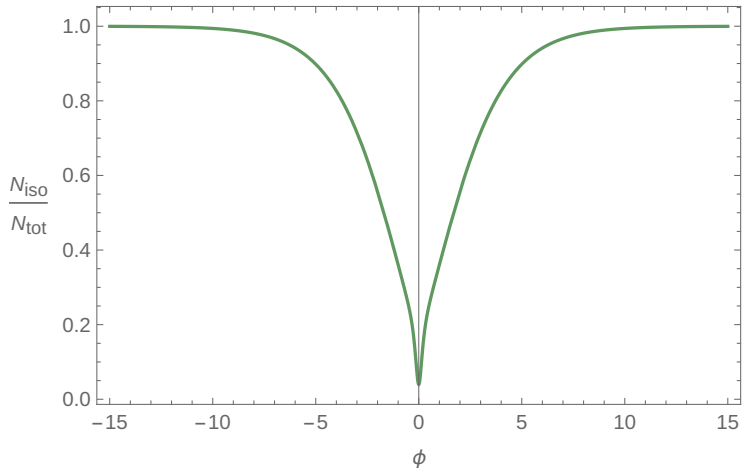

Figure 2.11: The ratio between the number of isotropic tetrahedra (N_{iso}) and that of total tetrahedra (N_{tot}), where $\epsilon = 0.0001$ and $\pi_0 = 10000$, and isotropy is represented by regular tetrahedra.

a large number of GFT quanta, which increases in the clock time. Therefore, the early state may not contain enough number of the tetrahedra and thus it fails to recover the Bianchi I dynamics.

Another possibility is that the number is large enough, but an improper definition of GFT observables measuring anisotropy yields corrections that are too small. For instance, (2.73) and (2.76) average over all tetrahedra, making the quantity almost a constant in clock time, so the derivative with respect to the clock ϕ will be relatively small comparing with V'/V. Same result can be found from the calculation, where the quantities measuring anisotropy in the same way as an average [165]. So far, such an average is inevitable, because $\beta_\pm$ or k_i is definitely an intensive quantity, while the number of tetrahedra (or the volume of a system) should not change their values and properties. Therefore, this may suggests that one needs a better way to characterise an anisotropic GFT state, or we may need a suitable operator measuring anisotropy directly instead of using functions of operators in this dissertation.

Finally, we may need a fundamentally different definition of anisotropic GFT condensates, instead of an approximate linear combination of different modes. If one studies each GFT mode alone, either 'isotropic' or 'anisotropic' modes will effectively yield Friedmann equation, since every single mode can be used as isotropic building block if they are not put together. For example, a regular mode $\{1/2\}$ can be perturbed into $\{1/2, 1/2, 1/2, 3/2\}$, which is called an 'anisotropic' perturbation. Then let us think about a question, what type of dynamics a state will yield if it only contains tetrahedra $\{1/2, 1/2, 1/2, 3/2\}$? At first sight, one may think it has an effective equation similar with Bianchi I universe (2.17), since it consists of only 'anisotropic' mode. However, if we are more careful, we will find

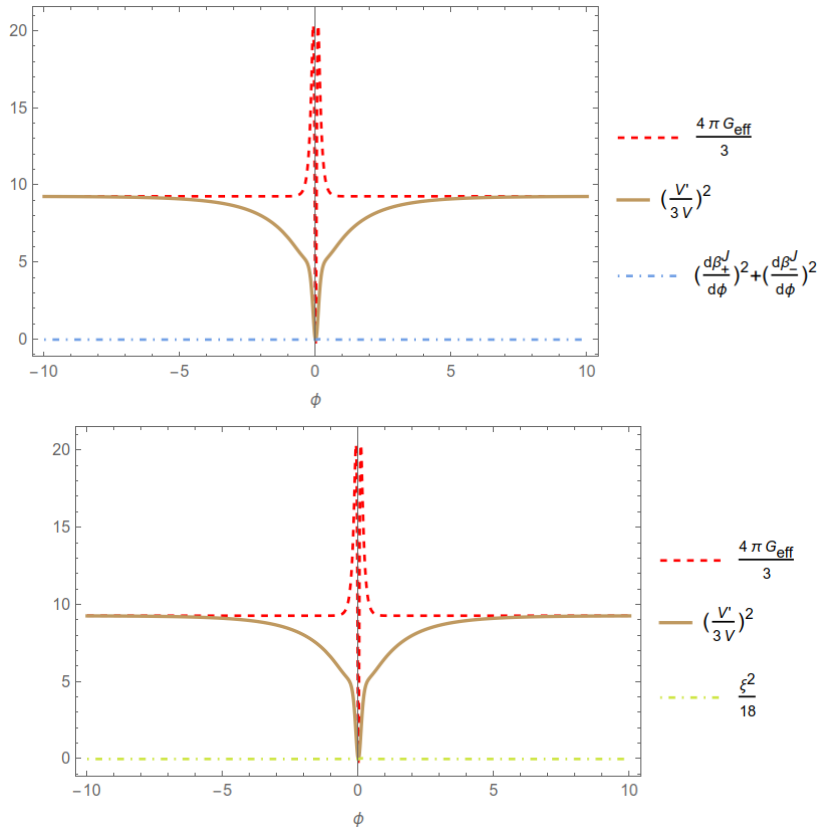

Figure 2.12: Effective dynamics of GFT condensates, where isotropic background consists of equilateral tetrahedra. The brown line represents $(V'/3V)^2$, and anisotropic part is shown by the blue or green dot-dashed line. The effective matter term $4\pi G_{eff}/3$ is illustrated by the red dashed line.

that this state also reproduce an isotropic Friedmann equation (2.98). Because β_+ and β_- are both constants over this state, though they are non-zero, this state still satisfy an isotropic equation of motion. Therefore, it is not surprising that Friedmann equation is reproduced when isotropic building blocks are not dominant.

2.7 Discussion

In this chapter, we tried using GFT quantum gravity condensates to build a model describing a homogeneous anisotropic universe. In this model, a bouncing universe with anisotropic 'perturbations' is constructed, and it evolves from an anisotropic state to an isotropic state as the clock time passes by.

Compared with previous study [164, 165], following improvements are made in this

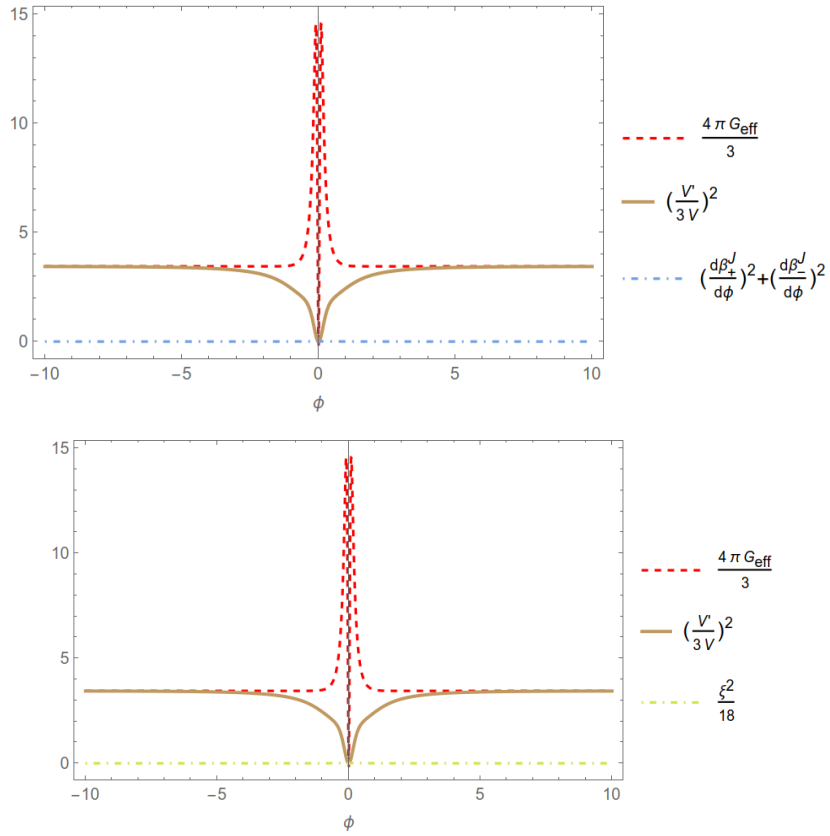

Figure 2.13: Effective dynamics of GFT condensates, where isotropy is defined as tri-rectangular tetrahedra with three edges of same length. The brown line represents $(V'/3V)^2$, and anisotropic part is shown by the blue or green dot-dashed line. The effective matter term $4\pi G_{eff}/3$ is illustrated by the red dashed line.

project:

i. Neither [164] nor [165] used the coherent peaked state, which is applied in our new model to control the quantum fluctuations;

ii. Neither [164] nor [165] took the low-spin dominance into consideration, but in our model, the parameters in kinetic kernel are chosen to ensure the low-spin dominance;

iii. The model in [164] has no classical correspondence, but the states in [165] and in this chapter aim to recover a Bianchi I universe;

iii. Compared with [165], where only a special Bianchi I universe with $\beta_- = 0$ is considered, our model considers a Bianchi I model where Misner's variables $\beta_\pm$ are both non-vanishing;

v. Compared with [165], which uses only β_+ to characterise the anisotropy, our state

uses $\beta_{\pm}$, shear term, as well as the anisotropy parameter as quantities to measure the anisotropy;

vi. Both states from [164] and [165] consist of a background isotropic mode and certain anisotropic mode(s), but our state is obtained by including all possible modes, with constraints on spins found as well.

This chapter focuses on the Bianchi I universe. To get deeper insight on early universe, it is helpful to study Bianchi IX model, where the curvature is non-zero. An significant feature of Bianchi IX universe is its mixmaster dynamics and chaotic behaviour near singularity. However, hitherto we are not able to construct such a state. One difficult task is adding curvatures in GFT condensates. On one hand, the dynamics studied in this paper ignored interactions $\mathcal{V}$ among SNWs, which result in a solution that yield flat Friedmann equation. It is possible that involving interactions gives us information on the curvature when the tetrahedra are connected. Unfortunately, this brings computational challenges and the equation cannot be solved exactly for the time being. On the other hand, one lacks GFT curvature operator to test the dynamics from condensates even we successfully construct such a state. Therefore, it is of our interest to improve the GFT quantum cosmological model to study the early universe as well as to explain present anomalies in the future.

Chapter 3

Quantum Schwarzschild Black Hole

This chapter is based on a project in collaboration with Daniele Oriti.

In this chapter, including both quantum geometric and scalar matter degrees of freedom, candidate GFT micro-states of a spherically symmetric geometry will be constructed in a material reference frame. The scalar fields realises the localisation of the various elements of quantum geometry. By computing geometric observables over the GFT quantum states, we will match the quantum states with a spherically symmetric classical geometry, with a suitable matter reference frame found as well.

3.1 Background

Spherically symmetric geometries, especially Schwarzschild black holes, play a special role in both classical and quantum gravity. For classical theories, they are an important simplified model for large massive objects and for the result of gravitational collapse. In quantum gravity, they are crucial for mainly three reasons. Firstly, any quantum gravity theory is called to provide a microscopic derivation of the black hole dynamics [196–200]. Second, the curvature singularity of black holes is expected to be resolved by quantum gravity theories; more generally, Planckian regime, which is reached in the last phase of black hole evaporation [198, 201], needs to be revealed by these theories. Third, Schwarzschild black hole represents a simple but highly non-trivial space-time geometries, which is only more complicated than the homogeneous geometries in cosmological backgrounds. Therefore, they are one of the first targets for reconstructing space-time from fundamental quantum gravity degrees of freedom.

We have reviewed in Chapter 1 the GFT formalism as well as quantum gravity condensates. This chapter will use GFT condensates to construct a candidate micro-state of a Schwarzschild black hole in a matter reference frame, which is a generalisation of the previous work [185, 186]. We will show how to find explicit solutions for scalar fields which act as a relational reference frame. In this reference system, expectation values of geometric

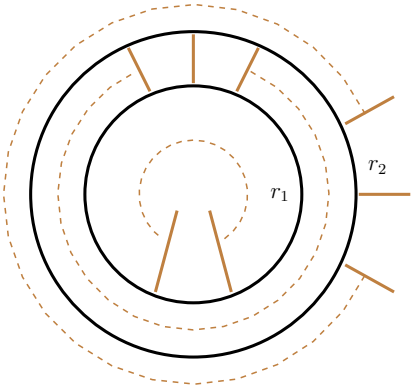

Figure 3.1: A foliation of a spherically symmetric space into concentric homogeneous shells. The outer boundary of shell r_1 and inner boundary on shell r_2 are glued.

observables will be computed, and we will obtain a GFT state which is able to reproduce continuum Schwarzschild geometry.

3.2 Spherically Symmetric GFT States

3.2.1 Seed State and Refinements

To begin with, let us first introduce the basic idea. The Schwarzschild geometry considered in this chapter is no longer homogeneous, but the quantum state can still be constructed from homogeneous GFT condensates. We consider a spherically symmetric $3D$ space foliated into thin concentric shells [185, 186], as is shown by Figure 3.1. Each shell is labelled by r_i, which can be understood as a radial parameter. The outer boundary of one shell r_1 is glued with the inner boundary of another shell r_2, and the full spatial foliation is obtained by repeating this procedure on every shell. In such a way, every single shell alone is homogeneous, and one can define every shell state through GFT condensate states.

The next step is to define the quantum states of these shells, endowed with a continuum and semi-classical homogeneous geometry [137, 184]. These states should have the following six features:

1. *Spherical topology*: the shell state are defined as a superposition of quantum states dual to spherically symmetric simplicial complexes with shell topology, and the states are obtained by increasing the number of 3-simplices (tetrahedra) from a 'seed state';

2. *Homogeneity*: GFT quanta assigned with the same quantum geometric information form a shell state, i.e. each building block is characterised by the same wave-function;

3. *Near-flatness*: the geometry inside the tetrahedra is nearly flat in order to have a better geometric interpretation in a continuum embedding, which, however, plays little role in this chapter;

4. *Continuum approximation*: the number of GFT building blocks consisting the shell will be infinitely large, and the combinatorial aspect of the continuum approximation will be considered as well;

5. *Reference frame peakedness*: matter d.o.f. from scalar fields will be included in these states, and the wave-function governing the GFT quanta is sharply peaked around given values of the scalar fields, with the scalar fields being good clock or rods;

6. *Semi-classicality*: the observables of shell states will match the ones in classical geometry with controllable quantum fluctuations.

The first four requirements have been met by the model from [186], and we will include the last two features in our generalised black hole state.

Then let us define a state with the features mentioned above. Each shell state corresponds to the triangulation of a spherical shell with two boundaries, so they have topology $S^2 \times [0,1]$. These state can be constructed from a *seed state* $|\tau\rangle$ by increasing the number of building blocks through *refinement operators* $\hat{\mathcal{M}}$. In order to control the connectivity, each tetrahedron (or each vertex in dual complex) is associated with a colour $t \in \{B(lack), W(hite)\}$.

The seed state is the simplest triangulation of a spherical shell, as illustrated by Figure 3.2, where every four-valent vertex corresponds to a tetrahedron. Links associated to a vertex is labelled by a colour labeled from 1 to 4, and only vertices with different colours can be connected together. A shell state consists of three parts: inner boundary, bulk, and outer boundary, where the bulk part has no open links. Similarly, only links with same colour can be glued. For instance, assume Figure 3.2 represents the shell r_1 in Figure 3.1, then the open links from inner boundary of shell r_2 must be of colour 1 in order to glue them with those from outer boundary of shell r_1. To distinguish three parts of a shell, let us introduce another label, $s \in \{+, 0, -\}$, representing outer boundary, bulk, and inner boundary respectively.

Given a seed state, one can define the refinement operator, which eliminates one vertex and adds three new ones without changing the spherical topology. Such a movement can be achieved by requiring that the new vertices are connected to form a melonic graph, or a 'dipole insertion' in the language of tensor models [90]. To control the connectivity of the

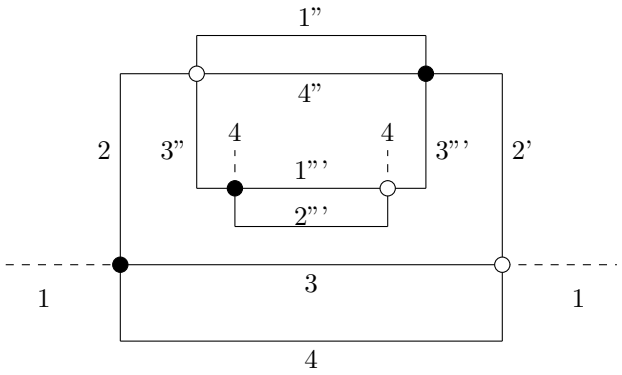

Figure 3.2: The seed state of a shell, consisting of three layers.

graph, each layer has its own refinements acting on the state independently. The action of a refinement on white vertices of a outer boundary $\hat{\mathcal{M}}_{W+}$ is graphically [184]

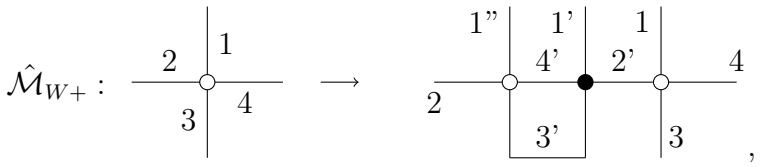

and for black vertices, it is

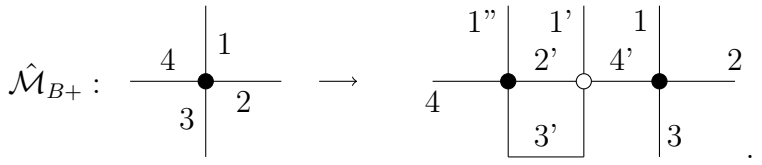

The ones for inner boundary is rather similar, where

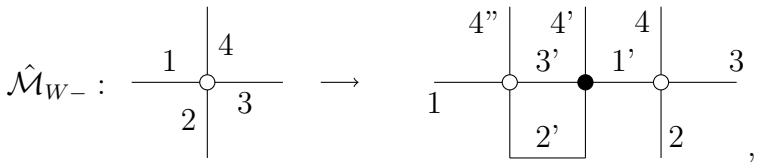

and

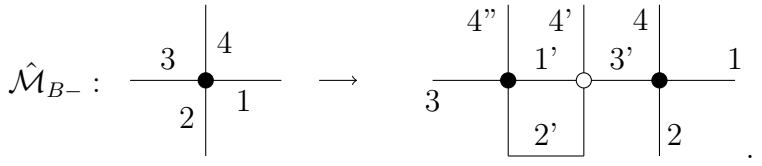

For the bulk, the refinements are

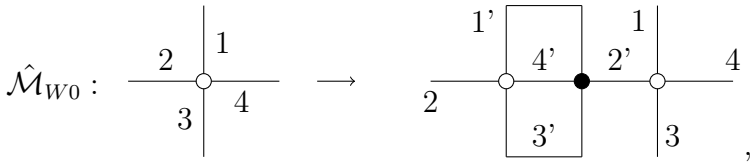

and

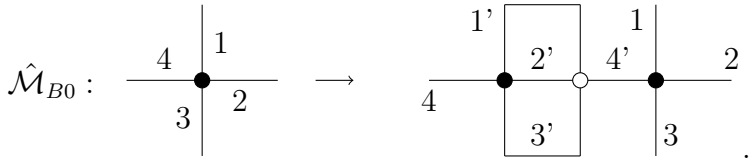

By repeating refinements, one increases the number of building blocks of a shell and obtains a continuum limit of the quantum state.

3.2.2 Ladder Operators

In addition to graphic definition, the seed state and the refinements can also be defined algebraically in terms of GFT condensate states. To this end, we first assume that our shell state is a superposition of quantum states, which correspond to the triangulations of a spherical shell. Moreover, the information of connectivity should be equipped to GFT condensates, since the seed state or the refinements are all represented by connected SNWs and only with connectivity can a state recover a continuum topology.

A black 4-valent vertex, dual to a tetrahedron, is created by $\hat{\varphi}^\dagger_B(g_1, g_2, g_3, g_4)$, where the colours of edges are assigned in a clockwise order. Similarly, a white vertex is created by $\hat{\varphi}^\dagger_W(g_1, g_2, g_3, g_4)$, while the labels are in an anti-clockwise order:

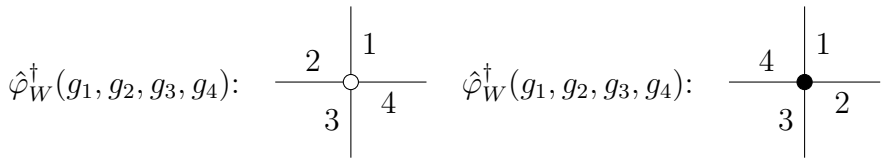

The group element on a links can be interpreted as the parallel transport from one tetrahedron to another. Suppose one link associated to vertex v is assigned with g_v, while a second link associated to vertex w has group element g_w. Connecting these two links, one should obtain another link with geometric information provided by $g_w^{-1} g_v$:

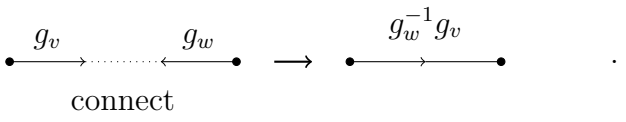

To do this, an auxiliary variable h_v is required, making sure that a connection can be achieved through convolution. For instance, the connection between two links above can be written as

$$\psi(g_v)\psi(g_w) \to \int \mathrm{d}h\psi(hg_v)\psi(hg_w), \tag{3.1}$$

resulting in a wave-function depending only on $g_w^{-1}g_v$, where ψ is a general wave-function assigned on the vertices.

Therefore, we can require that a shell state is created by ladder operators [184]

$$\hat{\sigma}_t(h_v) = \int \mathrm{d}g_v \overline{\sigma(h_v g_v)}\hat{\varphi}_t(g_v), \tag{3.2}$$

$$\hat{\sigma}_t^\dagger(h_v) = \int \mathrm{d}g_v \sigma(h_v g_v)\hat{\varphi}_t^\dagger(g_v), \tag{3.3}$$

annihilating or creating a superposition of tetrahedra of colour t, which is the new building block from now on, and h is associated to the endpoints of the links to be connected.

Remember that each shell is labelled by a radial parameter r, and we can encode this information into the GFT wave-function by coupling GFT state with a matter reference frame. Generally for $(3+1)$ dimensions, one needs a clock and three rods to localise a tetrahedron. For simplicity, here we again use four scalar fields to build a relational frame, $\{\phi_1, \phi_2, \phi_3, \phi_4\}$ with ϕ_1 the clock. Then the coherent peaked state introduced in Chapter 1 is applied again here to control the quantum fluctuations. An operator

$$\hat{\sigma}_t^\dagger(h_v; \{\phi_\tau, \phi_u, \phi_\theta, \phi_\chi\}) = \int \mathrm{d}g_v \mathrm{d}\phi_v \sigma_{\tau,u,\theta,\chi}(h_v g_v; \phi_v)\hat{\varphi}^\dagger(g_v; \phi_v), \tag{3.4}$$

with

$$\sigma_{\tau,u,\theta,\chi}(g;\phi) \equiv \eta_{\epsilon_1}(\phi_1 - \phi_\tau, \pi_\tau)\eta_{\epsilon_2}(\phi_2 - \phi_u, \pi_u)\eta_{\epsilon_3}(\phi_3 - \phi_\theta, \pi_\theta)\eta_{\epsilon_4}(\phi_4 - \phi_\chi, \pi_\chi)\varsigma(g;\phi), \tag{3.5}$$

creates a superposition of tetrahedra at $(\phi_0 = \phi_\tau, \phi_1 = \phi_u, \phi_2 = \phi_\theta, \phi_3 = \phi_\chi)$.

Such a state with four scalar fields is rather complicated. Fortunately, we expect this GFT state will yield Schwarzschild geometry, so the shell state should be static, which significantly simplify the construction. Being static, there should be no dependence on clock time. Additionally, as we deal with a shell as a whole, there is no need to localise every tetrahedra consisting the shell, and only one parameter r is enough to tell the difference among shells. As a result, we take ϕ_2 to be a 'radial' rod characterising the shells, and there is no dependence on neither ϕ_3 nor ϕ_4. From now on, we denote ϕ_2 by ϕ for convenience, and the ladder operators are simplified into

$$\hat{\sigma}_t^\dagger(h;\phi_u) \equiv \int \mathrm{d}g\mathrm{d}\phi \sigma_u(hg;\phi)\hat{\varphi}_t^\dagger(g;\phi), \tag{3.6}$$

$$\hat{\sigma}_t(h;\phi_u) \equiv \int \mathrm{d}g\mathrm{d}\phi \overline{\sigma_u(hg;\phi)}\hat{\varphi}_t(g;\phi), \tag{3.7}$$

where

$$\sigma_u(g;\phi) = \eta_\epsilon(\phi - \phi_u, \pi_u)\varsigma(g;\phi). \tag{3.8}$$

A shell u is the one whose bulk part is created by ladder operators peaking at $\phi = \phi_u$, with two boundaries having slightly different peaks:

$$\hat{\sigma}^\dagger_{u,t0}(h) \equiv \hat{\sigma}^\dagger_t(h;\phi_u), \tag{3.9}$$

$$\hat{\sigma}^\dagger_{u,t+}(h) \equiv \hat{\sigma}^\dagger_t(h;\phi_u + \delta\phi_u), \tag{3.10}$$

$$\hat{\sigma}^\dagger_{u,t-}(h) \equiv \hat{\sigma}^\dagger_t(h;\phi_u - \delta\phi_u), \tag{3.11}$$

where $\delta\phi_u \in \mathbb{R}$ is a small number.

In order that we can distinguish different layers s, or equivalently, states of different layers must be orthogonal, there should be a constraint on $\delta\phi_u$, i.e. it cannot be too small. According to the definition (1.42) and (1.43), what contributes to the states is a Gaußian function $\exp((\phi - \phi_u)^2/2\epsilon)$, as the other parts will be canceled or will be integrated away in calculation. As $\epsilon \ll 1$, the peaking function approximately perform a measurement at $\phi = \phi_a$. However, ϵ is small but finite, so the peaking function η actually counts the contribution from $\phi = \phi_u - 3\sqrt{\epsilon}$ to $\phi = \phi_u + 3\sqrt{\epsilon}$. A straightforward choice is to make peaks not to overlap with each other,

$$|\phi_{u_1} - \phi_{u_2}| \geq 6\sqrt{\epsilon}. \tag{3.12}$$

With condition (3.12), one obtains

$$[\hat{\sigma}(h;\phi_{u_1}), \hat{\sigma}^\dagger(h,\phi_{u_2})] \simeq 0. \tag{3.13}$$

Therefore, we always require $\delta\phi_u \geq 6\sqrt{\epsilon}$ in this chapter.

To further ensure the homogeneity of a shell state, ladder operators should obey Bosonic statistics. Let us work out the commutator in spin representation, which is more convenient than other representations. Again, Peter-Weyl decomposition on reduced wave-function ς is performed where

$$\varsigma(g_v,\phi_v) = \sum_{j,l_L,l_R} \iota^{j_1j_2j_3j_4l_L}_{m_1m_2m_3m_4} \iota^{j_1j_2j_3j_4l_R}_{n_1n_2n_3n_4} \varsigma^{j_1j_2j_3j_4l_Ll_R}(\phi_v) \prod_{i=1}^4 D^{j_i}_{m_in_i}(g_{v,i}), \tag{3.14}$$

where the intertwiner

$$\iota^{j_1j_2j_3j_4}_{m_1m_2m_3m_4} = \sum_{m,m'} C^{j_1j_2l}_{m_1m_2m} C^{j_3j_4l'}_{m_3m_4m'} C^{ll'0}_{mm'0} \tag{3.15}$$

is assigned on the vertex of a SNW to combine four links together, and $C^{jj_1j_2}_{mm_1m_2}$ the Clebsch-Gordon coefficient [115, 116]. We use the convention

$$\int \mathrm{d}g D^j_{mn}(g)\overline{D^{j'}_{m'n'}(g)} = \frac{1}{d_j}\delta_{mm'}\delta_{nn'}\delta_{jj'}, \tag{3.16}$$

where $d_j = 2j+1$, and normalise the intertwiners with n [184]

$$\sum_m \iota^{j_1 j_2 j_3 j_4 l}_{m_1 m_2 m_3 m_4} \iota^{j_1 j_2 j_3 j_4 l'}_{m_1 m_2 m_3 m_4} = \delta^{l,l'} n(j_1, j_2, j_3, j_4, l). \tag{3.17}$$

If one assumes

$$\varsigma^{j_1 j_2 j_3 j_4 l_L l_R}(\phi_u) = \delta_{l_L, l_R} \varsigma^{j_1 j_2 j_3 j_4 l_L}(\phi_u), \tag{3.18}$$

and

$$\varsigma^{j_1 j_2 j_3 j_4 l_R}(\phi_u) \overline{\varsigma^{j_1 j_2 j_3 j_4 l_R}(\phi_u)} = \frac{1}{\tilde{\varsigma}(\phi_u)} \frac{d_{j_1}^2 d_{j_2}^2 d_{j_3}^2 d_{j_4}^2}{n(j_1, j_2, j_3, j_4, l_R)}, \tag{3.19}$$

the commutator reads

$$[\hat{\sigma}_t(h_v; \phi_u), \hat{\sigma}^\dagger_{t'}(h_w; \phi_{u'})] = \delta_{u,u'} \delta_{t,t'} \frac{1}{\tilde{\varsigma}(\phi_u)} \int_{SU(2)} \mathrm{d}\gamma \prod_{i=1}^{4} \delta(\gamma h_{v_i} h_{w_i}^{-1}) \equiv \delta_{r,r'} \delta_{t,t'} \frac{1}{\tilde{\varsigma}(\phi_u)} \Delta_L(h_v, h_w). \tag{3.20}$$

The assumption (3.19) is necessary to obtain a Bosonic commutator (3.20), which provides the states with homogeneity. This commutator also agrees with the idea of space-time being quantum gravity quanta condensate [202, 203].

For simplicity, $\tilde{\varsigma}(\phi_u)$ is replaced by $\tilde{\varsigma}_{us}$, where

$$\tilde{\varsigma}_{u0} = \tilde{\varsigma}(\phi_u), \tag{3.21}$$

$$\tilde{\varsigma}_{u+} = \tilde{\varsigma}(\phi_u + \delta\phi_u), \tag{3.22}$$

$$\tilde{\varsigma}_{u-} = \tilde{\varsigma}(\phi_u - \delta\phi_u). \tag{3.23}$$

Then we can write the states in terms of these ladder operators. A seed state of u-shell is

$$\begin{aligned} |\tau_u\rangle \equiv & \int \mathrm{d}g^{10} \hat{\sigma}^\dagger_{u,B+}(e, g_2, g_3, g_4) \hat{\sigma}^\dagger_{u,W+}(e, g_2', g_3, g_4) \hat{\sigma}^\dagger_{u,B0}(g_1'', g_2', g_3''', g_4'') \\ & \hat{\sigma}^\dagger_{u,W0}(g_1'', g_2, g_3'', g_4'') \hat{\sigma}^\dagger_{u,B-}(g_1'''', g_2'''', g_3'', e) \hat{\sigma}^\dagger_{u,W-}(g_1'''', g_2'''', g_3''', e) \, |0\rangle \,, \end{aligned} \tag{3.24}$$

and the refinement operators reads

$$\begin{aligned} \hat{\mathcal{M}}_{u,W+} \equiv & \tilde{\varsigma}_{us}^2 \int \mathrm{d}k_2 \mathrm{d}k_3 \mathrm{d}k_4 \mathrm{d}h_{4'} \mathrm{d}h_{3'} \mathrm{d}h_{2'} \hat{\sigma}^\dagger_{u,W+}(e, k_2, h_{3'}, h_{4'}) \hat{\sigma}^\dagger_{u,B+}(e, h_{2'}, h_{3'}, h_{4'}) \\ & \hat{\sigma}^\dagger_{u,W+}(e, h_{2'}, k_3, k_4) \hat{\sigma}_{u,W+}(e, k_2, k_3, k_4), \end{aligned} \tag{3.25}$$

where we take the one acting on the white vertices at outer boundary for example. The expression for a generic shell state is

$$|\Psi_u\rangle = F(\hat{\mathcal{M}}_{u,Bs}, \hat{\mathcal{M}}_{u,Ws}) \, |\tau_u\rangle \,, \tag{3.26}$$

where F is a generic function. By taking large number of refinements such that the number of building blocks goes to infinity, this state can be interpreted as continuum geometry.

Since the number will be large enough, one can assume that each layer contains the same number of vertices, n white and n black.

In order to find the expectation values over GFT shell states, we need a more precise expression for (3.26). Let $|\Gamma_n\rangle$ be a general linear combination of $|\Psi_u\rangle$ with $6n$ vertices, obtained from the seed state through $(n-1)$ refinements on each layer:

$$\begin{aligned}|\Gamma_n(\phi_u)\rangle \equiv & \frac{1}{(n!)^3}\prod_{s=\{+,0,-\}}\tilde{\varsigma}_{us}^{n-1}\int\prod_{i=1}^{6n}\mathrm{d}h_i J_\Gamma(h_1,...,h_{6n})\hat{\sigma}^\dagger_{u,B+}(h_1)...\hat{\sigma}^\dagger_{u,W+}(h_{n+1})...\hat{\sigma}^\dagger_{u,B0}(h_{2n+1})\\ & ...\hat{\sigma}^\dagger_{u,W0}(h_{3n+1})...\hat{\sigma}^\dagger_{u,B-}(h_{4n+1})...\hat{\sigma}^\dagger_{u,W-}(h_{5n+1})...\hat{\sigma}^\dagger_{u,W-}(h_{6n})\,|0\rangle\,, \end{aligned} \tag{3.27}$$

where J_Γ are Dirac delta functions to connects the links in the graph and form the spherical-shell topology. Such a state is equipped with coarse grained microscopic degrees of freedom as well as only a few controllable variables. We do not normalise this state in order that the data contained in wave-function will not be erased away.

3.3 Operators and Expectation Values

3.3.1 Extended $(1+1)-$body Operators

To ensure the semi-classicality of GFT states, we will compute the geometric observables over the shell state and compare them with their classical correspondence. In this chapter, we consider the area and the volume of a shell, since they are all the GFT geometric observables available.

To continue, let us define the *extended* GFT operators. As illustrated in chapter 2, a generic GFT operator takes the form of (2.44):

$$\hat{\mathcal{O}}_t \equiv \int \mathrm{d}g_v\mathrm{d}g_w\mathrm{d}\phi_v\mathrm{d}\phi_w O(g_v,g_w;\phi_v,\phi_w)\hat{\varphi}^\dagger_t(g_v;\phi_v)\hat{\varphi}_t(g_w;\phi_w), \tag{3.28}$$

However, a shell contains three layers, so (3.28) is unable to distinguish these layers. For instance, one only needs to count the area of the outer boundary when computing the area of a shell, but (2.44) will compute the total area of three layers together, which makes no sense. Therefore, one should extend (3.28) to separately calculate the observables over three layers respectively. Such an extended version can be achieved by placing appropriate ladder operators $\hat{\sigma}_{ts}$ and $\hat{\sigma}^\dagger_{ts}$ in (3.28) [184]:

$$\hat{\mathbb{O}}_{u,ts} \equiv \int \mathrm{d}h_v\mathrm{d}h_w O_{us}(h_v,h_w)\hat{\sigma}^\dagger_{u,ts}(h_v)\hat{\sigma}_{u,ts}(h_w), \tag{3.29}$$

where

$$\begin{aligned}O_{us}(h,h') = & \tilde{\varsigma}^3_{us}\prod_{s'\neq s}\tilde{\varsigma}^2_{us'}\\ & \int \mathrm{d}g_v\mathrm{d}g_w\mathrm{d}\phi_v\mathrm{d}\phi_w\sigma_{u,s}(h_vg_v,\phi_v)O(g_v,g_w;\phi_v,\phi_w)\overline{\sigma_{u,s}(h_wg_w,\phi_w)}. \end{aligned} \tag{3.30}$$

In order that the extended operator will give a right result, we have applied the requirement that

$$\langle\tau_u|\,\hat{\mathbb{O}}_{u,ts}\,|\tau_u\rangle \sim \int \mathrm{d}h\mathrm{d}h'\,\langle 0|\,\hat{\sigma}_{u,ts}(h)\hat{\mathcal{O}}_t\hat{\sigma}^\dagger_{u,ts}(h')\,|0\rangle\,. \tag{3.31}$$

Before we continue, let us give a brief interpretation of the constraint (3.31). Note that there is no 'single-particle' state in this construction, and a seed state is the simplest case one can consider in our case. Requirement (3.31) means that the extended operator acting on a seed state will yield a similar result with (3.28) on a 'single-particle' state. Because of the connectivity on the left-hand side, two quantities in (3.31) should only differ by some Dirac delta functions.

The extended number operator in this chapter, which reads

$$\hat{n}_{u,ts} \equiv \tilde{\varsigma}^3_{us}\prod_{s'\neq s}\tilde{\varsigma}^2_{us'}\int \mathrm{d}h_v\hat{\sigma}^\dagger_{u,ts}(h_v)\hat{\sigma}_{u,ts}(h_v), \tag{3.32}$$

will count the number of tetrahedra condensates in a state. It can be verified that $\langle\Gamma_n(\phi_u)|\,\hat{n}_{u,ts}\,|\Gamma_n(\phi_u)\rangle = n$ as expected. Similarly, one can extend area operators and volume (density) operators, and compute their expectation value over a u-shell respectively.

3.3.2 Area and Volume

In spin representation, SNW states are the eigen-states of area operators as well as volume operator. So let us again move to spin representation to simplify the calculation.

In spin representation, the group creation operator $\hat{\varphi}^\dagger_t(g,\phi)$ is decomposed into

$$\hat{\varphi}^\dagger_t(g,\phi) = \sum_{j,m,n,l}\hat{\varphi}^{\dagger j_1j_2j_3j_4l}_{(t)m_1m_2m_3m_4}(\phi)\iota^{j_1j_2j_3j_4l}_{n_1n_2n_3n_4}\prod_{i=1}^4 D^{j_i}_{m_in_i}(g_i), \tag{3.33}$$

where the gauge invariance of $\hat{\varphi}$ is represented by the intertwiner. The field operators in spin basis satisfies

$$[\hat{\varphi}^{j_1j_2j_3j_4l}_{(t)m_1m_2m_3m_4}(\phi),\hat{\varphi}^{\dagger j'_1j'_2j'_3j'_4l'}_{(t')m'_1m'_2m'_3m'_4}(\phi')] = \delta_{t,t'}\delta_{j_i,j'_i}\delta_{m_i,m'_i}\delta_{l,l'}\delta^4(\phi-\phi'). \tag{3.34}$$

Then the condensate field operator reads

$$\begin{aligned}\hat{\sigma}^\dagger_t(h_I) &= \int \mathrm{d}g_I\mathrm{d}\phi\sum_{j,m,n,o,l_L,l_R}\sigma^{j_1j_2j_3j_4l_Ll_R}(\phi)\iota^{j_1j_2j_3j_4l_L}_{m_1m_2m_3m_4}\iota^{j_1j_2j_3j_4l_R}_{n_1n_2n_3n_4}\\ &\quad\prod_{I=1}^4 D_{m_Io_I}(h_I)D_{o_In_I}(g_I)\hat{\varphi}^\dagger_t(g_I,\phi)\\ &\equiv \sum_{j,m,o,l_L}\hat{\tilde{\sigma}}^{\dagger\ j_1j_2j_3j_4l_L}_{(t)o_1o_2o_3o_4}\iota^{j_1j_2j_3j_4l_L}_{m_1m_2m_3m_4}\prod_{I=1}^4 D^{j_I}_{m_Io_I}(h_I),\end{aligned} \tag{3.35}$$

where the wave-function assigned to the new operator is

$$\tilde{\sigma}^{j_1j_2j_3j_4l_L}_{(t)o_1o_2o_3o_4}(g_I,\phi) \equiv \langle g_t,\phi_t|\,\hat{\sigma}^{\dagger j_1j_2j_3j_4l_L}_{(t)o_1o_2o_3o_4}\,|0\rangle = \sum_{l_R}\sigma^{j_1j_2j_3j_4l_Ll_R}(\phi)\iota^{j_1j_2j_3j_4l_R}_{n_1n_2n_3n_4}\prod_{I=1}^{4}D^{j_I}_{o_In_I}(g_I). \quad (3.36)$$

The operator can be extended as

$$\hat{\tilde{\sigma}}^{\dagger j_1j_2j_3j_4l_L}_{(u,t)o_1o_2o_3o_4} = \sum_{l_R}\int \mathrm{d}g_I\mathrm{d}\phi\sigma^{j_1j_2j_3j_4l_Ll_R}_u(\phi)\iota^{j_1j_2j_3j_4l_R}_{n_1n_2n_3n_4}\prod_{I=1}^{4}D^{j_I}_{o_In_I}(g_I)\hat{\varphi}^\dagger(g_I,\phi), \quad (3.37)$$

peaked at $\phi=\phi_u$.

Let area operator count the area of the outer boundary with open links labelled 1 on $u-$shell, such that

$$\hat{\mathbb{A}}_1(\phi_u) = \sum_{t=W,B}\hat{\mathbb{A}}_{1,t+} \equiv \prod_{s=\{+,0,-\}}\tilde{\varsigma}^2_{us}\kappa\sum_{t=B,W}\int \mathrm{d}h^v_I\hat{\sigma}^\dagger_{r,t+}(h^v_I)\sqrt{E^i_1E^j_1\delta_{ij}}\rhd\hat{\sigma}_{r,t+}(h^v_I), \quad (3.38)$$

which is an extended version of the usual area operator (2.48). The expectation value of area operator (3.38) is

$$\begin{aligned}
&\langle\Gamma_n(\phi_u)|\,\hat{\mathbb{A}}_1(\phi_u)\,|\Gamma_n(\phi_u)\rangle\\
=&\sum_{t=\{B,W\}}\kappa\langle\hat{n}_{u,ts}\rangle\int \mathrm{d}g^v_I\mathrm{d}h^v_I\mathrm{d}\phi_v\sigma_{\phi_u+\delta\phi_u}(h^v_Ig^v_I;\phi_v)\sqrt{E^i_1E^j_1\delta_{ij}}\rhd\overline{\sigma_{\phi_u+\delta\phi_u}(h^v_Ig^v_I;\phi_v)}\\
\equiv&\sum_{t=\{B,W\}}\langle\hat{n}_{u,t+}\rangle a_{1,u+}, \quad (3.39)
\end{aligned}$$

where $a_{1,us}$ is the area for a single open link 1 on the boundary + of shell u, whose wave-function peaks at $\phi_u+\delta\phi_u$:

$$\begin{aligned}
a_{1,u+} &= \kappa\sum_{l_L,j,o}\int \mathrm{d}h\mathrm{d}\phi\tilde{\sigma}^{j_1j_2j_3j_4l_L}_{(u+)o_1o_2o_3o_4}(h,\phi)\sqrt{E^i_1E^j_1\delta_{i,j}}\rhd\overline{\tilde{\sigma}^{j_1j_2j_3j_4l_L}_{(u+)o_1o_2o_3o_4}(h;\phi)}\\
&\simeq \kappa\tilde{\varsigma}^{-1}_{u+}\sum_{l_L,j,o,n,n'}\int \mathrm{d}h\frac{d^2_{j_1}d^2_{j_2}d^2_{j_3}d^2_{j_4}}{n(j_1,j_2,j_3,j_4,l_L)}\\
&\quad \iota^{j_1j_2j_3j_4l_L}_{n_1n_2n_3n_4}\iota^{j_1j_2j_3j_4l_L}_{n'_1n'_2n'_3n'_4}\prod_{I=1}^{4}D^{j_I}_{o_In_I}(h)\overline{D^{j_I}_{o_In'_I}(h)}\sqrt{j_1(j_1+1)}\\
&= \kappa\tilde{\varsigma}(\phi_u+\delta\phi_u)^{-1}\sum_j d_{j_1}d_{j_2}d_{j_3}d_{j_4}\sqrt{j_1(j_1+1)}. \quad (3.40)
\end{aligned}$$

Though $\hat{\mathbb{A}}(\phi_u)$ acts on a shell labeled by u, it actually computes the area of a layer whose 'radial coordinate' is $\phi_u+\delta\phi_u$. So we have

$$\langle\mathbb{A}_{sphere}(\phi_u)\rangle \propto \tilde{\varsigma}^{-1}(\phi_u). \quad (3.41)$$

The expectation value of volume operator can be found in a similar vein. The extended volume density operator reads

$$\hat{\mathbb{V}}_{u,ts} = \int \mathrm{d}h_v \mathrm{d}h_w \hat{\sigma}^{\dagger}_{u,ts}(h_v) V(h_v, h_w) \hat{\sigma}_{u,ts}(h_w), \tag{3.42}$$

which results in

$$\begin{aligned} \langle \hat{\mathbb{V}}_{u,ts} \rangle &= \langle \hat{n}_{u,ts} \rangle \int \mathrm{d}h \mathrm{d}h' \mathrm{d}g \mathrm{d}g \mathrm{d}\phi \mathrm{d}\phi' \delta(h,h') \sigma_{us}(hg;\phi) V(g,g') \overline{\sigma_{us}(h'g';\phi')} \\ &\equiv \langle \hat{n}_{u,ts} \rangle \bar{V}_{(a)ts}(\phi_u). \end{aligned} \tag{3.43}$$

The spatial-volume of a shell reads

$$\langle V_3(\phi_u) \rangle = \sum_{t=\{B,W\}} \sum_{s=\{+,0,-\}} \langle \hat{n}_{u,ts} \rangle \bar{V}_{(a)ts}(\phi) \mathrm{d}\phi|_{\phi=\phi_u}, \tag{3.44}$$

where $\mathrm{d}\phi$ is the infinitesimal variation in field space [204]. Letting $V_{j_1 j_2 j_3 j_4}$ be the eigenvalue of a volume density operator acting on a SNW with links $\{j_1, j_2, j_3, j_4\}$, one finds the average volume is

$$\begin{aligned} \bar{V}_{(a)us} &= \sum_{j,j',m,m',l,l'} \int dh dh' d\phi_v d\phi_w \delta_{j,j'} \delta_{m,m'} V_{j_1 j_2 j_3 j_4} \\ &\quad \tilde{\sigma}^{j_1 j_2 j_3 j_4 l}_{(u,ts) m_1 m_2 m_3 m_4}(h, \phi_v)) \delta(l,l') \overline{\tilde{\sigma}^{j_1' j_2' j_3' j_4' l'}_{(u,ts) m_1' m_2' m_3' m_4'}(h;\phi_w)} \\ &= \sum_{j,m,l_R,l_R',n,n'} \int dh d\phi_w \delta(l_R, l_R') \sigma^{j_1 j_2 j_3 j_4 l_R}_{us}(\phi_w) \overline{\sigma^{j_1 j_2 j_3 j_4 l_R'}_{us}(\phi_w)} \\ &\quad \iota^{j_1 j_2 j_3 j_4 l_R}_{n_1 n_2 n_3 n_4} \iota^{j_1 j_2 j_3 j_4 l_R'}_{n_1' n_2' n_3' n_4'} \prod_{i=1}^{4} D^{j_i}_{m_i n_i}(h_i) \overline{D^{j_i}_{m_i n_i'}(h_i)} V_{j_1 j_2 j_3 j_4} \\ &\simeq \tilde{\varsigma}_{us}^{-1} \sum_j V_{j_1 j_2 j_3 j_4} d_{j_1} d_{j_2} d_{j_3} d_{j_4}. \end{aligned} \tag{3.45}$$

So we finally find the total effective volume of shell-u

$$\begin{aligned} \langle V_3(\phi_u) \rangle &\propto \tilde{\varsigma}(\phi)^{-1} \mathrm{d}\phi|_{\phi=\phi_u} + \tilde{\varsigma}(\phi)^{-1} \mathrm{d}\phi|_{\phi=\phi_u+\delta\phi_u} + \tilde{\varsigma}(\phi)^{-1} \mathrm{d}\phi|_{\phi=\phi_u-\delta\phi_u} \\ &\simeq 3\tilde{\varsigma}(\phi)^{-1} \mathrm{d}\phi|_{\phi=\phi_u}. \end{aligned} \tag{3.46}$$

Before we go to classical side and match these observables to find properties of wavefunction σ, let us take a quick investigation on the general properties of these shell states, where a horizon-like structure obeying the area law will be found.

3.4 Gluing States and Properties

The full space foliation is obtained by gluing the shells. One will find that coupling of matter d.o.f. does not change the properties such as entanglement structure, which are

the same with the state without scalar fields [186]. Since the process and the results are almost the same with that in [186], this section will simply give a brief summary.

A generic complete-foliation state reads

$$\left|\tilde{\Psi}\right\rangle = \prod_u |\Psi_u\rangle\,, \tag{3.47}$$

with a density matrix

$$\hat{\rho} = \left|\tilde{\Psi}\right\rangle\left\langle\tilde{\Psi}\right|. \tag{3.48}$$

To find the entanglement structure between shells, let us consider a graph A describing the outer boundary of a shell at ϕ_1, and a graph B for the inner boundary of a shell at ϕ_2. Both graphs have the same number n of vertices, so they could be glued properly. Then the wave-function of the glued graph $A\cup B$ is

$$\begin{aligned}
&\psi(g_I^{A_1},...,g_I^{A_n},g_I^{B_1},...,g_I^{B_n};\phi^{A_1},...\phi^{A_n},\phi^{B_1},...\phi^{B_n})\\
=&\prod_{i=1}^{n}\tilde{\sigma}^{j_1j_2j_3j_4l_R}_{A_im_1^im_2^im_3^im_4^i}(g_I^{A_i},\phi^{A_i})\tilde{\sigma}^{j_1j_2j_3j_4l_R}_{B_in_1^in_2^in_3^in_4^i}(g_I^{B_i},\phi^{B_i})\\
&\delta_{m_1^i,-n_1^{t_1^m(i)}}\prod_{J=2}^{4}\delta_{m_J^i,-m_J^{t_J^m(i)}}\delta_{n_J^i,-n_J^{t_J^n(i)}},
\end{aligned}\tag{3.49}$$

where $t_J^m(i)/t_J^n(i)$ represents the target vertex in graph A/B of edge J departing from vertex i, and δ's are used to keep track of the connectivity of graph $A\cup B$.

Integrating away the B part results in a reduced density matrix for part A

$$\begin{aligned}
&\rho_A^{(n)}(g_I^1,...,g_I^n,g'^1_I,...,g'^n_I;\phi^1,...\phi^n,\phi'^1,...,\phi'^n)\\
=&\left(\frac{\tilde{\varsigma}(\phi_1+\delta\phi_u)}{\prod_{I=1}^4 d_{j_I}}\right)^n\prod_{i=1}^{n}\tilde{\sigma}^{j_1j_2j_3j_4l_L}_{A_im_1^im_2^im_3^im_4^i}(g_I^i,\phi^i)\overline{\tilde{\sigma}^{j_1j_2j_3j_4l_L}_{A_im_1'^im_2'^im_3'^im_4'^i}(g'^i_I,\phi'^i)}\\
&\delta_{m_1^i,m'^i_1}\prod_{J=2}^{4}\delta_{m_J^i,-m_J^{t_J^m(i)}}\delta_{m'^i_J,-m'^{t_J^{m'}(i)}_J}.
\end{aligned}\tag{3.50}$$

This implies that no information about bulk degrees of freedom can be found from a reduced density matrix, so only the shells nearby will contribute to the entanglement entropy [186].

If A has combinatorial pattern α, then (3.50) has eigen-states

$$\Psi^n_{u,s}(\Gamma_\alpha)=\Psi_A^{(n)}(n_1,g,\phi)=\left(\frac{\tilde{\varsigma}(\phi_1+\delta\phi_u)}{\prod_{I=1}^4 d_{j_I}}\right)^{\frac{n}{2}}\prod_{I=1}^{n}\overline{\tilde{\sigma}^{j_1j_2j_3j_4l_L}_{A_in_1^in_2^in_3^in_4^i}(g_I^i,\phi^i)}\prod_{J=2}^{4}\delta_{n_J^i,-n_J^{t_J^n(i)}}, \tag{3.51}$$

which satisfies

$$\left\langle\Psi_A^{(n)}(n_1,g,\phi')\middle|\Psi_A^{(n)}(n_1',g,\phi)\right\rangle=\prod_{i=1}^{n}\delta_{n_1^i,n'^i_1}. \tag{3.52}$$

We find that

$$\begin{aligned}&\int\prod_{i=1}^{n}\mathrm{d}g^i\mathrm{d}\phi^i\rho_A^{(n)}(g_I^1,...,g_I^n,g'^1_I,...,g'^n_I;\phi^1,...\phi^n,\phi'^1,...,\phi'^n)\Psi_A^{(n)}(n_1,g,\phi)\\ =\;&\Psi_A^{(n)}(m_1,g',\phi').\end{aligned}\tag{3.53}$$

The orthogonality between states has been proved that [186]

$$\left\langle\Psi^n_{u,s}(\Gamma_\alpha)\middle|\Psi^n_{u,s}(\Gamma_{\alpha'})\right\rangle=\delta_{\alpha,\alpha'}\prod_{i=1}^{n}\delta_{n_1^i,n'^i_1},\tag{3.54}$$

which indicates

$$\rho^{(n)}_{u,s}(\Gamma_\alpha)\Psi^{(n)}_{u,s}(\Gamma_{\alpha'})=\begin{cases}\Psi^{(n)}_{u,s}(\Gamma_{\alpha'}) & \alpha=\alpha'\\ 0 & \alpha\neq\alpha'\end{cases}.\tag{3.55}$$

Computation above shows that the matter reference frame do not affect the entanglement structure of the states, and the reduced density matrix can be diagonalised. Therefore, the entropy of a shell can be obtained by counting the number of the states (or graphs), which is the same as the Boltzmann entropy [186].

Then we can identify a shell state as a black hole horizon by maximising its entropy. This strategy is supported by the argument that horizon entropy has an upper bound [205, 206], describing the dynamics in this purely kinematic model to a certain degree.

The entropy consists of two parts: one from combinatorial structure, and the other from geometric information. The combinatorial entropy is contributed from graphs Γ_α at fixed topology,

$$S_{comb}=-\sum_{\alpha=1}^{\mathfrak{N}}\omega_n(\Gamma_\alpha)\log[\omega_n(\Gamma_\alpha)],\tag{3.56}$$

and ω_n is the weight. Let $\mathfrak{N}$ be the total number of graphs with a given number of vertices (which is $2n$ in each layer). The most disordered configuration is the one that all weights are equal, i.e.

$$\omega_n^{max}(\Gamma)=\frac{1}{\mathfrak{N}}.\tag{3.57}$$

Thus,

$$S_{comb}^{max}=\log(\mathfrak{N}).\tag{3.58}$$

The number of distinct graphs obtained with $(n-1)$ refinement moves acting on l layers of the shell initial seed states is found to be

$$\mathfrak{N}=\left(\frac{(2n-2)!}{n!(n-1)!}\right)^l.\tag{3.59}$$

Scalar fields do not affect the combinatorial structure of the graphs, so $\mathfrak{N}$ here is exactly the same with that in case where only geometrical degrees of freedom are considered [186].

Taking n to be large and applying Stirling's formula

$$\log(n!) \simeq n\log(n) - n + \frac{1}{2}\log(2\pi n), \tag{3.60}$$

one obtains

$$S_{comb}^{max} \simeq 2ln\log(2) - \frac{3}{2}l\log(n). \tag{3.61}$$

This is the entropy from combinatorial degrees of freedom on the horizon.

The 'geometric' entropy relies on the degeneracy of the Hilbert space for a single vertex, whose macroscopic quantities are given by fixed values. Suppose a_H is the average area dual to the links on the horizon, and the degeneracy of the Hilbert space for a single vertex is $\Delta(a_H)$ for the fixed values of the macroscopic quantities. The total entropy of the horizon is

$$S(n, a_H) = \log(\mathfrak{N}\Delta(a_H)) = 2nl\log(2) + \log(\Delta(a)) - \frac{3l}{2}\log(n). \tag{3.62}$$

Assume the classical horizon area is of A_H. Consider a function [186] $\Sigma(n, a_H, \lambda)$, where

$$\Sigma(n, a_H, \lambda) = S(n, a_H) + \lambda(A_H - 2na_H), \tag{3.63}$$

and $\lambda \simeq 1/8\ell_P^2$ is a Lagrange multiplier that imposes the area constraint [186]. To maximise the entropy at large n, one requires

$$\frac{\partial\Sigma}{n} = 2l\log(2) - \frac{3l}{2n} - 2\lambda a_H \simeq 2l\log(2) - 2\lambda a_H = 0, \tag{3.64}$$

$$\frac{\partial\Sigma}{a_H} = \frac{\Delta'(a_H)}{\Delta(a_H)} - 2\lambda n = 0, \tag{3.65}$$

$$\frac{\partial\Sigma}{\lambda} = A_H - 2na_H = 0. \tag{3.66}$$

Then one obtains

$$a_H = \frac{l\log(2)}{\lambda}, \tag{3.67}$$

$$2na_H = A_H, \tag{3.68}$$

$$\Delta(a_H) = \exp(2\lambda a_H n) = \exp(\lambda A_H). \tag{3.69}$$

One also supposes that $a_H \sim \ell_P^2$, with ℓ_P the Planck length. Then the entropy reads

$$\begin{aligned} S(A_H) &\simeq 2nl\log(2) + \log(\Delta(a_H)) - \frac{3l}{2}\log\left(\frac{A_H}{l_P^2}\right) \\ &= 2a\lambda n + \lambda A_H - \frac{3l}{2}\log\left(\frac{A_H}{l_P^2}\right) \\ &= 2\lambda A_H - \frac{3l}{2}\log\left(\frac{A_H}{l_P^2}\right). \end{aligned} \tag{3.70}$$

Finally, one finds

$$S(A_H) \simeq \frac{A_H}{4\ell_P^2} - \frac{3l}{2}\log\left(\frac{A_H}{\ell_P^2}\right), \tag{3.71}$$

If the combinatorial structures of the three layers are the same, through entropy maximisation, one obtains

$$S(A_H) \simeq \frac{A_H}{4\ell_P} - \frac{3}{2}\log\left(\frac{A_H}{\ell_P^2}\right). \tag{3.72}$$

The logarithm correction is consistent with results in LQG [207–209]. Thus, if a horizon exists in this full state, its entropy will obey the area law.

3.5 Recovery of Schwarzschild Geometry

Both area and volume of quantum shell states are still abstract because wave-function σ is unknown. In this chapter, we only consider a GFT black hole candidate state at kinetic level, with no dynamics be of concern. Unlike Chapter 2, where we consider the dynamics and obtain the GFT wave-function by solving the Schwinger-Dyson equation, in this chapter, we will find the wave-function by matching the quantum expectation values with classical geometric observables. To do this, the key point here is to have the precise scalar fields.

3.5.1 Klein-Gordon Equation

The scalar fields are clocks and rods, so their existence cannot affect the original space-time too much. If we consider the precise black hole solution of a Schwarzschild space-time coupled with a scalar field, the main features of the black hole will be changed dramatically. Focusing on reproducing a Schwarzschild black hole, we will approximately solve equations of motion of the scalar fields in a Schwarzschild background:

$$ds^2 = -\left(1-\frac{2GM}{r}\right)\mathrm{d}t^2 + \left(1-\frac{2GM}{r}\right)^{-1}\mathrm{d}r^2 + r^2(\mathrm{d}\theta^2 + \sin^2(\theta)\mathrm{d}\chi^2). \tag{3.73}$$

So far, we only consider the model at kinetic level, and GFT model does not restrict the scalar fields with dynamics. As a result, there no reason to presume that these fields are massless ($\mathfrak{m} = 0$) or free ($V(\phi) = 0$). Thus, the only information one has is that the scalar fields satisfy the Klein-Gordon equations,

$$\nabla_\mu\nabla^\mu\phi_i - \mathfrak{m}_i^2\phi_i - V_i'(\phi_i) = 0, \tag{3.74}$$

with negligible energy-momentum tensors.

$$R_{\mu\nu} - \frac{1}{2}g_{\mu\nu}R = \frac{1}{2}\sum_{i=1}^{4}\left[\partial_\mu\phi_i\partial_\nu\phi_i - \frac{1}{2}g_{\mu\nu}\left((\partial\phi_i)^2 + \mathfrak{m}_i^2\phi_i^2 + 2V_i(\phi_i)\right)\right] \simeq 0. \tag{3.75}$$

Furthermore, depending on the role it plays, the field should also be monotonic in a temporal or a spatial direction.

The metric (3.73) can be rewritten in arbitrary coordinates, but the GFT foliation discussed in previous section has picked a preferred form of the metric facilitating the calculation, which reads

$$\mathrm{d}s^2 = -f_1(\tau,u)\mathrm{d}\tau^2 + f_2(\tau,u)\mathrm{d}u^2 + 2f_3(\tau,u)\mathrm{d}\tau\mathrm{d}u + r^2(\tau,u)\mathrm{d}\Omega^2, \tag{3.76}$$

where τ, u are arbitrary time-like and space-like coordinates. By requiring $f_1 > 0$ and $f_2 > 0$, the constant-τ hypersurface is space-like. The metric (3.76) foliates a space into nested spheres, compatible with what GFT has assumed. Then analytical solutions of scalar fields in (3.76) can be used to rewrite the spatial part of the Schwarzschild metric in a 'relational' manner, such that

$$\mathrm{d}h^2_{relational} \;=\; \frac{f_2[\tau(\phi_1),u(\phi_2)]}{\phi_2'(u)^2}\mathrm{d}\phi_2^2 + r(\phi_1,\phi_2)^2\mathrm{d}\Omega^2(\phi_3,\phi_4), \tag{3.77}$$

According to the relational metric (3.77), at a fixed clock time $\phi_1 = \phi_\tau$, the area and the volume of a sphere at $\phi_2 = \phi_u$ are

$$A_{rel}(\phi_u) = 4\pi r^2(\phi_\tau,\phi_u), \tag{3.78}$$

$$V_{3rel}(\phi_u) = 4\pi r^2(\phi_\tau,\phi_2)\frac{\sqrt{f_2[\phi_\tau,\phi_2]}}{\phi_2'(u)}\mathrm{d}\phi_2|_{\phi_2=\phi_u}. \tag{3.79}$$

By requiring that

$$A_{rel}(\phi_u) \propto \langle \mathbb{A}_{sphere}(\phi_u)\rangle_{GFT}, \tag{3.80}$$

and

$$V_{3rel}(\phi_u) \propto \langle V_3(\phi_u)\rangle_{GFT}, \tag{3.81}$$

one will find what wave-function σ should be assigned to GFT building blocks in order to reproduce the continuum Schwarzschild geometry.

With a few conditions put on the scalar fields, it seems to be impossible to find the precise solutions, but we will show how ambiguities are exhausted in the following analysis. In addition, the expectation values (3.41) and (3.46) are invariant under a scalar field redefinition such as choosing $\tilde{\phi}(\phi)$ as a new variable. So even redefining the fields, we will explore all possibilities.

First of all, we have shown that GFT construction has a preferred form of coordinates (3.76) that yields a spherical foliation. Next, we do not have to find all scalar fields, since ϕ_1 and ϕ_2 are sufficient to give relational description. It is not only because ϕ_3 and ϕ_4 will break the spherical symmetry, but also because it is meaningless to localise a point on a sphere if a sphere as a whole is the most basic quantity, which has been argued already. Thus one could leave them abstract and implicitly assume their energy-momentum density is negligible. However, unlike ϕ_3 and ϕ_4, an exact solution of ϕ_1 is necessary, even though there is no clock-dependence in GFT states, because a clock is essential to define an equal-time hypersurface. Therefore, we need to solve classical Klein-Gordon equations for ϕ_1 and ϕ_2.

From condition (3.80), one knows that the usual radial coordinate r should have no ϕ_1-dependence, or equivalently no τ-dependence. Without losing any generality, one can choose $u = r$, and the foliation (3.76) becomes

$$\mathrm{d}s^2 = -f_1(r)\mathrm{d}\tau^2 + f_2(r)\mathrm{d}r^2 + 2f_3(r)\mathrm{d}\tau dr + r^2\mathrm{d}\Omega^2. \tag{3.82}$$

Assume $\phi_1(\tau)$ has a potential $V(\phi_1)$ and a mass term $\mathfrak{m}_1$. Its Klein-Gordon equation reads

$$\begin{aligned} 0 &= \nabla_\mu\nabla^\mu\phi_1 - V'(\phi_1) - \mathfrak{m}_1^2\phi_1(\tau) \\ &= -\frac{f_2(r)}{f_1(r)f_2(r)+f_3(r)^2}\phi_1''(\tau) - V'(\phi_1) - \mathfrak{m}_1^2\phi_1(\tau) \\ &\quad -\frac{rf_2(r)f_3(r)f_1'(r) + f_1(r)\left(rf_3(r)f_2'(r) - 2f_2(r)\left(rf_3'(r)+2f_3(r)\right)\right) - 4f_3(r)^3}{2r\left(f_1(r)f_2(r)+f_3(r)^2\right)^2}\phi_1'(\tau). \end{aligned} \tag{3.83}$$

Since $f_2(r) > 0$, the first term on the right-hand side is non-zero unless $\phi_1''(\tau) = 0$, which is not allowed since ϕ_1 must be monotonic in τ. So this term is non-vanishing. Meanwhile, ϕ_1 and $V(\phi_1)$ have no r-dependence while other terms contain r, so the contribution from potential and mass should be zero in order that the equation makes sense. For the same reason, the remaining terms containing r needs to be canceled. An option is that the last term equals zero for any $r \in \mathbb{R}^+$, which results in a solvable equation. The equation

$$rf_2(r)f_3(r)f_1'(r) + f_1(r)\left(rf_3(r)f_2'(r) - 2f_2(r)\left(rf_3'(r)+2f_3(r)\right)\right) - 4f_3(r)^3 = 0 \tag{3.84}$$

has the following solutions

$$f_3(r) = 0, \tag{3.85}$$

$$f_3(r) = \frac{\sqrt{f_1(r)f_2(r)}}{\sqrt{-1+C_1r^4}}, \tag{3.86}$$

$$f_3(r) = -\frac{\sqrt{f_1(r)f_2(r)}}{\sqrt{-1+C_1r^4}}, \tag{3.87}$$

where C_1 is a constant. Both ϕ_1 and ϕ_2 must be real, so the last two solutions, yielding a solution ϕ_1 with non-vanishing imaginary part, are ruled out. When $f_3 = 0$, one obtains

a Schwarzschild metric in usual spherical coordinates (3.73) if $\tau = t$. The Klein-Gordon equation of $\phi_1(t)$ reads

$$\phi_1''(t) = 0, \tag{3.88}$$

whose solution is

$$\phi_1(t) = \beta_1 t, \tag{3.89}$$

where $\beta_1^2 \ll 1$ so the energy-momentum tensor $T_{tt} \simeq 0$.

To find ϕ_1, one first notes that conditions (3.80) and (3.81) together imply

$$\frac{\mathrm{d}\phi_2(r)}{\mathrm{d}r} = \frac{\beta_2}{\sqrt{f(r)}}, \tag{3.90}$$

where

$$f(r) = 1 - \frac{2GM}{r}, \tag{3.91}$$

with β_2 an arbitrary constant. It is immediate to obtain

$$\phi_2(r) = \beta_2 r\sqrt{1 - \frac{2GM}{r}} + 2\beta_1 GM\mathrm{arctanh}\left(\sqrt{1 - \frac{2M}{r}}\right), \tag{3.92}$$

for positive mass M with $r > 2GM$. Then let us find its mass or potential. Absorbing the mass term in potential term $V(\phi_2)$, one has

$$\nabla_\mu \nabla^\mu \phi - V'(\phi) = 0. \tag{3.93}$$

Substituting the solution into this equation yields

$$\beta_2 \frac{2r - 3GM}{r^2\sqrt{f(r)}} = V'(\phi_2). \tag{3.94}$$

The inverse $r(\phi_2)$ tells how area and volume of a thin shell depend on ϕ_2. Though the inverse cannot be expressed analytically for the time being, we can find it at different limits separately. First is the asymptotic infinity $r \to \infty$. In this region, $V'(\phi_2) \simeq 0$, and the simplest choice is that $V(\phi_2) = 0$. Then for the rod, we have $\phi_2'(r) \simeq 0$, and

$$\phi_2(r) \simeq \beta_2 r. \tag{3.95}$$

Therefore, $\phi_2 \to \infty$ corresponds the asymptotic infinity. In the near-horizon regime, one finds $f(r) \simeq r/2M - 1$, and

$$\frac{\mathrm{d}\phi_2(r)}{\mathrm{d}r} \simeq \frac{\beta_2}{\sqrt{\frac{r}{2GM} - 1}}. \tag{3.96}$$

Therefore,

$$\phi_2(r) \simeq 4\beta_1 GM\sqrt{\frac{r}{2M} - 1}, \tag{3.97}$$

and $\phi_2 \simeq 0$ at the event horizon. Its inverse reads

$$r = \frac{\phi_2^2}{8\beta_2^2 GM} + 2GM. \tag{3.98}$$

Consequently,

$$V'(\phi_2) \simeq \frac{\beta_2^2}{\phi_2}, \tag{3.99}$$

so

$$V(\phi_2) \simeq \beta_2^2 \ln(\phi_2). \tag{3.100}$$

It can be checked that ϕ_1 and ϕ_2 are good clock and rod. As $\phi_1 = \beta_1 t$, there is a one-to-one correspondence between ϕ_1 and t. For ϕ_2, $\phi_2'(r) \propto 1/\sqrt{f(r)}$, and it is always true that $f(r) > 0$. So ϕ_2 is a monotonic function of r.

We have shown that, starting at kinematical trial states, all ambiguities on scalar field dynamics are eventually removed, and the precise scalar fields are obtained.

3.5.2 Macroscopic GFT Wave-function

It is straightforward to find the relational observables and match them with quantum expectation values, and the GFT wave-function σ will be fixed. The relational spatial metric reads

$$\mathrm{d}h^2_{\mathrm{rel}} = \frac{1}{\beta_2^2}\mathrm{d}\phi_1^2 + r^2(\phi_2)\mathrm{d}\Omega^2. \tag{3.101}$$

At asymptotic infinity, $\phi_2 \to \infty$, a sphere at $\phi_2 = \phi_u$ has the area and the 3-volume

$$A_{rel}(\phi_u) = 4\pi \left(\frac{\phi_u}{\beta_2}\right)^2, \tag{3.102}$$

$$V_{3rel}(\phi_u) = \frac{4\pi}{\beta_2}\left(\frac{\phi_2}{\beta_2}\right)^2 \mathrm{d}\phi_2|_{\phi_2=\phi_u}. \tag{3.103}$$

In near-horizon regime when $M > 0$,

$$A_{rel}(\phi_u) = 4\pi \left(\frac{\phi_u^2}{8\beta_2^2 GM} + 2GM\right)^2, \tag{3.104}$$

$$V_{3rel}(\phi_u) = \frac{4\pi}{\beta_1}\left(\frac{\phi_2^2}{8\beta_2^2 GM} + 2GM\right)^2 \mathrm{d}\phi_2|_{\phi_2=\phi_u}. \tag{3.105}$$

To summarise, the GFT wave-functions should have such properties in order to build micro-states of spherically symmetric geometries:

$$\text{Schwarzschild} \begin{cases} \text{Asymptotic infinity}(\phi \to \infty) & \tilde{\varsigma}(\phi)^{-1} \propto \phi^2 \\ \text{Near-horizon}(\phi \sim 0) & \tilde{\varsigma}(\phi)^{-1} \propto (\phi^2 + 16\beta_1^2(GM)^2)^2 \\ \text{Near-singularity} & \text{Not available} \end{cases}. \tag{3.106}$$

Because $\phi(r)$ ends at $r = 2GM$, the rod cannot pass the horizon. As a result, no wave-function corresponds to the near-singularity behaviour is available.

3.6 Discussion

In this chapter, we construct a candidate quantum state of spherically symmetric black hole in a matter reference frame at kinetic level. With SNW connectivity and a proper wave-function assigned to GFT building blocks, these states can reproduce the continuum Schwarzschild geometries.

Admittedly, some limitations exist. The first one is that scalar field as a rod cannot extend into the horizon, which also occurs in a previous paper [210]. Neither GFT model can describe both interior and exterior Schwarzschild regions. In our case, real solutions of Klein-Gordon equations can only be found for scalar fields monotonic in usual spherical coordinates $\{t, r, \theta, \chi\}$ separately. When crossing the horizon, r is no longer space-like and it becomes a temporal coordinate, so $\phi_2(r)$ is no longer a rod inside the horizon. Such a limitation suggests a possible improvement in the future. An important set-up in our model is that the condensates are labeled by the value of ϕ_2, which is assumed to be a 'radial parameter'. A 'radial coordinate' will inevitably encounter a coordinate singularity on event horizon $r = 2GM$. Therefore, the construction is more likely to reach inside if the scalar fields behave like Kruskal-Szekeres coordinates. It is hopeful to find a suitable choice in future the by generalising the states further and labeling each shell with appropriate parameters. Another limitation is that dynamics has not been included in this model, and it is assumed implicitly the states satisfy the microscopic quantum dynamics. Finally, we did not calculate curvatures, which is of great importance when investigating black holes and resolving the curvature singularity. However, the absence of curvature operator has been a problem for long, and it is beyond the scope of this dissertation.

A similar research on GFT black hole as quantum gravity condensate coupled with scalar fields has been conducted previously [210], where the wave-function were found by matching the observables as well. The wave-functions and the scalar fields in our paper are different from those in [210], because these two models are fundamentally different. The model in this dissertation benefits from several improvements. First, the connectivity is introduced to the graph, whilst the previous work simply considers the disconnected tetrahedra. As mentioned, only with connected states can one recover the continuum topological structure, so the model in this chapter is physically more rigorous. Next, the coherent peaked state is applied in our model, which makes quantum fluctuations controllable. Moreover, our result could match all available geometrical quantities, but only the volume is considered in [210]. Additionally, the scalar fields in our model do not necessarily satisfy the harmonic gauge ($\Box\phi = 0$) applied in previous papers. Instead, mass and potential terms are included to make the fields as general as possible, which leads to different

solutions for Klein-Gordon equations. Lastly, our state can reproduce the area law with the same corrections with those from LQG.

Despite the limitations, which are not really problems at early stage, our model has made a great progress. The results suggests that we are working on a correct direction, and it is our interest to improve the model and generalise it to various black holes in the future.

Chapter 4

Amit-Roginsky Model from Boulatov Model

This chapter is based on a project in collaboration with Victor Nador, Daniele Oriti, Xian-Kai Pang, and Adrian Tanasa.

In this chapter, an Amit-Roginsky-like model will be obtained as a perturbation around the $3D$ Boulatov GFT in a matter reference frame, which consists of three scalar fields. The explicit conditions on the classical solutions of Boulatov model as well as the perturbations will be studied, in order to recover an Amit-Roginsky-like effective action. This work explores the possibility of combining an interesting matter theory with melonic dominance and a $3D$ GFT.

4.1 Background

The role of matter in quantum gravity, however, is not limited to a relational reference frame. Let us first forget the relational matter reference system, and take a closer look at the GFT action (1.20). As introduced, containing of geometric d.o.f., this is a quantum theory of space-time. In addition to gravity, there are various types of matter in our real world. So as a candidate for quantum gravity, GFT should be able to describe the interaction between the matter and the gravity. Furthermore, the construction of quantum gravity needs guidance from experiments. The inclusion of matter within GFT is a promising way towards the quantum gravity phenomenology [211], which is possible to provide observational test on a theory.

The coupling of matter fields in GFT has been studied for a long time [133, 134, 212]. Beside the direct coupling, the scalar matter can be introduced to $3D$ GFT as a particular phase of geometry [213], which a simpler method. The strategy starts from a GFT action S_{GFT}, and finds its classical solution φ_f. After doing a perturbation φ around the solution, one obtains a field $\varphi_f + \varphi$. Finally, substituting the perturbed field into S_{GFT} yields an

effective action S_{eff}

$$S_{\text{eff}} = S_{\text{GFT}}(\varphi_f + \varphi) - S_{\text{GFT}}(\varphi_f), \tag{4.1}$$

and this effective action turns out to be the one describing the dynamics of a scalar field.

In this chapter, we will continue with a GFT coupled with scalar fields as physical reference frame. Starting from the GFT action and its classical solution, we will follow the work done in [213] and show how an effective Amit-Roginsky-like matter field emerges as a perturbation over the geometry.

4.2 Boulatov Model

The first quantum gravity model is the Ponzano-Regge quantisation of a (2+1)-dimensional Euclidean gravity [214], which belongs to the sum-over-histories quantum gravity programme and can be viewed as a SF model. As mentioned in Chapter 1, GFT has a correspondence with SF, and the dual GFT of Ponzano-Regge theory is the Boulatov model [106], whose dynamical object is a field $T(g_1, g_2, g_3) : G^3 \to \mathbb{C}$, where $G = SU(2)$ for Riemannian quantum gravity in Euclidean signature.

The field $T(g_1, g_2, g_3)$ satisfies the reality condition [213]

$$T(g_1, g_2, g_3) = \bar{T}(g_3, g_2, g_1), \tag{4.2}$$

as well as the right gauge invariance

$$T(g_1 h, g_2 h, g_3 h) = T(g_1, g_2, g_3) \quad \forall h \in SU(2). \tag{4.3}$$

The dynamics of field T is governed by the action

$$\begin{aligned} S = &\frac{\mu^2}{2} \int \mathrm{d}g_1 \mathrm{d}g_2 \mathrm{d}g_3 T(g_1, g_2, g_3) \bar{T}(g_1, g_2, g_3) \\ &- \frac{\lambda}{4!} \int \prod_{i=1}^{6} \mathrm{d}g_i T(g_1, g_2, g_3) T(g_3, g_5, g_4) T(g_4, g_2, g_6) T(g_6, g_5, g_1), \end{aligned} \tag{4.4}$$

where μ is the 'mass', and λ is a coupling constant. Thus, the action (4.4) yields the equation of motion

$$\mu^2 T(g_3, g_2, g_1) = \frac{\lambda}{3!} \int \mathrm{d}g_4 \mathrm{d}g_5 \mathrm{d}g_6 T(g_3, g_5, g_4) T(g_4, g_2, g_6) T(g_6, g_5, g_1). \tag{4.5}$$

As performed in previous chapters, we again work in the spin representation for convenience. Then according to Peter-Weyl theorem, $T(g_1, g_2, g_3)$ can be decomposed into

$$T(g_1, g_2, g_3) = \sum_{\{j,m,n\}} T^{m_1 m_2 m_3}_{j_1 j_2 j_3} \prod_{i=1}^{3} \sqrt{2j_i + 1} D^{j_i}_{m_i n_i}(g_i) \begin{pmatrix} j_1 & j_2 & j_3 \\ n_1 & n_2 & n_3 \end{pmatrix}, \tag{4.6}$$

with

$$T^{m_1 m_2 m_3}_{j_1 j_2 j_3} = \int \mathrm{d}g_1 \mathrm{d}g_2 \mathrm{d}g_3 \sum_{\{n\}} T(g_1, g_2, g_3) \prod_{i=1}^{3} \sqrt{2j_i + 1} \bar{D}^{j_i}_{m_i n_i}(g_i) \begin{pmatrix} j_1 & j_2 & j_3 \\ n_1 & n_2 & n_3 \end{pmatrix}. \tag{4.7}$$

Thus, the spin-representation version of the action (4.4) is

$$S_B[T] = \sum_{j_1, j_2, j_3} \frac{\mu^2}{2} |T^{m_1, m_2, m_3}_{j_1, j_2, j_3}|^2 - \frac{\lambda}{4!} \sum_{j_1, .., j_6} \begin{Bmatrix} j_1 & j_2 & j_3 \\ j_4 & j_5 & j_6 \end{Bmatrix} T^{4_{6j}}, \tag{4.8}$$

where

$$|T^{m_1, m_2, m_3}_{j_1, j_2, j_3}|^2 = \sum_{\substack{j_1, j_2, j_3 \\ m_1, m_2, m_3}} (-1)^{\sum_{i=1}^{3} (j_i - m_i)} T^{m_1, m_2, m_3}_{j_1, j_2, j_3} T^{-m_1, -m_2, -m_3}_{j_1, j_2, j_3}, \tag{4.9}$$

and

$$T^{4_{6j}} = \sum_{\{j,m\}} (-1)^{\sum_{i=1}^{6} (j_i - m_i)} T^{-m_1, -m_2, -m_3}_{j_1 j_2 j_3} T^{m_3, m_5, -m_4}_{j_3 j_5 j_4} T^{m_4, m_2, -m_6}_{j_4 j_2 j_6} T^{m_6, -m_5, m_1}_{j_6 j_5 j_1}. \tag{4.10}$$

Correspondingly, the equation of motion in spin representation reads

$$\mu^2 T^{m_1, m_2, m_3}_{j_1, j_2, j_3} = \frac{\lambda}{3!} \sum_{j_4, j_5, j_6} \begin{Bmatrix} j_1 & j_2 & j_3 \\ j_4 & j_5 & j_6 \end{Bmatrix} T^{4_{6j}}_{\setminus \{m_1, m_2, m_3\}}, \tag{4.11}$$

where

$$T^{4_{6j}}_{\setminus \{m_1, m_2, m_3\}} = \sum_{m_4, m_5, m_6} (-1)^{\sum_{i=4}^{6} (j_i - m_i)} T^{m_3, m_5, -m_4}_{j_3 j_5 j_4} T^{m_4, m_2, -m_6}_{j_4 j_2 j_6} T^{m_6, -m_5, m_1}_{j_6 j_5 j_1}. \tag{4.12}$$

means that magnetic indices m_1,m_2 and m_3 are not summed on.

A field T represents a triangle, and the interaction term glues four triangles to form a tetrahedron as a building block of a $3D$ Euclidean space. The kinetic term connects the faces of these tetrahedron, so one obtains the triangulation, as illustrated in Figure 4.1 and Figure 4.2.

4.2.1 Matter Reference Frame and Homogeneous Solution

In this chapter, real scalar fields are used as relational reference frame as well. The coupling of matter d.o.f. will facilitate the following computation where a matter field will occur

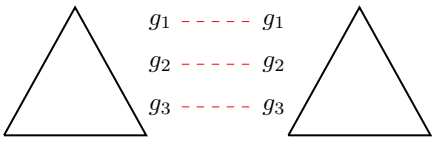

Figure 4.1: The field $T(g_1, g_2, g_3)$ corresponds to a triangle, and its kinetic term tells how to glue two triangles, which are the faces of tetrahedra.

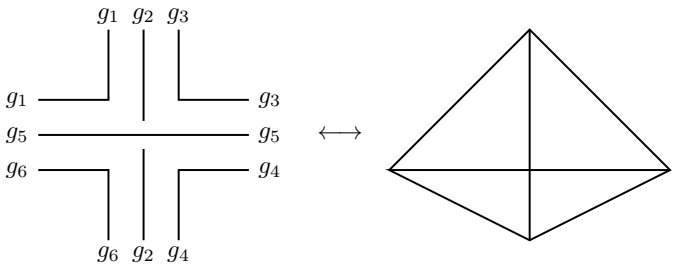

Figure 4.2: The interaction term of $T(g_1, g_2, g_3)$ combines four fields, corresponding to a tetrahedron as a building block of $3D$ Euclidean gravity.

effectively as a perturbation over geometry. For simplicity, the scalar fields in this chapter are assumed to be free and massless, same with those applied in chapter 2.

In three dimensions, one needs three scalar fields in total, χ_1, χ_2, and χ_3, to localise a triangle. Let $\chi = (\chi_1, \chi_2, \chi_3)$, and as illustrated in Chapter 1, the field T is extended to $T(g_1, g_2, g_3; \chi) : SU(2)^3 \times \mathbb{R}^3 \to \mathbb{C}$. The new action then reads

$$S[T] = \int [\mathrm{d}g]^3 \mathrm{d}^3\chi \left[\frac{1}{2}\nabla T(g_1, g_2, g_3; \chi)\nabla \bar{T}(g_1, g_2, g_3; \chi) + \frac{\mu^2}{2} T(g_1, g_2, g_3; \chi)\bar{T}(g_1, g_2, g_3; \chi)\right]$$
$$- \frac{\lambda}{4!}\int \prod_{i=1}^{6} \mathrm{d}g_i \mathrm{d}^3\chi T(g_1, g_2, g_3; \chi)T(g_3, g_5, g_4; \chi)T(g_4, g_2, g_6; \chi)T(g_6, g_5, g_1; \chi)., \qquad (4.13)$$

where $\nabla = (\partial_{\chi_1}, \partial_{\chi_2}, \partial_{\chi_3})$. The first term in (4.13) shows an invariance under translation $\chi_i \to \chi_i + a_i$, where a_i are some real constants. The equation of motion of (4.13) reads

$$\nabla^2 T(g_3, g_2, g_1; \chi) + \mu^2 T(g_3, g_2, g_1; \chi)$$
$$= \frac{\lambda}{3!}\int \mathrm{d}g_4 \mathrm{d}g_5 \mathrm{d}g_6 T(g_3, g_5, g_4; \chi)T(g_4, g_2, g_6; \chi)T(g_6, g_5, g_1; \chi). \qquad (4.14)$$

In spin representation, the action (4.14) becomes

$$S_B[T(\chi)] = \sum_{j_1, j_2, j_3} \int \mathrm{d}^3\chi \left[\frac{1}{2}\left|\nabla T^{m_1, m_2, m_3}_{j_1, j_2, j_3}(\chi)\right|^2 + \frac{\mu^2}{2}\left|T^{m_1, m_2, m_3}_{j_1, j_2, j_3}(\chi)\right|^2\right.$$
$$\left. - \frac{\lambda}{4!}\sum_{j_1, .., j_6} \begin{Bmatrix} j_1 & j_2 & j_3 \\ j_4 & j_5 & j_6 \end{Bmatrix} \int \mathrm{d}^3\chi T(\chi)^{4_{6j}}\right]. \qquad (4.15)$$

This leads to the equation of motion:

$$\nabla^2 T^{m_1,m_2,m_3}_{j_1,j_2,j_3}(\chi) + \mu^2 T^{m_1,m_2,m_3}_{j_1,j_2,j_3}(\chi) = \frac{\lambda}{3!}\sum_{j_4,j_5,j_6}\begin{Bmatrix} j_1 & j_2 & j_3 \\ j_4 & j_5 & j_6 \end{Bmatrix} T(\chi)^{4_{6j}}_{\backslash\{m_1,m_2,m_3\}}. \tag{4.16}$$

Boulatov model has a family of classical homogeneous solution [213], which is independent of χ:

$$T_f(g_1,g_2,g_3) = \mu\sqrt{\frac{3!}{\lambda}}\int \mathrm{d}h\delta(g_1 h)f(g_2 h)\delta(g_3 h), \tag{4.17}$$

where f is an arbitrary function $f : SU(2) \to \mathbb{C}$ and it is normalised such that $\int \mathrm{d}g f^2 = 1$. In (4.17), δ denotes the Dirac delta over $SU(2)$, such that

$$\int \mathrm{d}h\delta(h) = 1,\ \int \mathrm{d}h\delta(h)f(h) = f(I), \tag{4.18}$$

where I is $SU(2)$ group identity. Its spin-representation dual is

$$(T_f)^{m_1,m_2,m_3}_{j_1,j_2,j_3} = \mu\sqrt{\frac{3!}{\lambda}}\sqrt{d_{j_1}d_{j_3}}\sum_{l_2} f^{j_2}_{m_2,l_2}\begin{pmatrix} j_1 & j_2 & j_3 \\ m_1 & l_2 & m_3 \end{pmatrix}, \tag{4.19}$$

where $d_j = 2j+1$. In spin representation, f^j_{mn} reads

$$f^j_{mn} = \sqrt{2j+1}\int \mathrm{d}g f(g)\bar{D}^j_{mn}(g), \tag{4.20}$$

and satisfies the normalization condition

$$\sum_{j,m,n}(-1)^{m-n} f^j_{mn} f^j_{-m,-n} = 1. \tag{4.21}$$

Before we move on, let us discuss briefly a special type of solution which is regularised by the *heat kernel*. One finds a divergent action if one substitutes (4.17) into (4.13), due to the Dirac delta. To control the divergences, we can replace the Dirac delta with a heat-kernel delta:

$$\delta(g) = \sum_{j,m}(2j+1)D^j_{mm}(g) \to \delta_\varepsilon(g) = \sum_{j,m}(2j+1)D^j_{mm}(g)e^{-\varepsilon C_j}, \tag{4.22}$$

where $C_j = j(j+1)$ is the quadratic Casimir of $SU(2)$ spin-j representation. If $\varepsilon \to 0$, this is simply a Dirac delta. Accordingly, function f is decomposed into

$$f_\varepsilon(g) = \sum_{j,m,n} f^j_{mn} D^j_{mn}(g)e^{-\varepsilon C_j}. \tag{4.23}$$

When $\varepsilon \to 0$, one recovers the original function f.

Assume the norm of δ_ε to be α_ε^{-2}, and the normalised version for δ_ε is

$$\Delta_\varepsilon(g) = \alpha_\varepsilon \sum_{j,m,n} \sqrt{d_j} (\Delta_\varepsilon)^j_{mn} D^j_{mn}(g) e^{-\varepsilon C_j}, \tag{4.24}$$

where the Peter-Weyl coefficients $(\Delta_\varepsilon)^j_{mn}$ reads

$$(\Delta_\varepsilon)^j_{mn} = \alpha_\varepsilon \sqrt{d_j} \delta_{mn} e^{-\varepsilon C_j}. \tag{4.25}$$

Then a regularised and symmetric solution can be

$$\begin{aligned} T_\varepsilon(g_1, g_2, g_3) &= \mu \sqrt{\frac{3!}{\lambda}} \int \mathrm{d}h \delta_\varepsilon(g_1 h) \Delta_\varepsilon(g_2 h) \delta_\varepsilon(g_3 h) \\ &= \mu \alpha_\varepsilon \sqrt{\frac{3!}{\lambda}} \int \mathrm{d}h \delta_\varepsilon(g_1 h) \delta_\varepsilon(g_2 h) \delta_\varepsilon(g_3 h), \end{aligned} \tag{4.26}$$

in group representation, or

$$(T_\varepsilon)^{m_1 m_2 m_3}_{j_1 j_2 j_3} = \mu \alpha_\varepsilon \sqrt{\frac{3!}{\lambda}} \prod_{i=1}^{3} \sqrt{d_{j_i}} e^{-\varepsilon C_{j_i}} \begin{pmatrix} j_1 & j_2 & j_3 \\ m_1 & m_2 & m_3 \end{pmatrix}, \tag{4.27}$$

in spin representation. However, (4.26) is only an approximate solution of Boulatov model, so we will continue with solution (4.17) in following sections.

4.3 Amit-Roginsky Theory as a Phase of Boulatov Model

4.3.1 Amit-Roginsky Model

Systems with a large number of d.o.f. are of great interest in physics. Take the matrix model for example, where the dynamical objects are $N \times N$ matrices. The large-N limit is also known as the 'planar limit' [82], where only spherical topology contributes to the Feynman diagrams [82, 215]. Extending to tensor models, one finds that tensor models are dominated by melonic graphs when $N \to \infty$ [90, 215].

Another interesting example with large d.o.f. is the Sachedev-Ye-Kitaev (SYK) model [216–219], which becomes increasingly important in both condensate matter physics and fundamental physics. It is a model of strongly coupled quantum many-body systems. One remarkable feature of SYK model is being solvable, and it is believed that SYK model has a gravitational dual with maximal chaos. A typical action of an SYK$_q$ model containing N fermions has an interaction among q Majorana fermions,

$$S_q = \int d\tau \left(\sum_{i=1}^{N} \psi_i \frac{d}{d\tau} \psi_i - \frac{i^{q/2}}{q!} \sum_{i_1,\ldots,i_q=1}^{N} \mathfrak{J}_{i_1 \ldots i_q} \psi_{i_1} \ldots \psi_{i_q} \right), \tag{4.28}$$

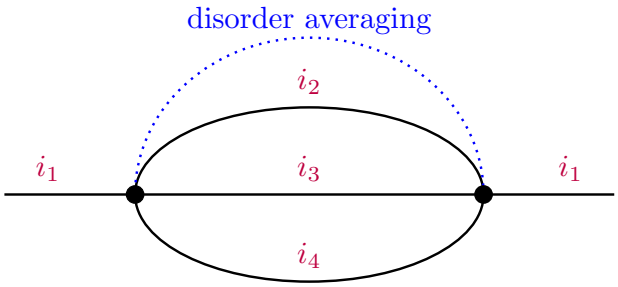

Figure 4.3: The self energy of an SYK_4 model at large N is a melonic graph. The fully dressed Green function is represented by black lines, and the correction from disorder averaging is denoted by the blue dotted line.

where the coupling constant $\mathfrak{J}_{i_1\ldots i_q}$ are independent random Gaußian variables. This model can be solved if $\mathfrak{J}_{i_1\ldots i_q}$ has zero mean and $N \to \infty$, and one can apply the self-averaging properties of SYK model to find the correlation functions up to $1/N$ corrections. At large-N limit, the Feynman graphs of SYK model are melonic [220], as is shown by Figure 4.3 which takes $q = 4$ for example.

Motivated by Razvan Gurau's work on tensor models [221, 222], Edward Witten made an important step and defined an 'SYK-like' model without quenched disorder [223]. Witten's new model describes a system sharing similar properties with SYK model, but in a more conventional large-N limit. This theory is also known as the Gurau-Witten model. In this theory, N real fermionic tensors are the dynamical objects, and the action reads

$$S_{\text{Gurau-Witten}} = \int dt \left(\sum_{i=1}^{N} \psi_i \frac{d}{dt} \psi_i - \frac{i^{q/2}}{q!} \mathfrak{J} \psi_{i_1} \ldots \psi_{i_q} \right), \tag{4.29}$$

where $\mathfrak{J}$ is a real coupling constant. The Feynman diagrams are represented by ribbon graphs like those for a matrix model. It is encouraging that at large-N limit, Gurau-Witten model is also dominated by melonic graphs. For this reason, such models are called 'SYK-like'. When $q = 4$, the tensors are of rank-3 and it is described by the Klebanov-Tarnopolsky model [224].

There is another type of theory which also possesses melonic dominance, named Amit-Roginsky (AR) model [225]. It is a ϕ^3 theory where the bosonic field ϕ is self-coupled through a Wigner's $3j$ symbol:

$$\begin{aligned} S_{AR}[\phi] = \int \mathrm{d}^d x \Bigg\{ & \frac{1}{2} \sum_m (-1)^{j-m} \left[(\nabla \phi^j_m)(\nabla \phi^j_{-m}) + \mu \phi^j_m \phi^j_{-m} \right] \\ & + \sum_{m_1, m_2, m_3} \frac{\lambda}{3!} \sqrt{2j+1} \begin{pmatrix} j & j & j \\ m_1 & m_2 & m_3 \end{pmatrix} \phi^j_{-m_1} \phi^j_{-m_2} \phi^j_{-m_3} \Bigg\}, \end{aligned} \tag{4.30}$$

and $m = 1, \ldots, N$. According to $SU(2)$ recoupling theory, j in the $3j$ symbol from (4.30) should be an integer, in order that the $3j$ symbol is non-vanishing [115, 116]. As a result,

the model lives in an irreducible representation of $SO(3)$ of dimension $N = 2j + 1$. When $N \to \infty$, it is found that AR model is also governed by melonic graphs [226].

It has been shown that a scalar field can be obtained from Boulatov model as a '$2D$ phase ' excitation over the geometry [213]. The strategy is perturbing the classical solution of Boulatov model and substituting the perturbed solution to the action. One will find an effective action in addition to the original Boulatov action, and this effective action generates the dynamics of a matter field [213]. In this chapter, it is our interest to verify whether the AR model can be recovered as a effective field if we do a perturbation on Boulatov model.

4.3.2 Perturbations over Homogeneous Solution

The so-called '$2D$ phases' of Boulatov model is a type of surface-like perturbations over the field T which only depends on two of the groups elements [213]:

$$T(g_1, g_2, g_3; \chi) = \psi(g_1, g_3; \chi). \tag{4.31}$$

The perturbation ψ becomes

$$\begin{aligned}\psi^{m_1m_2m_3}_{j_1j_2j_3}(\chi) &= \sum_{\{n\}} \int [\mathrm{d}g]^3 \psi(g_1, g_3; \chi) \prod_{i=1}^{3} \sqrt{2j_i + 1} \bar{D}^{j_i}_{m_i n_i} \begin{pmatrix} j_1 & j_2 & j_3 \\ n_1 & n_2 & n_3 \end{pmatrix} \\ &\equiv \delta^{j_2,0} \delta_{m_2,0} \delta^{j_1,j_3} \sqrt{2j_1 + 1} \psi^{j_1}_{m_1,m_3}(\chi)\end{aligned} \tag{4.32}$$

in spin representation. Let ψ be a perturbation around the homogeneous solution (4.17), then the perturbed field is

$$T_\psi(g_1, g_2, g_3; \chi) = T_f(g_1, g_2, g_3) + \xi \psi(g_1, g_3; \chi), \tag{4.33}$$

where ξ is a small real positive constant such that $0 < \xi \ll 1$. The dual of perturbed field in spin representation is

$$(T_\psi)^{m_1m_2m_3}_{j_1j_2j_3}(\chi) = (T_f)^{m_1m_2m_3}_{j_1j_2j_3} + \xi \delta^{j_2,0} \delta_{m_2,0} \delta^{j_1,j_3} \psi^{j_1}_{m_1,m_3}(\chi). \tag{4.34}$$

Substituting (4.34) into the action (4.15), one obtains an action

$$S_B[T_\psi(\chi)] = S_B[T] + \xi^2 \cdot S_{\text{eff}}[\psi] + \mathcal{O}(\xi^4), \tag{4.35}$$

where terms at the first order of ξ vanishes since T_f (4.17) is a solution to the equation of motion. Terms at the first order are approximately vanishing if one applies the heat kernel solution (4.27). Since the action $S_{\text{eff}}[\psi]$ represents the effective action of the perturbation field ψ^j_{mn} and contains corrections up to ξ, $\xi^2 S_{\text{eff}}[\psi]$ contains corrections up to order ξ^3.

We expect that S_{eff} takes a form similar with the AR model (4.30), which means that an effective dynamics of matter can be obtained as a $2D$-phase excitation around the Boulatov

model [213]. Now we are going to compute the effective action and show how to achieve this goal in detail.

Note that the AR model involves a field ϕ transforming in a representation of $SU(2)$, and it carries only one magnetic index m. Therefore, we can make the situation easier by first specialising the type of perturbations and requiring that

$$\psi^{j_1}_{m_1 m_3}(\chi) = \sum_m \sqrt{2j_1+1}\phi^{j_1}_m(\chi) \begin{pmatrix} j_1 & j_1 & j_1 \\ m_1 & m & m_3 \end{pmatrix}. \tag{4.36}$$

Now let us continue to find the effective action S_{eff}. One finds that the quadratic term of ξ receives three kinds of contributions. First, the kinetic term of Boulatov action contributes terms with a form $\psi\psi$. Then, the interaction term gives two distinct type of contributions, depending on how the two perturbative fields are connected in the action. Schematically, these two terms can be represented under the form $TT\psi\psi$ when the two perturbative fields $\psi_{m_a m_b}$ share one magnetic indices, and $T\psi T\psi$ is used in the case where they share none.

Quadratic terms I: $\psi\psi$ The kinetic term $\sum_{j_1,j_2,j_3} \left|(T_\psi)^{m_1,m_2,m_3}_{j_1,j_2,j_3}(\chi)\right|^2$ of the Boulatov action contributes the following term $\psi\psi$ to the effective action:

$$\begin{aligned}
&\sum_{\substack{j_1,j_2,j_3 \\ m_1,m_2,m_3}} (-1)^{\sum_{i=1}^3 (j_i - m_i)} \left[\delta^{j_2,0}\delta_{m_2,0}\delta^{j_1,j_3}\psi^{j_1}_{m_1,m_3}\right]\left[\delta^{j_2,0}\delta_{-m_2,0}\delta^{j_1,j_3}\psi^{j_1}_{-m_1,-m_3}\right] \\
&= \sum_{\substack{j_1,m_1,m_3 \\ m,m'}} (-1)^{2j_1-m_1-m_3}\phi^{j_1}_m\phi^{j_1}_{m'}(2j_1+1) \begin{pmatrix} j_1 & j_1 & j_1 \\ m_1 & m & m_3 \end{pmatrix}\begin{pmatrix} j_1 & j_1 & j_1 \\ -m_1 & m' & -m_3 \end{pmatrix} \\
&= \sum_{j_1,m_1} (-1)^{j_1-m_1}\phi^{j_1}_{m_1}\phi^{j_1}_{-m_1}.
\end{aligned} \tag{4.37}$$

This term shares the same form with the quadratic term of the AR action (4.30). Note that this contribution is independent of the solution $T^{m_1 m_2 m_3}_{j_1 j_2 j_3}$ and therefore it does not impose any restriction on the homogeneous solution considered.

Quadratic terms II: $TT\psi\psi$ Terms of $TT\psi\psi$ come from the interaction term from the action, and they have four types, each contributing to the effective action with

$$\begin{aligned}
&\sum_{\substack{m_1,\cdots,m_6\\ j_1,\cdots,j_6}} \begin{Bmatrix} j_1 & j_2 & j_3 \\ j_4 & j_5 & j_6 \end{Bmatrix} (-1)^{\sum_i (j_i - m_i)} T^{-m_1,-m_2,-m_3}_{j_1 j_2 j_3} T^{m_3,m_5,-m_4}_{j_3 j_5 j_4} \\
&\times \delta^{j_2,0}\delta_{m_2,0}\delta^{j_4,j_6}\psi^{j_4}_{m_4,-m_6}\delta^{j_5,0}\delta_{m_5,0}\delta^{j_6,j_1}\psi^{j_6}_{m_6,m_1} \\
=& \sum_{\substack{m_1,m_3,m_4,m_6\\ j_1,j_3,j_4,j_6}} \begin{Bmatrix} j_1 & 0 & j_3 \\ j_4 & 0 & j_6 \end{Bmatrix} (-1)^{\sum_{i\neq 2,5}(j_i - m_i)} T^{-m_1,0,-m_3}_{j_1,0,j_3} T^{m_3,0,-m_4}_{j_3,0,j_4} \delta^{j_4,j_6}\delta^{j_6,j_1}\psi^{j_1}_{m_4,-m_6}\psi^{j_1}_{m_6,m_1} \\
=& \sum_{\substack{m_1,m_3,m_4,m_6\\ j_1}} (-1)^{6j_1 - \sum_{i\neq 2,5} m_i} T^{-m_1,0,-m_3}_{j_1,0,j_1} T^{m_3,0,-m_4}_{j_1,0,j_1} \psi^{j_1}_{m_4,-m_6}\psi^{j_1}_{m_1,m_6} \\
=& \sum_{j_1,m_1,m_6,m_4} \left[\sum_{m_3} (-1)^{-m_3-m_4} T^{-m_1,0,-m_3}_{j_1,0,j_1} T^{m_3,0,-m_4}_{j_1,0,j_1} \right] (-1)^{2j_1 - m_1 - m_6} \psi^{j_1}_{m_4,-m_6}\psi^{j_1}_{m_1,m_6} \qquad (4.38)
\end{aligned}$$

If the homogeneous solution $T^{m_1 m_2 m_3}_{j_1 j_2 j_3}$ satisfies

$$\sum_{m_3} (-1)^{-m_3-m_4} T^{-m_1,0,-m_3}_{j_1,0,j_1} T^{m_3,0,-m_4}_{j_1,0,j_1} = c_{1,j_1}\delta_{m_1,-m_4} \qquad (4.39)$$

with c_{1,j_1} some constant to be fixed later, then one finds

$$\begin{aligned}
&\sum_{\substack{m_1,\cdots,m_6\\ j_1,\cdots,j_6}} \begin{Bmatrix} j_1 & j_2 & j_3 \\ j_4 & j_5 & j_6 \end{Bmatrix} (-1)^{\sum_i (j_i - m_i)} T^{-m_1,-m_2,-m_3}_{j_1 j_2 j_3} T^{m_3,m_5,-m_4}_{j_3 j_5 j_4} \\
&\times \delta^{j_2,0}\delta_{m_2,0}\delta^{j_4,j_6}\psi^{j_4}_{m_4,-m_6}\delta^{j_5,0}\delta_{m_5,0}\delta^{j_6,j_1}\psi^{j_6}_{m_6,m_1} \\
=& \sum_{j_1,m_1,m_6,m_4} \left[\sum_{m_3} (-1)^{-m_3-m_4} T^{-m_1,0,-m_3}_{j_1,0,j_1} T^{m_3,0,-m_4}_{j_1,0,j_1} \right] (-1)^{2j_1 - m_1 - m_6} \psi^{j_1}_{m_4,-m_6}\psi^{j_1}_{m_1,m_6} \\
=& \sum_{j_1,m_1} c_{1,j_1} (-1)^{j_1 - m_1} \phi^{j_1}_{m_1}\phi^{j_1}_{-m_1}, \qquad (4.40)
\end{aligned}$$

where (4.36) is applied. This is similar with the kinetic term of the AR model (4.30).

Quadratic terms III: $T\psi T\psi$ The second type contribution from interactions is $T\psi T\psi$, which contains two terms. Each of this term contributes to the effective action as follows

$$\begin{aligned}
&\sum_{\substack{m_1,\cdots,m_6\\ j_1,\cdots,j_6}} (-1)^{\sum_i (j_i-m_i)} T^{-m_1,-m_2,-m_3}_{j_1 j_2 j_3} \delta^{j_5,0}\delta_{m_5,0}\delta^{j_3,j_4}\psi^{j_3}_{m_3,-m_4} \\
&\times T^{m_4,m_2,-m_6}_{j_4 j_2 j_6}\delta^{j_5,0}\delta_{m_5,0}\delta^{j_1,j_6}\psi^{j_6}_{m_6 m_1}\begin{Bmatrix} j_1 & j_2 & j_3 \\ j_4 & j_5 & j_6 \end{Bmatrix} \\
&= \sum_{\substack{m_1,m_3,m_4,m_6\\ j_1,j_3}} (-1)^{j_1+j_3-m_4-m_6}\psi^{j_3}_{m_3,-m_4}\psi^{j_1}_{m_6,m_1}\frac{1}{\sqrt{(2j_1+1)(2j_3+1)}} \\
&\times \sum_{j_2,m_2} (-1)^{\sum_{i=1}^3 (2j_i-m_i)} T^{-m_1,-m_2,-m_3}_{j_1,j_2,j_3} T^{m_4,m_2,-m_6}_{j_3,j_2,j_1}.
\end{aligned} \tag{4.41}$$

For a general solution of the equation of motion, this term leads to a non-diagonal kinetic term for the ψ field . By requiring that the homogeneous solution satisfies

$$\sum_{j_2,m_2} (-1)^{\sum_{i=1}^3 (2j_i-m_i)} T^{-m_1,-m_2,-m_3}_{j_1,j_2,j_3} T^{m_4,m_2,-m_6}_{j_3,j_2,j_1} = c_{2,j_1} c_{2,j_3}\delta_{m_1,-m_6}\delta_{m_3,m_4}, \tag{4.42}$$

where $c_{2,j}$ is again a constant to be found later, one finds the contribution from $T\psi T\psi$ becomes

$$\begin{aligned}
&\sum_{\substack{m_1,m_3,m_4,m_6\\ j_1,j_3}} (-1)^{j_1+j_3-m_4-m_6}\psi^{j_3}_{m_3,-m_4}\psi^{j_1}_{m_6,m_1}\frac{1}{\sqrt{(2j_1+1)(2j_3+1)}} \\
&\times \sum_{j_2,m_2} (-1)^{\sum_{i=1}^3 (2j_i-m_i)} T^{-m_1,-m_2,-m_3}_{j_1,j_2,j_3} T^{m_4,m_2,-m_6}_{j_3,j_2,j_1} \\
&= \left[\sum_{j_1,m_1} (-1)^{j_1-m_1}\frac{c_{2,j_1}}{\sqrt{2j_1+1}}\psi^{j_1}_{m_1,-m_1}\right]^2.
\end{aligned} \tag{4.43}$$

When specializing to the type of perturbation given by equation (4.36), we obtain

$$\begin{aligned}
\sum_{j_1,m_1} (-1)^{j_1-m_1}\frac{c_{2,j_1}}{\sqrt{2j_1+1}}\psi^{j_1}_{m_1,-m_1} &= \sum_{j_1,m_1,m} (-1)^{j_1-m_1} c_{2,j_1}\phi^{j_1}_m \begin{pmatrix} j_1 & j_1 & j_1 \\ m_1 & m & -m_1 \end{pmatrix}, \\
&= \sum_{j_1} c_{2,j_1}\phi^{j_1}_0 \sum_{m_1} (-1)^{j_1-m_1}\begin{pmatrix} j_1 & j_1 & j_1 \\ m_1 & 0 & -m_1 \end{pmatrix}, \\
&= \sum_{j_1} c_{2,j_1}\phi^{j_1}_0\delta_{j_1,0}\sqrt{2j_1+1}, \\
&= c_{2,0}\phi^0_0.
\end{aligned} \tag{4.44}$$

Therefore, the quadratic term obtained from $T\psi T\psi$ term can also be diagonal under certain choices of homogeneous solution and perturbations mentioned above.

Cubic terms There is only one type of cubic contribution which also comes from the interaction term of (4.16), say $T\psi\psi\psi$. Their contribution reads

$$\sum_{\{j,m\}} (-1)^{\sum_i (j_i - m_i)} T^{-m_1,-m_2,-m_3}_{j_1,j_2,j_3} \delta^{j_5,0}\delta_{m_5,0}\psi^{j_3}_{m_3,-m_4}\delta^{j_2,0}\delta_{m_2,0}\psi^{j_4}_{m_4,-m_6}\delta^{j_5,0}\delta_{m_5,0}\psi^{j_6}_{m_6,m_1} \begin{Bmatrix} j_1 & j_2 & j_3 \\ j_4 & j_5 & j_6 \end{Bmatrix}$$

$$= \sum_{\substack{m_1,m_3,m_4,m_6 \\ j_1}} (-1)^{-\sum_{i\neq 2,5} m_i} T^{-m_1,0,-m_3}_{j_1,0,j_1} \frac{(-1)^{2j_1}}{2j_1+1} \psi^{j_1}_{m_3,-m_4}\psi^{j_1}_{m_4,-m_6}\psi^{j_1}_{m_6,m_1}. \tag{4.45}$$

If we assume that the homogeneous solution T satisfies

$$T^{-m_1,0,-m_3}_{j_1,0,j_1} = c_{3,j_1}(-1)^{-m_3}\delta_{m_1,-m_3}, \tag{4.46}$$

with c_{3,j_1} a constant, this contribution becomes

$$\sum_{\substack{m_1,m_3,m_4,m_6 \\ j_1}} (-1)^{-\sum_{i\neq 2,5} m_i} T^{-m_1,0,-m_3}_{j_1,0,j_1} \frac{(-1)^{2j_1}}{2j_1+1} \psi^{j_1}_{m_3,-m_4}\psi^{j_1}_{m_4,-m_6}\psi^{j_1}_{m_6,m_1}$$

$$= \sum_{\substack{m_3,m_4,m_6 \\ j_1}} (-1)^{2j_1-m_3-m_4-m_6} \frac{c_{3,j_1}}{2j_1+1} \psi^{j_1}_{m_3,-m_4}\psi^{j_1}_{m_4,-m_6}\psi^{j_1}_{m_6,-m_3}. \tag{4.47}$$

Substituting (4.36) into the equation above, one finds

$$\sum_{\substack{m_1,m_3,m_4,m_6 \\ j_1}} (-1)^{-\sum_{i\neq 2,5} m_i} T^{-m_1,0,-m_3}_{j_1,0,j_1} \frac{(-1)^{2j_1}}{2j_1+1} \psi^{j_1}_{m_3,-m_4}\psi^{j_1}_{m_4,-m_6}\psi^{j_1}_{m_6,m_1}$$

$$= \sum_{\substack{m_3,m_4,m_6 \\ j_1}} (-1)^{2j_1-m_3-m_4-m_6} \frac{c_{3,j_1}}{2j_1+1} \sum_{m,m',m''} \phi^{j_1}_m \phi^{j_1}_{m'} \phi^{j_1}_{m''}$$

$$\times \begin{pmatrix} j_1 & j_1 & j_1 \\ m_3 & m & -m_4 \end{pmatrix} \begin{pmatrix} j_1 & j_1 & j_1 \\ m_4 & m' & -m_6 \end{pmatrix} \begin{pmatrix} j_1 & j_1 & j_1 \\ m_6 & m'' & -m_3 \end{pmatrix}$$

$$\times (-1)^{j_1} \sum_{m_3,m_4,m_6} (-1)^{3j_1-m_3-m_4-m_6} \begin{pmatrix} j_1 & j_1 & j_1 \\ m & -m_4 & m_3 \end{pmatrix} \begin{pmatrix} j_1 & j_1 & j_1 \\ m_6 & m'' & -m_3 \end{pmatrix} \begin{pmatrix} j_1 & j_1 & j_1 \\ -m_6 & m_4 & m' \end{pmatrix}$$

$$= \sum_{\substack{m,m',m'' \\ j_1}} \frac{c_{3,j_1}}{2j_1+1} \begin{Bmatrix} j_1 & j_1 & j_1 \\ j_1 & j_1 & j_1 \end{Bmatrix} \phi^{j_1}_m \phi^{j_1}_{m'} \phi^{j_1}_{m''} \begin{pmatrix} j_1 & j_1 & j_1 \\ m & m' & m'' \end{pmatrix}. \tag{4.48}$$

We have used the fact that $(-1)^{2j_1} = 1$, since j_1 here has to be an integer so that the $3j$ symbol will not vanish. Thus, when imposing the condition (4.46), one obtains a contribution which corresponds to the interaction term of the AR model (4.30).

Furthermore, when comparing two conditions (4.39) and (4.46), one notes that the former will be automatically satisfied when the later is true, and two coefficients are related through the relation

$$c_{1,j_1} = c^2_{3,j_1}. \tag{4.49}$$

Based on the calculation above, let us continue to show the emergence of an AR-like model as an effective field.

4.3.3 The Emergence of Amit-Roginsky Model

With conditions (4.42) as well as (4.46), for a perturbation (4.36), one finds the effective action $S_{\text{eff}}[\psi]$ in (4.35)

$$S_{\text{eff}}[\psi] \equiv S[\phi^j_m] = S_0[\phi^0_0] + \sum_j S_j[\phi^j_m], \tag{4.50}$$

where

$$S_0[\phi^0_0] = \int \mathrm{d}^3\vec{\chi} \left(\frac{1}{2} \left\{ (\nabla\phi^0_0)^2 + \left[\mu^2 + \frac{\lambda}{3!}(2c^2_{3,0} + c^2_{2,0}) \right] (\phi^0_0)^2 \right\} - \frac{\xi\lambda}{3!} c_{3,0} \left(\phi^0_0\right)^3 \right), \tag{4.51}$$

and

$$\begin{aligned} S_j[\phi^j_m] = \int \mathrm{d}^3\vec{\chi} \Bigg\{ & \frac{1}{2} \left[|\nabla\phi^j_n|^2 + \left(\mu^2 + \frac{\lambda}{3!} c^2_{3,j} \right) |\phi^j_n|^2 \right] \\ & - \frac{c_{3,j_1}}{2d_j} \frac{\xi\lambda}{3!} \begin{Bmatrix} j & j & j \\ j & j & j \end{Bmatrix} \sum_{m_1,m_2,m_3} \phi^j_{m_1}\phi^j_{m_2}\phi^j_{m_3} \begin{pmatrix} j & j & j \\ m_1 & m_2 & m_3 \end{pmatrix} \Bigg\}, \end{aligned} \tag{4.52}$$

with $\sum_n |\phi^j_n|^2 = \sum_n (-1)^{j-n} \phi^j_n \phi^j_{-n}$. The fields ϕ with different spin label j decouple and each of them has the form of an AR action (4.30) with j-dependent mass term and coupling.

Explicit values of coefficients Before closing this section, it is also interesting to make the constraints in (4.39), (4.42), and (4.46) more explicit. Here we briefly show how to find the precise values of $c_{1,j}$, $c_{2,j}$, and $c_{3,j}$.

Substituting (4.19) into (4.46), one obtains

$$\mu \sqrt{\frac{3!}{\lambda}} d_{j_1} f^0_{00} \begin{pmatrix} j_1 & 0 & j_1 \\ -m_1 & 0 & -m_3 \end{pmatrix} = \mu \sqrt{\frac{3! d_{j_1}}{\lambda}} f^0_{00} (-1)^{j_1+m_3} \delta_{m_1,-m_3} = c_{3,j_1} (-1)^{-m_3} \delta_{m_1,-m_3}, \tag{4.53}$$

which means

$$c_{3,j} = \begin{cases} (-1)^j \mu \sqrt{\frac{3! d_j}{\lambda}} f^0_{00} & \text{if } j \in \mathbb{N} \\ 0 & \text{otherwise} \end{cases}. \tag{4.54}$$

On the other hand, (4.42) yields

$$\begin{aligned} & \frac{3!\mu^2}{\lambda} \sum_{j_2,m_2} (-1)^{\sum_{i=1}^3 (4j_i - m_i)} d_{j_1} d_{j_3} \sum_{n_2,l_2} f^{j_2}_{-m_2,-n_2} f^{j_2}_{m_2,l_2} \begin{pmatrix} j_1 & j_3 & j_2 \\ m_1 & m_3 & n_2 \end{pmatrix} \begin{pmatrix} j_1 & j_3 & j_2 \\ -m_6 & m_4 & l_2 \end{pmatrix} \\ & = c_{2,j_1} c_{2,j_3} \delta_{m_1,-m_6} \delta_{m_3,m_4}, \end{aligned} \tag{4.55}$$

so one can assume

$$\sum_{m_2} (-1)^{n_2-m_2} f^{j_2}_{-m_2,-n_2} f^{j_2}_{m_2,l_2} \equiv d_{j_2} c^2_{f,j_2} \delta_{n_2,l_2}, \tag{4.56}$$

with $c^2_{f,2} \sim c_{2,j_1} c_{2,j_3}$ a constant. It can be determined with normalisation condition (4.21)

$$\begin{aligned} 1 &= \sum_{j_2,m_2,n_2,l_2} (-1)^{n_2-m_2} f^{j_2}_{-m_2,-n_2} f^{j_2}_{m_2,l_2} \delta_{n_2,l_2}, \\ &= \sum_{j_2} d^2_{j_2} c^2_{f,j_2}. \end{aligned} \tag{4.57}$$

We can also consider the heat-kernel regularised solution (4.26), which reads

$$(f_\varepsilon)^j_{mn} = \alpha_\varepsilon \sqrt{d_j} \delta_{mn} e^{-\varepsilon C_j}. \tag{4.58}$$

It is straightforward to find that

$$c_{3,j} = (-1)^j \mu \sqrt{\frac{3! d_j}{\lambda}} (\Delta_\varepsilon)^0_{00} = (-1)^j \mu \sqrt{\frac{3! d_j}{\lambda}} \alpha_\varepsilon, \tag{4.59}$$

and the coefficients $c_{f,j}$ should take the form

$$c_{f,j} = \alpha_\varepsilon d_j e^{-\varepsilon C_j}. \tag{4.60}$$

Similarly, the condition (4.42) is only satisfied approximately at first order in ε. Indeed at first order in ε,

$$\sum_{j,m} d_j e^{-2\varepsilon C_j} \begin{pmatrix} j_1 & j_2 & j \\ m_1 & m_2 & m \end{pmatrix} \begin{pmatrix} j_1 & j_2 & j \\ m'_1 & m'_2 & m \end{pmatrix} \approx \delta_{m'_1 m_1} \delta_{m'_2 m_2}. \tag{4.61}$$

Hence the coefficients $c_{2,j}$ from the condition (4.42)is found to be

$$c_{2,j} = \mu d_j \alpha_\varepsilon \sqrt{\frac{3!}{\lambda}}. \tag{4.62}$$

4.4 Melonic Dominance of Matter Perturbation

An important feature of AR model is its dominance of melonic graphs at large-$N(= 2j+1)$ limit [226]. However, the main difference between the effective action (4.50) and the original AR model (4.30) is the presence of a sum over spins j. Thus one needs to check whether such a summation spoils the existence of a melonic limit or not. Though the general behaviour of $\{3nj\}$ symbols as functions of j is still an open issue [227–230], one can qualitatively study the behaviour of the Feynman amplitudes and impose additional constraints to ensure the existence of a melonic limit.

4.4.1 Feynman Amplitude

For simplicity, we will forget in this paragraph the heat kernel regularisation and work with the actions given by (4.52). Our new model (4.50) contains a sum over actions labelled by j, and each action from the sum has a Feynman diagram γ, whose amplitudes consists of an isoscalar part I_γ and an isospin part S_γ [225, 226]. Therefore, the Feynman amplitude of the new model is

$$\mathsf{A}_\gamma = \sum_j c_\gamma \left(\frac{\lambda\{6j\}}{3!(2j+1)}\right)^v \mathsf{I}_\gamma \mathsf{S}_\gamma, \tag{4.63}$$

where c_γ is the combinatorial factor of the diagram and v is the number of vertices. The isoscalar part is simply an usual space integral [225, 226], and the isospin part is used to investigate the dependence on N of a Feynman diagram.

The melonic contributions are from Fully 2-Particle Reducible (F2PR) diagrams. They are graphs that always admit a 2-cut which gives another melonic graph with fewer vertices, until a trivial graph (the simplest 2-particle irreducible graph) is reached. Every isospin amplitude reads

$$\mathsf{S}_{F2PR} = (2j+1)^{1-n}, \tag{4.64}$$

for a graph with $v = 2n$ vertices. So the total contribution of F2PR graphs is

$$\mathsf{A}_{F2PR} \sim \sum_j (2j+1)^{1-3n} \{6j\}^{2n} \equiv \bar{\mathsf{A}}_{F2PR}, \tag{4.65}$$

according to (4.63).

For graphs which are not F2PR, their isospin amplitudes can be factorized as a product of 3-particle irreducible graphs

$$\mathsf{S}_{NF2PR} = (2j+1)^{-n_0} \prod_{i=1}^{k} \mathsf{S}_{\{3n_i j\}} \{6j\}^{2n}, \tag{4.66}$$

where

$$n = 1 + n_0 - k + \sum_{i=1}^{k} n_i, \tag{4.67}$$

and $\mathsf{S}_{\{3n_i j\}}$ ($3n_i j$ symbols) are amplitudes of three-particle irreducible diagrams with $2n_i$ vertices. Consequently, the full Feynman amplitude is of order

$$\mathsf{A}_{NF2PR} \sim \sum_j (2j+1)^{-n_0-2n} \prod_{i=1}^{k} \mathsf{S}_{\{3n_i j\}} \{6j\}^{2n} \equiv \bar{\mathsf{A}}_{NF2PR}, \tag{4.68}$$

When $N = 2j+1$ goes to infinity, their amplitudes is conjectured to have a scaling bounded where [225]

$$\mathsf{S}_{\{3n_i j\}} \leq (2j+1)^{1-n_i-\alpha_i}, \tag{4.69}$$

for some positive real numbers $\alpha_i > 0$. If one assumes (4.69) holds for any value of N, then the amplitude from NF2PR graphs has an upper bound

$$\bar{\mathsf{A}}_{NF2PR} \leq \sum_j (2j+1)^{1-3n-\alpha} \{6j\}^{2n}, \tag{4.70}$$

with $\alpha = \sum_i \alpha_i$. The contribution from F2PR graphs is

$$\bar{\mathsf{A}}_{F2PR} \sim \sum_j (2j+1)^{1-3n} \{6j\}^{2n} < \sum_j (2j+1)^{1-3n} = \left(1 - 2^{1-3n}\right) \zeta(3n-1), \tag{4.71}$$

since $\{6j\}$ is a very small number. In AR model, without a summation, when $N = 2j+1 \to \infty$, the contribution from F2PR graphs overwhelms the contribution from other diagrams. However, summing over j may make the two Feynman amplitudes be at the same order, since they are two infinite series that converge. Therefore, it is possible that A_{NF2PR} is comparable with A_{F2PR} because of the summation. Even if (4.69) fails for values of N satisfying $N < N_m$ for some bound N_m, the melonic graphs may not be dominant since the summation from N_m is still infinite. Moreover, it is also a subtle point to define how 'large' is a 'large N' is, or what is the exact value of N_m. If N_m is small, then (4.70) approximately give the correct behaviour.

Thus we can see that the sum over j might dramatically changes the amplitudes of the Feynman graphs of the Amit-Roginsky model and spoil the melonic limit at large j when including a summation over spin index j. However, the explicit properties of the summation is currently not available, so this is only a possibility. Fortunately, there is are two simple ways to exclude this possibility and ensure the melonic dominance to be preserved, which will be discussed below.

4.4.2 Melonic Dominance

Though the amplitudes of the perturbation fields ϕ^j_m may not be dominated by melonic graphs due to the summation over j. We can ensure the melonic dominance by make the summation finite with There exists one naïve way to get the melonic dominance back. One can further specialise the form of perturbation (4.34) in order to enforce the selection of one spin j, getting rid of the sum over spin labels and leading to the original AR model.

$$(T_\psi)^{m_1 m_2 m_3}_{j_1 j_2 j_3}(\chi) = T^{m_1 m_2 m_3}_{j_1 j_2 j_3} + \delta^{j_1 j} \delta^{j_2, 0} \delta_{m_2, 0} \psi^{j_1}_{m_1, m_3}(\chi). \tag{4.72}$$

Another example that recovers melonic dominance works with the approximate solution (4.26). When $j_2 = 0$, the solution becomes

$$(T_\varepsilon)^{m_1 m_2 m_3}_{j_1 j_2 j_3} = \mu \alpha_\varepsilon \sqrt{\frac{3!}{\lambda}} e^{-2\varepsilon C_{j_1}} \sqrt{2j_1 + 1} (-1)^{j_1 - m_1} \delta_{j_1, j_3} \delta_{m_1, -m_3}, \tag{4.73}$$

which scales as $\sqrt{2j_1+1}$ for $j_1 < j_{\max} < \infty$ if $\varepsilon = (2j_{\max}(j_{\max}+1))^{-1}$. For terms $j > j_{\max}$, the contribution are suppressed. Then in the Peter-Weyl expansion, the coefficients with

larger j are dominant, and $(T_\varepsilon)^{m_1m_2m_3}_{j_1j_2j_3}$ with $j_i < j_{\min}$ can be neglected for large $j_{\min}$. Then at first order of ε, the perturbed field is

$$(T_\psi)^{m_1m_2m_3}_{j_1j_2j_3}(\chi) \simeq \begin{cases} T^{m_1m_2m_3}_{j_1j_2j_3} + \delta^{j_1j}\delta^{j_2,0}\delta_{m_2,0}\psi^{j_1}_{m_1,m_3}(\chi), & j_{\min} \leq j_i \leq j_{\max} \\ 0, & \text{otherwise} \end{cases} .$$

In this case, we only sum over a finite number of j, so the non-F2PR graphs are higher order infinitesimals like those of AR model. Consequently, the melonic dominance is back.

While it is still unclear whether a summation over spins could spoil the dominance of melonic diagram in the most general framework, here we demonstrate that it is possible to preserve this melonic limit either by specialising the type of perturbation considered, or by making use of the heat kernel regularisation and taking a double scaling limit.

4.5 Discussion

This chapter we show the emergence of AR model as a $2D$-phase excitation over non-trivial geometry given by a Boulatov model. This is not new that matter can be 'defined as a particular phase of the geometry '[213], and our result is in fact a special case of that in [213]. However, instead of usual scalar fields, we managed to extract matter similar to an AR model which possesses melonic dominance at large d.o.f. with certain conditions.

Another important feature is that we work in a relational reference frame consisting of scalar fields χ. Though they seems to play no role in the computation above, they are actually of great importance such that the action changed accordingly to (4.13) which includes a Laplacian ∇ acting on the Euclidean space. This leads to the recovery of the effective action (4.50), which is our main result in this chapter. One can repeat the procedure without χ, but this will require a much more elaborate computation to proof the emergence of matter phase [213]. The application of a matter reference frame significantly simplifies the calculation and gives rise to an AR-like model.

There are two possible generalisations of this new model. The first one is to find other classical solutions to the Boulatov model and find if the effective field theory of matter, especially that of AR theory, can be recovered as well. The second is more difficult but may be more of physical interest, which aims to obtain an SYK model as a perturbative phase of geometry.

Chapter 5

Conclusion

This dissertation illustrates several applications of a matter reference frame in GFT formalism of quantum gravity. Due to general covariance in GR, the introduction of coordinates or the manifold is simply a way to facilitate the description of a system [231]. In fact, what is physical is the relative location and dynamics among various dynamical objects [52], and matter can act as a relational reference system for us to define local observables. All examples demonstrated in this dissertation use scalar fields as the matter reference frame, which is also a common choice that one makes in LQG.

Chapter 2 shows a very common application of material reference frame, extracting effective dynamics of GFT condensate comparing with the dynamics of a universe. In this chapter, based on different definitions of 'isotropic' GFT states, we accordingly define the 'anisotropic' condensates, in a most general way that we are able to deal with so far. We demonstrate the possibility of GFT condensate states to describe the very early universe which is homogeneous but anisotropic, described by a Bianchi I model.

In Chapter 3 is a more complicated example, where we exhaust all ambiguities and showed how to find the explicit scalar fields even start from a very general situation, without any information of their classical dynamics. We tackle the challenge and find such a physical reference frame. Coupled with this reference system, the GFT state reproduces an effective continuum Schwarzschild geometry, on the basis of a few relevant geometric observables.

Finally, Chapter 4 uses a matter reference system for a slightly different purpose. Instead of straightforwardly give an effective description of kinetics or dynamics of a GFT state, which is done in the previous two chapters, here the introduction of scalar fields brings a translationally invariant term in Boulatov model, and thus the perturbation over this new action yields an effective scalar matter field which is described by AR theory. This can be understood as the emergence of AR-like matter as geometric perturbations.

The anisotropic GFT state, GFT micro-state of black holes, and the effective melonic

dominant matter are all topics that are not well-developed in GFT, compared with other branches such as isotropic GFT cosmology. Here let us discuss some open issues and possible future directions related to or beyond these topics.

Spatial Curvature A main open issue for GFT cosmology is generalising the model to describe more complicated and physical states. So far, most research in GFT cosmology studies a spatially flat FLRW universe. Therefore, it is natural to ask whether an open or a closed universe can be reproduced by the GFT condensates effectively. The inclusion of curvature is quite a challenging task since it involves the construction of a curvature operator in GFT. However, we can start from two possible directions which are more feasible. First, the geometry inside each tetrahedron is assumed to be flat, and the information of curvature is encoded in the way we connect the tetrahedra. If the space-time and geometry is emergent from a large d.o.f., then we need a state containing a large number of connected GFT quanta. Second, the GFT condensates assume that the interaction among tetrahedra are negligible, but it is very likely that one has to include the interaction term in dynamics when non-zero curvature is considered.

Quantum Bounce An important feature of GFT cosmological model is that there is a quantum bounce, which can also be seen from Chapter 2. The bounce exists as the GFT wave-function σ is symmetric about a clock time $\phi = \Phi$. However, effective dynamics of a GFT condensate state is only valid with a large number of building blocks, or when the quantum fluctuations are small. Therefore, we shall ask if GFT really allows the existence of a quantum bounce? Either quantum bounce or early universe calls for a more accurate description of the state consisting only a limited number of GFT quanta, which may be too small that the condensate approximation breaks down.

Black Holes In chapter 3, the micro-state of a spherically symmetric vacuum space-time is built, while no quantum dynamics is considered. A possible improvement of this model can be achieved by including the dynamics. One may also ask if the black hole evaporation can be described in GFT. It is also of great interested if we can identify a GFT state with a black hole horizon, beside maximising the entropy. For example, one can check if Ryu-Takayanagi formula can be recovered from a GFT microscopic state, and identify a horizon-like region from GFT states [232–234]. Furthermore, as a test ground of quantum theory of gravity, more physical black holes are necessary to be investigated in GFT, such as the Kerr black hole. However, physical black holes are usually not highly symmetric. Foliation of a space into shells enables us to investigate a Schwarzschild black hole with GFT condensates, but a Kerr space-time can not be treated in a similar way. Before solving such a complicated problem, one can first try building inhomogeneous or anisotropic GFT state as the first step.

Inhomogeneity GFT condensate state is a state of homogeneous geometry. However, it is important to consider inhomogeneity in GFT in order to have a wider range of applications. To this end, one can explore the possibility of including inhomogeneity in GFT condensates. For example, it can be introduced as quantum fluctuations, and a better method is expected. If this direction is not correct, then we shall ask, how to make GFT reproduce an inhomogeneous geometry, or how to go beyond the homogeneous GFT condensates?

SYK Model As discussed in Chapter 4, AR-like matter can be viewed as a perturbation around Boulatov model. AR is similar with an SYK model that they are both dominated by melonic graphs at large N. So one can explore whether an true SYK matter can be recovered in a similar way. In addition, more recently, Jackiw-Teitelboim (JT)-dilaton gravity is suggested to be a bulk correspondence of a high-temperature double scaled SYK theory on boundary [235, 236], and it has been shown that JT gravity is dual to a matrix model [237, 238]. Therefore, it seems hopeful that we can get clue to the relation between the SYK theory and the GFT.

As a young candidate of quantum gravity, GFT has lots of aspects to be explored. Even for theories with long histories like String Theory and LQG, there is still a long journey to quantum gravity. Both quantum physics and GR brought conceptual revolutions to the way that people understand the world where we are living. The way to a quantum theory of gravity has not been found out completely, and what we are facing with is not only the computational challenges, but also conceptual issues, which have been illustrated by the three projects in this dissertation. There are still many aspects of physical reference frame to be explored. For example, what is the physical role of clocks in quantum gravity? How to solve the problem of time? As for GFT, it provides a promising scheme to explore the non-perturbative approaches to quantum gravity. We hope it will make more exciting progress including but not limited to the issues mentioned above in near future.

Appendix A

$SU(2)$ Recouping Theory and Spin Network States

This part gives a brief introduction to $SU(2)$ recoupling theory, which is essential in this dissertation. For detailed reviews, we refer nice papers written by Martin-Dussaud [115] and Mäkinen [116] for the interested readers.

A.1 Basics

A.1.1 Wigner Matrices

The Haar measure $\mathrm{d}g$ defines the integral over $SU(2)$. It is a unique normalised quasi-regular Borel measure such that

$$\int \mathrm{d}g = 1, \tag{A.1}$$

and

$$\int \mathrm{d}g f(gu) = \int \mathrm{d}g f(ug) = \int \mathrm{d}g f(g), \tag{A.2}$$

where $u \in SU(2)$ is a group element.

The Hilbert space of $SU(2)$ group is denoted by $L^2(SU(2))$, which is defined as a space of complex functions $f : SU(2) \to \mathbb{C}$ such that

$$\int_{SU(2)} \mathrm{d}g |f(g)|^2 \mathrm{d}g < \infty, \tag{A.3}$$

and its scalar product is

$$(f_1, f_2) \equiv \int_{SU(2)} f_1^*(g) f_2(g) \mathrm{d}g. \tag{A.4}$$

The spin-j representation of $SU(2)$ group is a $(2j+1)$-dimensional irreducible representation. It is associated with a j-Hilbert space whose canonical basis is the magnetic

basis, $|j,m\rangle$, where $m \in \{-j, -j+1, ..., j-1, j\}$. The action of an $SU(2)$ group element g over a j-Hilbert space can be represented in magnetic basis with a Wigner matrix, whose matrix elements are defined as

$$D^j_{mn}(g) \equiv \langle j,n|\, g\, |j,m\rangle\,. \tag{A.5}$$

Schur orthogonality relations implies the Wigner matrices form an orthogonal family such that

$$\int_{SU(2)} \mathrm{d}g \overline{D^{j'}_{m'n'}(g)} D^j_{mn}(g) = \frac{1}{d_j}\delta_{jj'}\delta_{mm'}\delta_{nn'}, \tag{A.6}$$

where $d_j = 2j+1$. An important property of Wigner matrix is that

$$\overline{D^j_{mn}(g)} = (-1)^{m-n} D^j_{-m,-n}(g). \tag{A.7}$$

The group multiplication rule reads

$$D^j_{mn}(g_1 g_2) = \sum_l D^j_{ml}(g_1) D^j_{ln}(g_2). \tag{A.8}$$

According to Peter-Weyl's theorem, any function $f \in L^2(SU(2))$ can be decomposed into

$$f(g) = \sum_{\{j,m,n\}} f^j_{mn} D^j_{mn}(g), \tag{A.9}$$

where the coefficients $f^j_{mn} \in \mathbb{C}$, and $D^j_{mn}(g)$ acts as a basis of $L^2(SU(2))$.

A.1.2 Intertwiners

If we have two irreducible representations of $SU(2)$ labelled by j_1 and j_2, then their tensor product is given by

$$|j_1, m_1; j_2, m_2\rangle \equiv |j_1, m_1\rangle \otimes |j_2, m_2\rangle\,. \tag{A.10}$$

This tensor product has another basis $|(j_1 j_2)j, m\rangle$ which relates with $|j_1, m_1; j_2, m_2\rangle$ through

$$|(j_1 j_2)j, m\rangle = \sum_{m_1, m_2} C^{j_1 j_2 j}_{m_1 m_2 m}\, |j_1, m_1; j_2, m_2\rangle\,, \tag{A.11}$$

and

$$C^{j_1 j_2 j}_{m_1 m_2 m} \equiv \langle j_1, m_1; j_2, m_2 | (j_1 j_2) j, m\rangle \tag{A.12}$$

is the Clebsch-Gordan coefficient. It has three important properties:

1. Clebsch-Gordan coefficient is well-defined and non-vanishing only if the spins satisfy the triangle inequality

$$|j_1 - j_2| \le j \le j_1 + j_2, \tag{A.13}$$

and

$$j_1 + j_2 + j = \text{integer}. \tag{A.14}$$

2. $C^{j_1 j_2 j}_{m_1 m_2 m} = 0$ if $m \neq m_1 + m_2$.

3. It satisfies the orthogonality relations

$$\sum_{m_1,m_2} C^{j_1 j_2 j}_{m_1 m_2 m} C^{j_1 j_2 j'}_{m_1 m_2 m'} = \delta_{jj'}\delta_{mm'}, \tag{A.15}$$

$$\sum_{m_1,m_2} C^{j_1 j_2 j}_{m_1 m_2 m} C^{j_1 j_2 j}_{m_1' m_2' m} = \delta_{m_1 m_1'}\delta_{m_2 m_2'}. \tag{A.16}$$

A Wigner's $3j$ symbol is defined as

$$\begin{pmatrix} j_1 & j_2 & j_3 \\ m_1 & m_2 & m_3 \end{pmatrix} \equiv \frac{(-1)^{j_1 - j_2 - m_3}}{\sqrt{2j_3+1}} C^{j_1 j_2 j_3}_{m_1, m_2, -m_3}. \tag{A.17}$$

If we have the tensor product among three representations, j_1, j_2, and j_3, then there exists an eigen-vector of the total angular momentum operator $J^{(1)} + J^{(2)} + J^{(3)}$

$$|0\rangle = \sum_{m_1,m_2,m_3} \begin{pmatrix} j_1 & j_2 & j_3 \\ m_1 & m_2 & m_3 \end{pmatrix} |j_1, m_1\rangle \otimes |j_2, m_2\rangle \otimes |j_3, m_3\rangle , \tag{A.18}$$

which is of zero eigen-value.

The $6j$ symbol is defined as

$$\begin{Bmatrix} j_1 & j_2 & j_3 \\ j_4 & j_5 & j_6 \end{Bmatrix} = \sum_{j_i, m_i} (-1)^{\sum_{a=1}^{6}(j_a - m_a)} \begin{pmatrix} j_1 & j_2 & j_3 \\ -m_1 & -m_2 & -m_3 \end{pmatrix} \begin{pmatrix} j_1 & j_5 & j_6 \\ m_1 & -m_5 & m_6 \end{pmatrix} \cdot \begin{pmatrix} j_4 & j_2 & j_6 \\ m_4 & m_2 & -m_6 \end{pmatrix} \begin{pmatrix} j_4 & j_5 & j_3 \\ -m_4 & m_5 & m_3 \end{pmatrix}. \tag{A.19}$$

It similarly gives a possible decomposition of the tensor production among four irreducible representations.

An intertwiner ι is an invariant tensor of $SU(2)$. We can imagine it as a knot that 'intertwines' the irreducible representations together, which is more obvious in graphic calculus to be discussed in the next section. For example, the only three-valent intertwiners are given by $3j$-symbols:

$$\iota_{m_1 m_2 m_3} = \begin{pmatrix} j_1 & j_2 & j_3 \\ m_1 & m_2 & m_3 \end{pmatrix}. \tag{A.20}$$

And the Wigner's $4j$-symbol is an example for 4-valent intertwiner, whose definition is

$$\begin{pmatrix} j_1 & j_2 & j_3 & j_4 \\ m_1 & m_2 & m_3 & m_4 \end{pmatrix}^{(j)} \equiv \sum_m (-1)^{j-m} \begin{pmatrix} j_1 & j_2 & j \\ m_1 & m_2 & m \end{pmatrix} \begin{pmatrix} j & j_3 & j_4 \\ m & m_2 & m_4 \end{pmatrix}, \tag{A.21}$$

which can be applied to give another possible decomposition of the production of four spin-j representations.

A.2 Graphic Formalism

The calculation in $SU(2)$ recoupling theory can be simplified by applying the graphic formalism. This section lists examples that are frequently used.

The Kronecker delta is a single line in graphic framework:

$$\delta_{mn} = m \overset{j}{\text{———}} n. \tag{A.22}$$

Invariant rank-2 tensors of $SU(2)$

$$\epsilon_{AB} = \begin{pmatrix} 0 & 1 \\ -1 & 0 \end{pmatrix}, \quad \epsilon^{AB} = \begin{pmatrix} 0 & 1 \\ -1 & 0 \end{pmatrix}, \tag{A.23}$$

are represented as

$$\epsilon^{(j)}_{mn} = m \overset{j}{\text{——}\rightarrow\text{——}} n, \tag{A.24}$$

and

$$\epsilon^{(j)mn} = m \overset{j}{\text{——}\rightarrow\text{——}} n. \tag{A.25}$$

The $3j$ symbol is the basic object of graphic calculus, which is

$$\begin{pmatrix} j_1 & j_2 & j_3 \\ m_1 & m_2 & m_3 \end{pmatrix} =$$

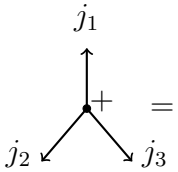

$=$

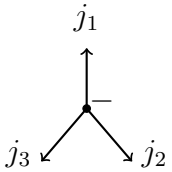

. (A.26)

Summation over a magnetic index m from $-j$ to j is achieved by gluing two links. Accordingly, the $4j$ symbols are

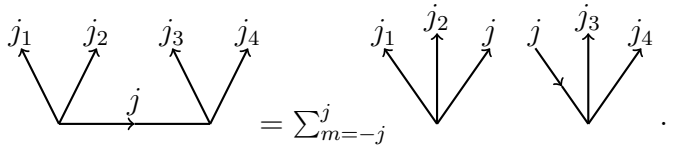

. (A.27)

The graph of a $6j$ symbol, similarly, can be obtained by gluing four $3j$ symbols according to (A.19):

$$\begin{Bmatrix} j_1 & j_2 & j_3 \\ k_1 & k_2 & k_3 \end{Bmatrix} =$$

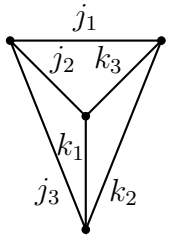

. (A.28)

A.3 Spin Network

The $SU(2)$ recoupling theory has an important application to LQG and GFT [52]. The basis of the Hilbert space in LQG is the SNW $|\Gamma, \iota, j\rangle$, where Γ denotes an abstract directed graph consisting of nodes and links. The intertwiner ι is assigned to the nodes, and the spin j is on the links.

Suppose we have a SNW containing N 4-valent nodes and l links. According to Peter-Weyl theorem, such a SNW can be written as a function $\Psi(g_1, g_2, g_3, g_4) \in L^2\left(SU(2)^N\right)_\Gamma$, where $L^2\left(SU(2)^N\right)_\Gamma$ is a subspace of $L^2\left(SU(2)^N\right)$. To this end, one first note that the Wigner matrices can be represented by a graph:

$$D^j_{mn}(g) = \quad m \xleftarrow{\quad g, j \quad} n, \tag{A.29}$$

and this can be associated to each link from Γ with $g \in SU(2)$. Then we can virtually split the nodes such that

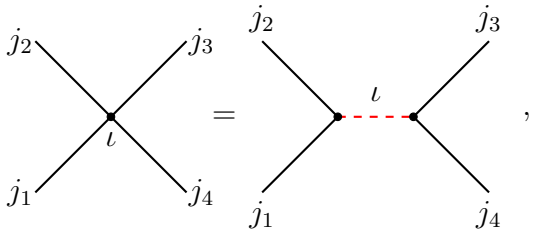

(A.30)

and assign a $4j$ symbol $\begin{pmatrix} j_1 & j_2 & j_3 & j_4 \\ m_1 & m_2 & m_3 & m_4 \end{pmatrix}^{(\iota)}$ to the split node. After summing over the magnetic indices, one obtains

$$\Psi(g_1, g_2, g_3, g_4) = \sum_{m,n} \prod_{N \in \Gamma} \begin{pmatrix} j_{N1} & j_{N2} & j_{N3} & j_{N4} \\ m_{N1} & m_{N2} & m_{N3} & m_{N4} \end{pmatrix}^{(\iota_N)} \prod_{N_i=1}^{4} D^{j_{N_i}}_{m_{N_i} n_{N_i}}(g_{N_i}) \tag{A.31}$$

as a SNW wave-function.

A.4 Useful Properties

This section lists properties of Wigner's $3j$ and $6j$ symbols which helps in Chapter 4, and they can be simply derived through graphic calculus.

First of all, the $3j$ symbol is invariant under the action of $SU(2)$ group,

$$D^{j_1}_{m_1 n_1} D^{j_2}_{m_2 n_2} D^{j_3}_{m_3 n_3} \begin{pmatrix} j_1 & j_2 & j_3 \\ n_1 & n_2 & n_3 \end{pmatrix} = \begin{pmatrix} j_1 & j_2 & j_3 \\ m_1 & m_2 & m_3 \end{pmatrix}. \tag{A.32}$$

Wigner $3j$ symbol is also symmetric under the even permutations of indices, and an additional phase under odd permutations

$$\begin{pmatrix} j_1 & j_2 & j_3 \\ m_1 & m_2 & m_3 \end{pmatrix} = (-1)^{j_1+j_2+j_3} \begin{pmatrix} j_2 & j_1 & j_3 \\ m_2 & m_1 & m_3 \end{pmatrix} = (-1)^{j_1+j_2+j_3} \begin{pmatrix} j_1 & j_2 & j_3 \\ -m_1 & -m_2 & -m_3 \end{pmatrix}. \tag{A.33}$$

The $3j$ symbols satisfy two orthonormal relations such that

$$(2j_3+1) \sum_{m_1,m_2} \begin{pmatrix} j_1 & j_2 & j_3 \\ m_1 & m_2 & m_3 \end{pmatrix} \begin{pmatrix} j_1 & j_2 & j_3' \\ m_1 & m_2 & m_3' \end{pmatrix} = \delta_{j_3,j_3'} \delta_{m_3,m_3'}, \tag{A.34}$$

$$\sum_{j_3,m_3} (2j_3+1) \begin{pmatrix} j_1 & j_2 & j_3 \\ m_1 & m_2 & m_3 \end{pmatrix} \begin{pmatrix} j_1 & j_2 & j_3 \\ m_1' & m_2' & m_3 \end{pmatrix} = \delta_{m_1,m_2'} \delta_{m_2,m_2'}, \tag{A.35}$$

Finally, the $3j$ symbol satisfies

$$\sum_m (-1)^{j-m} \begin{pmatrix} j & j & k \\ m & -m & 0 \end{pmatrix} = \sqrt{2j+1}\delta_{k,0}. \tag{A.36}$$

and

$$\begin{pmatrix} j_1 & j_2 & 0 \\ m_1 & m_2 & 0 \end{pmatrix} = \delta_{j_1,j_2} \frac{1}{\sqrt{2j_1+1}} \delta_{m_1,-m_2} \tag{A.37}$$

For the $6j$ symbol, one has

$$\begin{aligned} &\sum_{n_1,n_2,n_3} (-1)^{\sum_{a=1}^3 (k_a - n_a)} \begin{pmatrix} j_1 & k_2 & k_3 \\ m_1 & -n_2 & n_3 \end{pmatrix} \begin{pmatrix} k_1 & j_2 & k_3 \\ n_1 & m_2 & -n_3 \end{pmatrix} \begin{pmatrix} k_1 & k_2 & j_3 \\ -n_1 & n_2 & m_3 \end{pmatrix} \\ &= \begin{Bmatrix} j_1 & j_2 & j_3 \\ k_1 & k_2 & k_3 \end{Bmatrix} \begin{pmatrix} j_1 & j_2 & j_3 \\ m_1 & m_2 & m_3 \end{pmatrix}. \end{aligned} \tag{A.38}$$

Finally when one of the spin index (say j_6) vanishes we have

$$\begin{Bmatrix} j_1 & j_2 & j_3 \\ j_4 & j_5 & 0 \end{Bmatrix} = \frac{\delta_{j_1,j_5}\delta_{j_2,j_4}}{\sqrt{d_{j_1} d_{j_2}}} (-1)^{j_1+j_2+j_3}, \tag{A.39}$$

where j_1, j_2, and j_3 satisfy the triangle inequality.

Appendix B

Edge-Coloured Graph and Topology

This is a brief introduction to definitions of graph structures that are encoded with topological information, which are useful in Chapter 3. For interested readers, we refer to a nice paper [184], which illustrates the idea of homogeneous geometries as GFT condensates in detail. The review [90] also contains the basics of graph-encoded topologies.

A $d-$*simplex* is a $d-$dimensional object. For example, a $2-$simplex is a triangle, and a $3-$simplex a tetrahedron. The finite set of simplices is a *simplicial complex*, where the simplices are glued along their sub-simplices. The union of all simplices is a polyhedron $|K|$ of the simplicial complex K. If there exists a homeomorphism f mapping the polyhedron $|K|$ to a topological space X, then (f, K) is a triangulation of X [100].

A d-dimensional *simplicial manifold* is a simplicial complex, with the neighborhood of each point is homeomorphic to a d-dimensional ball [82]. A simplicial *pseudo-manifold* is obtained by gluing d-simplices along their $(d-1)$-subsimplices until a complex with no boundary is formed. A Riemannian metric can be equipped to a d-dimensional simplicial manifold with three assumptions [82]:

1) The space in the $d-$simplices is flat;

2) The $(d-1)-$faces are flat as well;

3) The metric is continuous at $(d-1)-$faces.

A closed graph $\mathcal{B}^{1234}$ of 4 colours is defined as an edge-coloured graph that is bipartite as well as 4-regular, and the four edges on a vertex should be labelled by different colours. A simple example is

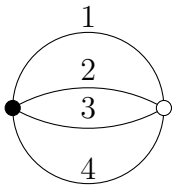

Then a d-bubble is a maximal connected d coloured sub-graph of $\mathcal{B}^{1234}$. For example, 3-bubbles of the example above can be

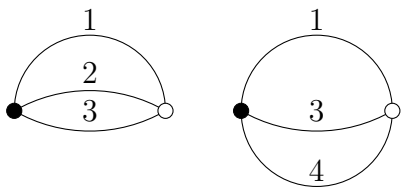

and so son. The 0-bubbles, 1-bubbles, 2-bubbles, and 3-bubbles are vertices, faces, and 3-dimensional cells respectively.

If we associate every d-bubble in $\mathcal{B}^{1234}$ with a $(3-d)$-simplex, and translate the nested structure of the bubbles to the dual nested structure of the simplicial cells, then we will obtain a non-branching, pure, strongly-connected simplicial complex, which is a *pseudo-manifold*.

A *melonic* move creates or removes melonic graph(s) as follows

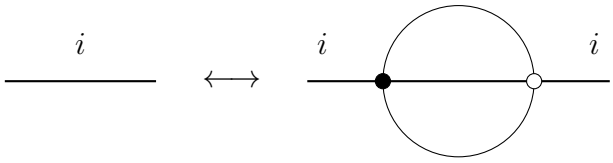

and preserves the topology of the graphs.

Appendix C

Negative-mass Black Hole

This part shows the relational description of a quantum GFT state built in Chapter 3, which corresponds to a classical negative-mass $M < 0$ Schwarzschild black hole. Though it is non-physical, here we use it as an example to show how to deal with a state corresponding to a black hole with a naked singularity.

When M is negative, the clock scalar field is unchanged with $\phi_1 = \beta_1 t$ and the rod scalar field has a real solution

$$\phi_2(r) = \sqrt{r(r-2GM)} + 2M\text{arcsinh}\left(\sqrt{-\frac{r}{2GM}}\right). \tag{C.1}$$

The Klein-Gordon equation (3.93) remains unchanged, and the derivatives of solution (3.92) and (C.1) with respect to r are the same. The expression (3.92) is modified to (C.1) because when $x > 1$, $\text{arctanh}(x)$ as a real-valued function is ill-defined. When $r \to 0$, $f(r) \simeq -2GM/r$. As a result, the $\phi_1(r)$ reads

$$\phi_2(r) \simeq \frac{\sqrt{2}\beta_1 r}{3\sqrt{-GM/r}}. \tag{C.2}$$

Thus, $\phi_2 \simeq 0$ corresponds to a naked singularity with

$$r = \left(-\frac{9GM\phi_2^2}{\sqrt{2}\beta_2^2}\right)^{\frac{1}{3}}. \tag{C.3}$$

For the potential, one obtains

$$V'(\phi_2) \simeq -\frac{\sqrt{2}\beta_2^2}{\phi_2}, \tag{C.4}$$

and

$$V(\phi_2) \simeq \sqrt{2}\beta_2^2 \ln\left(\frac{1}{\phi_2}\right). \tag{C.5}$$

In order that the energy-momentum tensor of ϕ_2 is negligible, $|\beta_2|$ is a very small constant too. Thus, the potential $V(\phi_1)$ at order β_2^2 can be dropped.

Repeating the same procedure, one obtains the near-singularity behaviour when $M < 0$,

$$A_{rel}(\phi_u) = 4\pi \left(\frac{9GM\phi_u^2}{\sqrt{2}\beta_1^2} \right)^{\frac{2}{3}}, \tag{C.6}$$

$$V_{3rel}(\phi_u) = \frac{4\pi}{\beta_1} \left(\frac{9GM\phi_1^2}{\sqrt{2}\beta_1^2} \right)^{\frac{2}{3}} \delta\phi_2|_{\phi_2=\phi_u}. \tag{C.7}$$

A negative-mass black hole has a naked singularity, and no horizon exists in this case. Hence, no wave-function corresponds to the near-horizon regime. Together with the positive-mass case, the wave-functions are

$$\text{Schwarzschild} \begin{cases} M > 0 & \begin{cases} \text{Asymptotic infinity}(\phi \to \infty) & \tilde{\varsigma}(\phi)^{-1} \propto \phi^2 \\ \text{Near-horizon}(\phi \sim 0) & \tilde{\varsigma}(\phi)^{-1} \propto (\phi^2 + 16\beta_1^2(GM)^2)^2 \\ \text{Near-singularity} & \text{Not available} \end{cases} \\ M < 0 & \begin{cases} \text{Asymptotic infinity}(\phi \to \infty) & \tilde{\varsigma}(\phi)^{-1} \propto \phi^2 \\ \text{Near-horizon} & \text{Non-existent} \\ \text{Near-singularity}(\phi \sim 0) & \tilde{\varsigma}(\phi)^{-1} \propto \phi^{\frac{4}{3}} \end{cases} \end{cases}. \tag{C.8}$$

The curvature singularity at $r = 0$ corresponds to a sphere of vanishing area. As mentioned, the simplest state is a seed state, so there is no such a GFT state describing a sphere with zero area, and we easily bypass the singularity even when $M < 0$. Certainly, the resolution of singularity needs an explicit calculation of the curvature. Lacking a GFT curvature operator, here we only give a very naïve argument to show the non-singularity of a GFT state.

Bibliography

[1] C. Rovelli, *Notes for a brief history of quantum gravity*, in *9th Marcel Grossmann Meeting on Recent Developments in Theoretical and Experimental General Relativity, Gravitation and Relativistic Field Theories (MG 9)*, p. 742–768, 6, 2000 [gr-qc/0006061].

[2] A. Einstein, *Näherungsweise Integration der Feldgleichungen der Gravitation*, *Sitzungsberichte der Königlich Preußischen Akademie der Wissenschaften* (1916) 688–696.

[3] O. Klein, *Zur fünfdimensionalen darstellung der relativitätstheorie*, *Zeitschrift für Physik* **46** (1928) 188–208.

[4] O. Klein, *Aktuella problem kring fysikens sma och stora tal*, *Kosmos* **32** (1954) 33.

[5] O. Klein, *Generalization of Einsteins theory of gravitation considered from the point of view of quantum field theory*, in *Fuenfzig Jahre Relativitätstheorie. Bern, 11–16 Juli 1955* (1956).

[6] L. Rosenfeld, *Zur quantelung der wellenfelder*, *Annalen der Physik* **397** (1930) 113–152 [https://onlinelibrary.wiley.com/doi/pdf/10.1002/andp.19303970107].

[7] L. Rosenfeld, *Über die gravitationswirkungen des lichtes*, *Zeitschrift für Physik* **65** (1930) 589–599.

[8] B. D.I. and G. F.M., *Neutrino Hypothesis and Conservation of Energy*, *Pod Znamenem Marxisma* **6** (1934) 147–157.

[9] M. Fierz, *Force-free particles with any spin*, *Helv. Phys. Acta* **12** (1939) 3–37.

[10] W. Pauli and M. Fierz, *On Relativistic Field Equations of Particles With Arbitrary Spin in an Electromagnetic Field*, *Helv. Phys. Acta* **12** (1939) 297–300.

[11] M. Bronstein, *Quantentheorie schwacher Gravitationsfelder*, *Physikalische Zeitschrift der Sowjetunion* **9** (1936) 140–157.

[12] P.G. Bergmann, *Non-linear field theories*, *Phys. Rev.* **75** (1949) 680–685.

[13] P.G. Bergmann and J.H.M. Brunings, *Non-linear field theories ii. canonical equations and quantization*, *Rev. Mod. Phys.* **21** (1949) 480–487.

[14] P.G. Bergmann, *Introduction of "true observables" into the quantum field equations*, *Nuovo Cim* **3** (1956) 1177–1185.

[15] P.A.M. Dirac, *Generalized hamiltonian dynamics*, *Canadian Journal of Mathematics* **2** (1950) 129–148.

[16] P.A.M. Dirac, *The Hamiltonian form of field dynamics*, *Can. J. Math.* **3** (1951) 1–23.

[17] S.N. Gupta, *On the elimination of divergencies from quantum electrodynamics*, *Proceedings of the Physical Society. Section A* **64** (1951) 426.

[18] S.N. Gupta, *Quantization of einstein's gravitational field: Linear approximation*, *Proceedings of the Physical Society. Section A* **65** (1952) 161.

[19] S.N. Gupta, *Quantization of einstein's gravitational field: General treatment*, *Proceedings of the Physical Society. Section A* **65** (1952) 608.

[20] C.W. Misner, *Feynman quantization of general relativity*, *Rev. Mod. Phys.* **29** (1957) 497–509.

[21] J. Polchinski, *String Theory*, vol. 1 of *Cambridge Monographs on Mathematical Physics*, Cambridge University Press (1998), 10.1017/CBO9780511816079.

[22] J. Polchinski, *String Theory*, vol. 2 of *Cambridge Monographs on Mathematical Physics*, Cambridge University Press (1998), 10.1017/CBO9780511618123.

[23] D. Rickles, *A brief history of string theory: From dual models to M-theory*, Springer (2016).

[24] R.P. Feynman, *Quantum theory of gravitation*, *Acta Phys. Polon.* **24** (1963) 697–722.

[25] B.S. DeWitt, *The quantization of geometry*, in *International Conference on Relativistic Theories of Gravitation*, p. 131–147, 1964.

[26] B.S. DeWitt, *Theory of radiative corrections for non-abelian gauge fields*, *Phys. Rev. Lett.* **12** (1964) 742–746.

[27] B.S. DeWitt, *Quantum theory of gravity. ii. the manifestly covariant theory*, *Phys. Rev.* **162** (1967) 1195–1239.

[28] B.S. DeWitt, *Quantum theory of gravity. iii. applications of the covariant theory*, *Phys. Rev.* **162** (1967) 1239–1256.

[29] L.D. Faddeev and V.N. Popov, *Feynman diagrams for the yang-mills field*, *Physics Letters B* **25** (1967) 29–30.

[30] G. 't Hooft, *Renormalizable Lagrangians for Massive Yang-Mills Fields*, *Nucl. Phys. B* **35** (1971) 167–188.

[31] G. 't Hooft and M.J.G. Veltman, *Regularization and Renormalization of Gauge Fields*, *Nucl. Phys. B* **44** (1972) 189–213.

[32] G. 't Hooft, *An algorithm for the poles at dimension four in the dimensional regularization procedure*, *Nuclear Physics B* **62** (1973) 444–460.

[33] G. 't Hooft and M.J.G. Veltman, *One loop divergencies in the theory of gravitation*, *Ann. Inst. H. Poincare Phys. Theor. A* **20** (1974) 69–94.

[34] S. Deser and P. van Nieuwenhuizen, *One-loop divergences of quantized einstein-maxwell fields*, *Phys. Rev. D* **10** (1974) 401–410.

[35] S. Deser and P. van Nieuwenhuizen, *Nonrenormalizability of the quantized dirac-einstein system*, *Phys. Rev. D* **10** (1974) 411–420.

[36] S. Weinberg, *Ultraviolet Divergences in Quantum Theories of Gravitation*, in *General Relativity: An Einstein Centenary Survey*, p. 790–831 (1980).

[37] D.Z. Freedman, P. van Nieuwenhuizen and S. Ferrara, *Progress toward a theory of supergravity*, *Phys. Rev. D* **13** (1976) 3214–3218.

[38] S. Deser and B. Zumino, *Consistent Supergravity*, *Phys. Lett. B* **62** (1976) 335.

[39] K.S. Stelle, *Renormalization of higher-derivative quantum gravity*, *Phys. Rev. D* **16** (1977) 953–969.

[40] G. Veneziano, *Construction of a crossing - symmetric, Regge behaved amplitude for linearly rising trajectories*, *Nuovo Cim. A* **57** (1968) 190–197.

[41] T. Yoneya, *Quantum gravity and the zero slope limit of the generalized Virasoro model*, *Lett. Nuovo Cim.* **8** (1973) 951–955.

[42] T. Yoneya, *Connection of Dual Models to Electrodynamics and Gravidynamics*, *Prog. Theor. Phys.* **51** (1974) 1907–1920.

[43] J. Scherk and J.H. Schwarz, *Dual Models for Nonhadrons*, *Nucl. Phys. B* **81** (1974) 118–144.

[44] M.B. Green and J.H. Schwarz, *Anomaly Cancellation in Supersymmetric D=10 Gauge Theory and Superstring Theory*, *Phys. Lett. B* **149** (1984) 117–122.

[45] D.J. Gross, J.A. Harvey, E. Martinec and R. Rohm, *Heterotic string*, *Phys. Rev. Lett.* **54** (1985) 502–505.

[46] P. Candelas, G.T. Horowitz, A. Strominger and E. Witten, *Vacuum configurations for superstrings*, *Nucl. Phys. B* **258** (1985) 46–74.

[47] M.B. Green, J.H. Schwarz and E. Witten, *SUPERSTRING THEORY. VOL. 1: INTRODUCTION*, Cambridge Monographs on Mathematical Physics (7, 1988).

[48] M.B. Green, J.H. Schwarz and E. Witten, *SUPERSTRING THEORY. VOL. 2: LOOP AMPLITUDES, ANOMALIES AND PHENOMENOLOGY* (7, 1988).

[49] P.A.M. Dirac, *The Theory of Gravitation in Hamiltonian Form*, *Proceedings of the Royal Society of London Series A* **246** (1958) 333–343.

[50] R. Arnowitt, S. Deser and C.W. Misner, *The Dynamics of General Relativity*, in *in Gravitation: An Introduction to Current Research (Chap. 7). Edited by Louis Witten. John Wiley & Sons Inc*, p. 227 (1962).

[51] B.S. DeWitt, *Quantum theory of gravity. i. the canonical theory*, *Phys. Rev.* **160** (1967) 1113–1148.

[52] C. Rovelli, *Quantum gravity*, Cambridge University Press (2008).

[53] C. Rovelli and F. Vidotto, *Covariant loop quantum gravity: An elementary introduction to quantum gravity and Spinfoam theory*, Cambridge University Press (2020).

[54] A. Ashtekar, *New hamiltonian formulation of general relativity*, *Phys. Rev. D* **36** (1987) 1587–1602.

[55] A. Ashtekar, *New Hamiltonian Formulation of General Relativity*, *Phys. Rev. D* **36** (1987) 1587–1602.

[56] A. Sen, *GRAVITY AS A SPIN SYSTEM*, *Phys. Lett. B* **119** (1982) 89–91.

[57] T. Jacobson and L. Smolin, *Nonperturbative Quantum Geometries*, *Nucl. Phys. B* **299** (1988) 295–345.

[58] C. Rovelli and L. Smolin, *Knot theory and quantum gravity*, *Phys. Rev. Lett.* **61** (1988) 1155–1158.

[59] C. Rovelli and L. Smolin, *Loop Space Representation of Quantum General Relativity*, *Nucl. Phys. B* **331** (1990) 80–152.

[60] R. Penrose, *Angular momentum: an approach to combinatorial space-time*, 1971.

[61] C. Rovelli and L. Smolin, *Spin networks and quantum gravity*, *Physical Review D* **52** (1995) 5743–5759.

[62] J.C. Baez, *Spin networks in nonperturbative quantum gravity*, .

[63] J.C. Baez, *An Introduction to Spin Foam Models of BF Theory and Quantum Gravity*, *Lect. Notes Phys.* **543** (2000) 25–93 [gr-qc/9905087].

[64] A. Perez, *Spin foam models for quantum gravity*, *Class. Quant. Grav.* **20** (2003) R43 [gr-qc/0301113].

[65] E.R. Livine, *The Spinfoam Framework for Quantum Gravity*, other thesis, 10, 2010, [1101.5061].

[66] A. Perez, *The Spin Foam Approach to Quantum Gravity*, *Living Rev. Rel.* **16** (2013) 3 [1205.2019].

[67] J.B. Hartle and S.W. Hawking, *Path Integral Derivation of Black Hole Radiance*, *Phys. Rev. D* **13** (1976) 2188–2203.

[68] S.W. Hawking, *Quantum Gravity and Path Integrals*, *Phys. Rev. D* **18** (1978) 1747–1753.

[69] S.W. Hawking, *THE PATH INTEGRAL APPROACH TO QUANTUM GRAVITY*, in *General Relativity: An Einstein Centenary Survey*, p. 746–789 (1980).

[70] J.J. Halliwell and S.W. Hawking, *The Origin of Structure in the Universe*, *Phys. Rev. D* **31** (1985) 1777.

[71] E. Witten, *Topological Quantum Field Theory*, *Commun. Math. Phys.* **117** (1988) 353.

[72] M.P. Reisenberger, *World sheet formulations of gauge theories and gravity*, in *7th Marcel Grossmann Meeting on General Relativity (MG 7)*, 12, 1994 [gr-qc/9412035].

[73] F. Markopoulou and L. Smolin, *Quantum geometry with intrinsic local causality*, *Phys. Rev. D* **58** (1998) 084032 [gr-qc/9712067].

[74] J.W. Barrett and L. Crane, *Relativistic spin networks and quantum gravity*, *J. Math. Phys.* **39** (1998) 3296–3302 [gr-qc/9709028].

[75] J.C. Baez, *Spin foam models*, *Class. Quant. Grav.* **15** (1998) 1827–1858 [gr-qc/9709052].

[76] D. Oriti, *Approaches to quantum gravity: Toward a new understanding of space, time and matter*, Cambridge University Press (2009).

[77] C. Rovelli, *A new look at loop quantum gravity*, *Class. Quant. Grav.* **28** (2011) 114005 [1004.1780].

[78] C. Rovelli, *Zakopane lectures on loop gravity*, *PoS* **QGQGS2011** (2011) 003 [1102.3660].

[79] C. Rovelli, *Covariant loop gravity*, *Lect. Notes Phys.* **863** (2013) 57–66.

[80] L. Bombelli, J. Lee, D. Meyer and R. Sorkin, *Space-Time as a Causal Set*, *Phys. Rev. Lett.* **59** (1987) 521–524.

[81] S. Surya, *The causal set approach to quantum gravity*, *Living Rev. Rel.* **22** (2019) 5 [1903.11544].

[82] F. David, *Simplicial quantum gravity and random lattices*, in *Les Houches Summer School on Gravitation and Quantizations, Session 57*, p. 0679–750, 7, 1992 [hep-th/9303127].

[83] P. Di Francesco, P.H. Ginsparg and J. Zinn-Justin, *2-D Gravity and random matrices*, *Phys. Rept.* **254** (1995) 1–133 [hep-th/9306153].

[84] R. Penrose, *Twistor algebra*, *J. Math. Phys.* **8** (1967) 345.

[85] R. Penrose, *Nonlinear Gravitons and Curved Twistor Theory*, *Gen. Rel. Grav.* **7** (1976) 31–52.

[86] D. Oriti, *Quantum gravity as a quantum field theory of simplicial geometry*, gr-qc/0512103.

[87] D. Oriti, *The Group field theory approach to quantum gravity*, gr-qc/0607032.

[88] D. Oriti, *The microscopic dynamics of quantum space as a group field theory*, in *Foundations of Space and Time: Reflections on Quantum Gravity*, p. 257–320, 10, 2011 [1110.5606].

[89] T. Krajewski, *Group field theories*, *PoS* **QGQGS2011** (2011) 005 [1210.6257].

[90] R. Gurau and J.P. Ryan, *Colored Tensor Models - a review*, *SIGMA* **8** (2012) 020 [1109.4812].

[91] V. Rivasseau, *Quantum Gravity and Renormalization: The Tensor Track*, *AIP Conf. Proc.* **1444** (2012) 18–29 [1112.5104].

[92] V. Rivasseau, *Random Tensors and Quantum Gravity*, *SIGMA* **12** (2016) 069 [1603.07278].

[93] T. Regge, *GENERAL RELATIVITY WITHOUT COORDINATES*, *Nuovo Cim.* **19** (1961) 558–571.

[94] R. Loll, *Quantum Gravity from Causal Dynamical Triangulations: A Review*, *Class. Quant. Grav.* **37** (2020) 013002 [1905.08669].

[95] D. Weingarten, *EUCLIDEAN QUANTUM GRAVITY ON A LATTICE*, *Nucl. Phys. B* **210** (1982) 229–245.

[96] V.A. Kazakov, *Bilocal Regularization of Models of Random Surfaces*, *Phys. Lett. B* **150** (1985) 282–284.

[97] F. David, *A model of random surfaces with non-trivial critical behaviour*, *Nuclear Physics B* **257** (1985) 543–576.

[98] J. Ambjorn, B. Durhuus and J. Frohlich, *Diseases of Triangulated Random Surface Models, and Possible Cures*, *Nucl. Phys. B* **257** (1985) 433–449.

[99] D. Boulatov, V. Kazakov, I. Kostov and A. Migdal, *Analytical and numerical study of a model of dynamically triangulated random surfaces*, *Nuclear Physics B* **275** (1986) 641–686.

[100] M. Nakahara, *Geometry, topology and physics*, CRC Press, 2nd ed. (2003).

[101] J.B. Hartle and S.W. Hawking, *Wave Function of the Universe*, *Phys. Rev. D* **28** (1983) 2960–2975.

[102] S. Gielen and D. Oriti, *Discrete and continuum third quantization of Gravity*, in *Quantum Field Theory and Gravity: Conceptual and Mathematical Advances in the Search for a Unified Framework*, pp. 41–64, 2012, DOI [1102.2226].

[103] J. Ambjorn, B. Durhuus and T. Jonsson, *Three-dimensional simplicial quantum gravity and generalized matrix models*, *Mod. Phys. Lett. A* **6** (1991) 1133–1146.

[104] N. Sasakura, *Tensor model for gravity and orientability of manifold*, *Mod. Phys. Lett. A* **6** (1991) 2613–2624.

[105] N. Godfrey and M. Gross, *Simplicial quantum gravity in more than two-dimensions*, *Phys. Rev. D* **43** (1991) 1749–1753.

[106] D.V. Boulatov, *A Model of three-dimensional lattice gravity*, *Mod. Phys. Lett. A* **7** (1992) 1629–1646 [hep-th/9202074].

[107] H. Ooguri, *Topological lattice models in four-dimensions*, *Mod. Phys. Lett. A* **7** (1992) 2799–2810 [hep-th/9205090].

[108] R. Dijkgraaf and E. Witten, *Topological Gauge Theories and Group Cohomology*, *Commun. Math. Phys.* **129** (1990) 393.

[109] A. Baratin and D. Oriti, *Group field theory with noncommutative metric variables*, *Physical Review Letters* **105** (2010) .

[110] L. Freidel and E.R. Livine, *Ponzano-regge model revisited: III. feynman diagrams and effective field theory*, *Classical and Quantum Gravity* **23** (2006) 2021–2061.

[111] L. Freidel and S. Majid, *Noncommutative harmonic analysis, sampling theory and the Duflo map in 2+1 quantum gravity*, *Class. Quant. Grav.* **25** (2008) 045006 [hep-th/0601004].

[112] E. Joung, J. Mourad and K. Noui, *Three Dimensional Quantum Geometry and Deformed Poincare Symmetry*, *J. Math. Phys.* **50** (2009) 052503 [0806.4121].

[113] E.R. Livine, *Matrix models as non-commutative field theories on R**3*, *Class. Quant. Grav.* **26** (2009) 195014 [0811.1462].

[114] C. Guedes, D. Oriti and M. Raasakka, *Quantization maps, algebra representation and non-commutative Fourier transform for Lie groups*, *J. Math. Phys.* **54** (2013) 083508 [1301.7750].

[115] P. Martin-Dussaud, *A Primer of Group Theory for Loop Quantum Gravity and Spin-foams*, *Gen. Rel. Grav.* **51** (2019) 110 [1902.08439].

[116] I. Mäkinen, *Introduction to SU(2) Recoupling Theory and Graphical Methods for Loop Quantum Gravity*, 1910.06821.

[117] D. Oriti, *Group field theory as the 2nd quantization of Loop Quantum Gravity*, *Class. Quant. Grav.* **33** (2016) 085005 [1310.7786].

[118] C. Rovelli, *The Basis of the Ponzano-Regge-Turaev-Viro-Ooguri quantum gravity model in the loop representation basis*, *Phys. Rev. D* **48** (1993) 2702 [hep-th/9304164].

[119] D. Oriti, *Group Field Theory and Loop Quantum Gravity*, 8, 2014 [1408.7112].

[120] M.P. Reisenberger and C. Rovelli, *Space-time as a Feynman diagram: The Connection formulation*, *Class. Quant. Grav.* **18** (2001) 121–140 [gr-qc/0002095].

[121] R.D. Pietri and L. Freidel, *so(4) plebanski action and relativistic spin-foam model*, *Classical and Quantum Gravity* **16** (1999) 2187–2196.

[122] B. Dittrich, *Diffeomorphism symmetry in quantum gravity models*, *Adv. Sci. Lett.* **2** (2008) 151 [0810.3594].

[123] A. Baratin and D. Oriti, *Group field theory and simplicial gravity path integrals: A model for Holst-Plebanski gravity*, *Phys. Rev. D* **85** (2012) 044003 [1111.5842].

[124] D. Oriti, *Disappearance and emergence of space and time in quantum gravity*, *Stud. Hist. Phil. Sci. B* **46** (2014) 186–199 [1302.2849].

[125] L. Marchetti and D. Oriti, *Effective relational cosmological dynamics from Quantum Gravity*, *JHEP* **05** (2021) 025 [2008.02774].

[126] L.d. Broglie, *Physics and Microphysics*, Harper (1960).

[127] D.P.A. M., *Lectures on Quantum Mechanics*, Belfer Graduate School of Science, Yeshiva University (1966).

[128] C. Rovelli, *What Is Observable in Classical and Quantum Gravity?*, *Class. Quant. Grav.* **8** (1991) 297–316.

[129] C. Rovelli, *Partial observables*, *Phys. Rev. D* **65** (2002) 124013 [gr-qc/0110035].

[130] B. Dittrich, *Partial and complete observables for canonical general relativity*, *Class. Quant. Grav.* **23** (2006) 6155–6184 [gr-qc/0507106].

[131] C.J. Isham, *Canonical quantum gravity and the problem of time*, *NATO Sci. Ser. C* **409** (1993) 157–287 [gr-qc/9210011].

[132] H.W. Hamber, *Discrete and continuum quantum gravity*, 0704.2895.

[133] D. Oriti and J. Ryan, *Group field theory formulation of 3-D quantum gravity coupled to matter fields*, *Class. Quant. Grav.* **23** (2006) 6543–6576 [gr-qc/0602010].

[134] Y. Li, D. Oriti and M. Zhang, *Group field theory for quantum gravity minimally coupled to a scalar field*, *Class. Quant. Grav.* **34** (2017) 195001 [1701.08719].

[135] A. Altland and B.D. Simons, *Condensed Matter Field Theory*, Cambridge University Press, 2 ed. (2010), 10.1017/CBO9780511789984.

[136] S. Gielen, D. Oriti and L. Sindoni, *Cosmology from Group Field Theory Formalism for Quantum Gravity*, *Phys. Rev. Lett.* **111** (2013) 031301 [1303.3576].

[137] S. Gielen, D. Oriti and L. Sindoni, *Homogeneous cosmologies as group field theory condensates*, *JHEP* **06** (2014) 013 [1311.1238].

[138] S. Gielen and L. Sindoni, *Quantum Cosmology from Group Field Theory Condensates: a Review*, *SIGMA* **12** (2016) 082 [1602.08104].

[139] L.P. Pitaevski and S. Stringari, *Bose-Einstein condensation*, Oxford University Press (2016).

[140] D. Oriti, L. Sindoni and E. Wilson-Ewing, *Emergent Friedmann dynamics with a quantum bounce from quantum gravity condensates*, *Class. Quant. Grav.* **33** (2016) 224001 [1602.05881].

[141] L. Marchetti and D. Oriti, *Quantum Fluctuations in the Effective Relational GFT Cosmology*, *Front. Astron. Space Sci.* **0** (2021) 110 [2010.09700].

[142] C.W. Misner, *Quantum cosmology. i*, *Phys. Rev.* **186** (1969) 1319–1327.

[143] R. Penrose, *Gravitational collapse and space-time singularities*, *Phys. Rev. Lett.* **14** (1965) 57.

[144] S. Hawking, *The occurrence of singularities in cosmology. III. Causality and singularities*, *Proc. Roy. Soc. Lond. A* **300** (1967) 187.

[145] S.W. Hawking and R. Penrose, *The Singularities of gravitational collapse and cosmology*, *Proc. Roy. Soc. Lond. A* **314** (1970) 529.

[146] V.N. Melnikov and S.V. Orlov, *NONSINGULAR COSMOLOGY AS A QUANTUM VACUUM EFFECT*, *Phys. Lett. A* **70** (1979) 263.

[147] M. Novello and J.M. Salim, *NONLINEAR PHOTONS IN THE UNIVERSE*, *Phys. Rev. D* **20** (1979) 377.

[148] M. Novello and S.E.P. Bergliaffa, *Bouncing Cosmologies*, *Phys. Rept.* **463** (2008) 127 [0802.1634].

[149] S. Foffa, *Bouncing pre - big bang on the brane*, *Phys. Rev. D* **68** (2003) 043511 [hep-th/0304004].

[150] M. Bojowald, *Loop quantum cosmology*, *Living Rev. Rel.* **8** (2005) 11 [gr-qc/0601085].

[151] A. Ashtekar and P. Singh, *Loop Quantum Cosmology: A Status Report*, *Class. Quant. Grav.* **28** (2011) 213001 [1108.0893].

[152] M. Bojowald, *Absence of singularity in loop quantum cosmology*, *Phys. Rev. Lett.* **86** (2001) 5227 [gr-qc/0102069].

[153] V.A. Belinsky, I.M. Khalatnikov and E.M. Lifshitz, *Oscillatory approach to a singular point in the relativistic cosmology*, *Adv. Phys.* **19** (1970) 525.

[154] V.a. Belinsky, I.m. Khalatnikov and E.m. Lifshitz, *A General Solution of the Einstein Equations with a Time Singularity*, *Adv. Phys.* **31** (1982) 639.

[155] L. Bianchi, *Sugli spazi a tre dimensioni che ammettono un gruppo continuo di movimenti.*, *Soc. Ital. Sci. Mem. di Mat.* **11** (1898) 267.

[156] M. Bojowald, *Canonical gravity and applications: Cosmology, black holes, and quantum gravity*, Cambridge University Press (2011).

[157] N.J. Secrest, S. von Hausegger, M. Rameez, R. Mohayaee, S. Sarkar and J. Colin, *A Test of the Cosmological Principle with Quasars*, *Astrophys. J. Lett.* **908** (2021) L51 [2009.14826].

[158] N.J. Secrest, S. von Hausegger, M. Rameez, R. Mohayaee and S. Sarkar, *A Challenge to the Standard Cosmological Model*, *Astrophys. J. Lett.* **937** (2022) L31 [2206.05624].

[159] A. Pontzen and A. Challinor, *Bianchi Model CMB Polarization and its Implications for CMB Anomalies*, *Mon. Not. Roy. Astron. Soc.* **380** (2007) 1387 [0706.2075].

[160] E. Russell, C.B. Kılınç and O.K. Pashaev, *Bianchi I model: an alternative way to model the present-day Universe*, *Monthly Notices of the Royal Astronomical Society* **442** (2014) 2331 [https://academic.oup.com/mnras/article-pdf/442/3/2331/3558602/stu932.pdf].

[161] W. Zhao and L. Santos, *Preferred axis in cosmology*, 1604.05484.

[162] P.K. Aluri et al., *Is the Observable Universe Consistent with the Cosmological Principle?*, 2207.05765.

[163] L. Perivolaropoulos and F. Skara, *Challenges for ΛCDM: An update*, *New Astron. Rev.* **95** (2022) 101659 [2105.05208].

[164] M. de Cesare, D. Oriti, A.G.A. Pithis and M. Sakellariadou, *Dynamics of anisotropies close to a cosmological bounce in quantum gravity*, *Class. Quant. Grav.* **35** (2018) 015014 [1709.00994].

[165] A. Calcinari and S. Gielen, *Towards anisotropic cosmology in group field theory*, 2210.03149.

[166] C.W. Misner, *Mixmaster universe*, *Phys. Rev. Lett.* **22** (1969) 1071.

[167] A. Ashtekar and E. Wilson-Ewing, *Loop quantum cosmology of Bianchi I models*, *Phys. Rev. D* **79** (2009) 083535 [0903.3397].

[168] D.C. Salisbury, J. Helpert and A. Schmitz, *Reparameterization invariants for anisotropic Bianchi I cosmology with a massless scalar source*, *Gen. Rel. Grav.* **40** (2008) 1475 [gr-qc/0503014].

[169] D.-W. Chiou, *Loop Quantum Cosmology in Bianchi Type I Models: Analytical Investigation*, *Phys. Rev. D* **75** (2007) 024029 [gr-qc/0609029].

[170] K.C. Jacobs, *Spatially homogeneous and euclidean cosmological models with shear*, *The Astrophysical Journal* **153** (1968) 661.

[171] K.A. Bronnikov, E.N. Chudayeva and G.N. Shikin, *Magneto-dilatonic bianchi-i cosmology: isotropization and singularity problems*, *Classical and Quantum Gravity* **21** (2004) 3389.

[172] B. Saha, *Nonlinear spinor field in Bianchi type-I cosmology: Inflation, isotropization, and late time acceleration*, *Phys. Rev. D* **74** (2006) 124030.

[173] B. Saha, *Spinor field in Bianchi type-IX space-time*, 1705.07773.

[174] D. Oriti and T. Tlas, *A New Class of Group Field Theories for 1st Order Discrete Quantum Gravity*, *Class. Quant. Grav.* **25** (2008) 085011 [0710.2679].

[175] D. Oriti and L. Sindoni, *Towards classical geometrodynamics from Group Field Theory hydrodynamics*, *New J. Phys.* **13** (2011) 025006 [1010.5149].

[176] A.G.A. Pithis and M. Sakellariadou, *Relational evolution of effectively interacting group field theory quantum gravity condensates*, *Phys. Rev. D* **95** (2017) 064004 [1612.02456].

[177] J. Engle, E. Livine, R. Pereira and C. Rovelli, *LQG vertex with finite Immirzi parameter*, *Nucl. Phys. B* **799** (2008) 136–149 [0711.0146].

[178] J. Ben Geloun and V. Bonzom, *Radiative corrections in the Boulatov-Ooguri tensor model: The 2-point function*, *Int. J. Theor. Phys.* **50** (2011) 2819–2841 [1101.4294].

[179] J. Ben Geloun and V. Rivasseau, *A Renormalizable 4-Dimensional Tensor Field Theory*, *Commun. Math. Phys.* **318** (2013) 69–109 [1111.4997].

[180] S. Carrozza, D. Oriti and V. Rivasseau, *Renormalization of Tensorial Group Field Theories: Abelian U(1) Models in Four Dimensions*, *Commun. Math. Phys.* **327** (2014) 603–641 [1207.6734].

[181] S. Carrozza, D. Oriti and V. Rivasseau, *Renormalization of a SU(2) Tensorial Group Field Theory in Three Dimensions*, *Commun. Math. Phys.* **330** (2014) 581–637 [1303.6772].

[182] S. Carrozza, *Group field theory in dimension* $4-\epsilon$, *Phys. Rev. D* **91** (2015) 065023 [1411.5385].

[183] M. de Cesare and M. Sakellariadou, *Accelerated expansion of the Universe without an inflaton and resolution of the initial singularity from Group Field Theory condensates*, *Phys. Lett. B* **764** (2017) 49 [1603.01764].

[184] D. Oriti, D. Pranzetti, J.P. Ryan and L. Sindoni, *Generalized quantum gravity condensates for homogeneous geometries and cosmology*, *Class. Quant. Grav.* **32** (2015) 235016 [1501.00936].

[185] D. Oriti, D. Pranzetti and L. Sindoni, *Horizon entropy from quantum gravity condensates*, *Phys. Rev. Lett.* **116** (2016) 211301 [1510.06991].

[186] D. Oriti, D. Pranzetti and L. Sindoni, *Black Holes as Quantum Gravity Condensates*, *Phys. Rev. D* **97** (2018) 066017 [1801.01479].

[187] C. Rovelli and L. Smolin, *Discreteness of area and volume in quantum gravity*, *Nuclear Physics B* **442** (1995) 593–619.

[188] J. Brunnemann and T. Thiemann, *Simplification of the spectral analysis of the volume operator in loop quantum gravity*, *Class. Quant. Grav.* **23** (2006) 1289 [gr-qc/0405060].

[189] E. Bianchi, P. Dona and S. Speziale, *Polyhedra in loop quantum gravity*, *Phys. Rev. D* **83** (2011) 044035 [1009.3402].

[190] E. Bianchi and H.M. Haggard, *Discreteness of the volume of space from Bohr-Sommerfeld quantization*, *Phys. Rev. Lett.* **107** (2011) 011301 [1102.5439].

[191] E. Bianchi and H.M. Haggard, *Bohr-Sommerfeld Quantization of Space*, *Phys. Rev. D* **86** (2012) 124010 [1208.2228].

[192] J.A. Wheeler, *The beam and stay of the taub universe*, in *Essays in General Relativity*, F.J. Tipler, ed., pp. 59–70, Academic Press (1980), DOI.

[193] D.H. King, *Gravity wave insights to Bianchi type IX universes*, *Phys. Rev. D* **44** (1991) 2356.

[194] S. Gielen, *Emergence of a low spin phase in group field theory condensates*, *Class. Quant. Grav.* **33** (2016) 224002 [1604.06023].

[195] D. Oriti, L. Sindoni and E. Wilson-Ewing, *Bouncing cosmologies from quantum gravity condensates*, *Class. Quant. Grav.* **34** (2017) 04LT01 [1602.08271].

[196] J.D. Bekenstein, *Black holes and the second law*, *Lett. Nuovo Cim.* **4** (1972) 737.

[197] J.D. Bekenstein, *Black holes and entropy*, *Phys. Rev. D* **7** (1973) 2333.

[198] S.W. Hawking, *Black hole explosions*, *Nature* **248** (1974) 30–31.

[199] S.W. Hawking, *Particle Creation by Black Holes*, *Commun. Math. Phys.* **43** (1975) 199–220.

[200] J.M. Bardeen, B. Carter and S.W. Hawking, *The Four laws of black hole mechanics*, *Commun. Math. Phys.* **31** (1973) 161–170.

[201] W.G. Unruh, *Notes on black hole evaporation*, *Phys. Rev. D* **14** (1976) 870.

[202] D. Oriti, *The universe as a quantum gravity condensate*, *Comptes Rendus Physique* **18** (2017) 235–245 [1612.09521].

[203] B.L. Hu, *Can spacetime be a condensate?*, *Int. J. Theor. Phys.* **44** (2005) 1785 [gr-qc/0503067].

[204] S. Gielen and D. Oriti, *Cosmological perturbations from full quantum gravity*, *Phys. Rev. D* **98** (2018) 106019 [1709.01095].

[205] J.D. Bekenstein, *A Universal Upper Bound on the Entropy to Energy Ratio for Bounded Systems*, *Phys. Rev. D* **23** (1981) 287.

[206] R. Bousso, *A Covariant entropy conjecture*, *JHEP* **07** (1999) 004 [hep-th/9905177].

[207] R.K. Kaul and P. Majumdar, *Logarithmic correction to the Bekenstein-Hawking entropy*, *Phys. Rev. Lett.* **84** (2000) 5255 [gr-qc/0002040].

[208] E.R. Livine and D.R. Terno, *Quantum black holes: Entropy and entanglement on the horizon*, *Nucl. Phys. B* **741** (2006) 131 [gr-qc/0508085].

[209] J. Engle, K. Noui, A. Perez and D. Pranzetti, *The SU(2) Black Hole entropy revisited*, *JHEP* **05** (2011) 016 [1103.2723].

[210] S. Gielen, *Group field theory and its cosmology in a matter reference frame*, *Universe* **4** (2018) 103 [1808.10469].

[211] G. Amelino-Camelia, *Introduction to quantum-gravity phenomenology*, *Lect. Notes Phys.* **669** (2005) 59 [gr-qc/0412136].

[212] L. Freidel, D. Oriti and J. Ryan, *A Group field theory for 3-D quantum gravity coupled to a scalar field*, gr-qc/0506067.

[213] W.J. Fairbairn and E.R. Livine, *3d Spinfoam Quantum Gravity: Matter as a Phase of the Group Field Theory*, *Class. Quant. Grav.* **24** (2007) 5277 [gr-qc/0702125].

[214] G. Ponzano and T. Regge, *Semiclassical limit of racah coefficients*, in *Spectroscopy and Group Theoretical Methods in Physics, F. Block et al*, North-Holland, Amsterdam, 1968.

[215] I.R. Klebanov, F. Popov and G. Tarnopolsky, *TASI Lectures on Large N Tensor Models*, *PoS* **TASI2017** (2018) 004 [1808.09434].

[216] S. Sachdev and J. Ye, *Gapless spin fluid ground state in a random, quantum Heisenberg magnet*, *Phys. Rev. Lett.* **70** (1993) 3339 [cond-mat/9212030].

[217] A. Kitaev, "A simple model of quantum holography (part 1)." Talk at KITP Program: Entanglement in Strongly-Correlated Quantum Matter, 2015.

[218] A. Kitaev, "A simple model of quantum holography (part 2)." Talk at KITP Program: Entanglement in Strongly-Correlated Quantum Matter, 2015.

[219] S. Sachdev, *Bekenstein-Hawking Entropy and Strange Metals*, *Phys. Rev. X* **5** (2015) 041025 [1506.05111].

[220] D. Chowdhury, A. Georges, O. Parcollet and S. Sachdev, *Sachdev-Ye-Kitaev models and beyond: Window into non-Fermi liquids*, *Rev. Mod. Phys.* **94** (2022) 035004 [2109.05037].

[221] R. Gurau, *Colored Group Field Theory*, *Commun. Math. Phys.* **304** (2011) 69 [0907.2582].

[222] R.G. Gurau, *Random tensors*, Oxford University Press (2017).

[223] E. Witten, *An SYK-Like Model Without Disorder*, *J. Phys. A* **52** (2019) 474002 [1610.09758].

[224] I.R. Klebanov and G. Tarnopolsky, *Uncolored random tensors, melon diagrams, and the Sachdev-Ye-Kitaev models*, *Phys. Rev. D* **95** (2017) 046004 [1611.08915].

[225] D.J. Amit and D.V.I. Roginsky, *Exactly soluble limit of ϕ^3 field theory with internal potts symmetry*, *Journal of Physics A: Mathematical and General* **12** (1979) 689.

[226] D. Benedetti and N. Delporte, *Remarks on a melonic field theory with cubic interaction*, *JHEP* **04** (2021) 197 [2012.12238].

[227] H.M. Haggard and R.G. Littlejohn, *Asymptotics of the Wigner 9j symbol*, *Class. Quant. Grav.* **27** (2010) 135010 [0912.5384].

[228] F. Costantino and J. Marche, *Generating series and asymptotics of classical spin networks*, 2011. 10.48550/ARXIV.1103.5644.

[229] V. Bonzom and P. Fleury, *Asymptotics of Wigner 3nj-symbols with Small and Large Angular Momenta: An Elementary Method*, *J. Phys. A* **45** (2012) 075202 [1108.1569].

[230] P. Donà, M. Fanizza, G. Sarno and S. Speziale, *SU(2) graph invariants, Regge actions and polytopes*, *Class. Quant. Grav.* **35** (2018) 045011 [1708.01727].

[231] A. Einstein, *Die Grundlage der allgemeinen Relativitätstheorie*, *Annalen der Physik* **354** (1916) 769.

[232] E. Colafranceschi and D. Oriti, *Quantum gravity states, entanglement graphs and second-quantized tensor networks*, *JHEP* **07** (2021) 052 [2012.12622].

[233] E. Colafranceschi, G. Chirco and D. Oriti, *Holographic maps from quantum gravity states as tensor networks*, *Phys. Rev. D* **105** (2022) 066005 [2105.06454].

[234] G. Chirco, E. Colafranceschi and D. Oriti, *Bulk area law for boundary entanglement in spin network states: Entropy corrections and horizon-like regions from volume correlations*, *Phys. Rev. D* **105** (2022) 046018 [2110.15166].

[235] A.A. Rahman, *dS JT Gravity and Double-Scaled SYK*, 2209.09997.

[236] L. Susskind, *De Sitter Space, Double-Scaled SYK, and the Separation of Scales in the Semiclassical Limit*, 2209.09999.

[237] P. Saad, S.H. Shenker and D. Stanford, *JT gravity as a matrix integral*, 1903.11115.

[238] E. Witten, *Matrix Models and Deformations of JT Gravity*, *Proc. Roy. Soc. Lond. A* **476** (2020) 20200582 [2006.13414].

Acknowledgement

First of all, I would like to thank my doctoral supervisor, Dr. Daniele ORITI. I learnt a lot when working with him, not only a wide range of knowledge on quantum gravity, but also how to become an independent mature scientific researcher.

I thank also all our group members at Ludwig-Maximilians-Universität München, Jibril Ben Achour, Ali Barzegar, Eugenia Colafrancheschi, Roukaya Dekhil, Christophe Goeller, Simon Langenscheidt, Luca Marchetti, Xiankai Pang, and Andreas G.A. Pithis, for inspiring discussions as well as the enthusiasm for physics shared with me.

Then I would like to show my deepest gratitude to Prof. GE Xian-Hui. I cannot have been here without your patient guidance and help over the past ten years. I cannot thank you enough, as no words can express my thanks to your great favour.

I am also grateful to Prof. NAKAHARA Mikio, and you are always a good example to me as a scientist. Your kind help and warm encouragement gave me the confidence to overcome the difficulties during my doctoral period.

I feel blessed to met Prof. PI Shi. You share with me your experience of becoming an outstanding young physicist, and nudge me to keep going. It is you that makes me look at the stars when in the gutter.

Finally, I am forever in-debt to my parents and grandparents. I am so lucky to have you as my family. Thank you for your strong support and love all the time.